THE ROLE OF COMPLEXING AGENTS IN THE FLOTATION OF PENTLANDITE-PYROXENE MIXTURES

Natalie Jean Shackleton

THE ROLE OF COMPLEXING AGENTS IN THE FLOTATION OF PENTLANDITE-PYROXENE MIXTURES

By

Natalie Jean Shackleton

A thesis submitted to the University of Cape Town in fulfilment of the requirements for a Masters Degree in Applied Science

Faculty of Chemical Engineering and Built Environment

University of Cape Town

June 2003

"Kill the snake of doubt in your soul, crush the worms of fear in your heart and mountains will move out of your way."

-- Kate Seredy

ACKNOWLEDGEMENTS

I would like to thank Anglo Platinum management for support during the study and permission to publish the thesis.

I also wish to express my gratitude to Professor Cyril O'Connor for his guidance and valuable suggestions during the course of this study and I would like to record my thanks to Vrat Malysiak for his guidance during the study.

To my husband, Andrew, for all his support and encouragement throughout the study and last but not least my Chihuahuas who faithfully sat with me till late at night while I was writing up the thesis.

TABLE OF CONTENTS

LIST OF APPENDICES

LIST OF FIGURES

PAGE NO

LIST OF TABLES

PAGE NO

NOMENCLATURE

e	Ion charge
E°	Standard reduction potential
E_h	Oxidation/reduction potential
E_{kin}	Kinetic energy
L_o	Effective length of spectrometer
m	Ion mass
m_o	Adjacent masses
Δm	Ion mass difference
t	Flight time
t_o	Length of primary ion pulse
Δt	Time difference
v	Ion velocity
V_o	Accelerating potential

GREEK LETTERS

ε	Fluid dielectric constant
η	Viscosity
κ_a	Ratio of particle radius to double layer thickness
ζ	Zeta potential

LIST OF ABBREVIATIONS

ATR	Attenuated total internal reflection
COS	Complex oxidised sulphide
$CuSO_4$	Copper sulphate
DETA	Diethylenetriamine
e^-	Standard reducing agent
EDA	Ethylenediamine
EDTA	Ethylenediaminetetraacetic acid
FTIR	Fourier transform infrared spectroscopy
H^+	Concentration of standard acid

I	Ionic Strength
iep	Isoelectric point
IR	Infrared spectroscopy
LIMS	Laser ionisation mass spectrometry
Log(Conc.)	Logarithmic concentration
M	Metal ion
M^+	Metal cation
MS	Metal sulphide
MA	Metal chelates
L	Ligand
ML	Metal ligand
Log K	Formation or stability constant
Log β	Cumulative formation constants
PAM	Polyacrylamide
pE	Equilibrium potential
PGM	Platinum group minerals
pH_{ie}	Isoeletric point pH
ppm	Parts per million
Rel Std Dev	Relative standard deviation
rpm	Revolutions per minute
SIBX	Sodium iso-butyl xanthate
$SIBX^-$	Xanthate anionic form
$(SIBX)_2$	Xanthate dimer
Std Dev	Standard deviation
ToF-SIMS	Time of flight secondary ion mass spectrometry
UV	Ultraviolet spectroscopy
wt.%	Weighted percent
X^-	Xanthate ion
XPS	X-ray photoelectron spectroscopy

SYNOPSIS

The major loss of base metals in beneficiation of the Merensky Reef ore occurs during the separation of the siliceous gangue from the platinum group and base metal sulphides by selective flotation. This study examines the role complexing agents play in pentlandite-pyroxene flotation and focuses on the surface chemistry and interaction between valuable and gangue minerals as well as the interaction of complexing agents and reagents (xanthate, copper sulphate) in the system at pH 9. Microflotation, zeta potential measurements, ToF-SIMS analyses (time of flight secondary ion mass spectrometry) and X-ray photoelectron spectroscopy (XPS) were used as tools in determining the extent of surface alteration.

Evaluation of the four-complexing agents, diethylenetriamine (DETA), ethylenediamine (EDA), triethylenetetramine (TETA) and ethylenediaminetetraacetic acid (EDTA), for use in the flotation of pentlandite and pyroxene systems, has revealed that there are differences as well as similarities with respect to floatability, selectivity and surface alteration of the system studied at pH 9.

DETA, TETA and EDTA gave ultimate recoveries similar to the copper sulphate followed by xanthate base case. The lowest selectivity between pentlandite and pyroxene was obtained in the presence of EDTA

Zeta potential, ToF-SIMS and XPS data have shown that pyroxene becomes copper activated in the presence of copper sulphate. When xanthate ions are added to the copper activated minerals true flotation of pyroxene occurs. Furthermore, the flotation and surface analysis data revealed that pyroxene could also be inadvertently activated by Ni(II) ions, which would result in a higher pyroxene recovery and thus lower selectivity.

In the presence of EDA the concentration of copper(II) and nickel(II) ions found on pyroxene and pentlandite surfaces was significantly reduced, but predominantly on pyroxene. The mechanism for the removal of the activating ions from the mineral

surfaces involves the formation of soluble stable metal-EDA chelates, which are removed into solution.
Variation in the sequence of addition of EDA and the variation in the concentration of copper sulphate or xanthate displayed no added benefit.

The optimum conditions, in terms of pentlandite recovery and selectivity at pH 9, appear to be the combination of copper sulphate, ethylenediamine (EDA) and SIBX at an EDA concentration of 4.00E-05M.

Keywords: Surface passivation, Microflotation, Sulphides, Gangue, Water quality, DETA, EDA, TETA, EDTA ToF-SIMS, Zeta potential, XPS, Copper activation / deactivation.

CHAPTER 1

INTRODUCTION

The Merensky ore is found in a platinum group mineral (PGM) bearing reef in the Bushveld Igneous Complex in South Africa. The predominant sulphide minerals are pentlandite, chalcopyrite and pyrrhotite. Non-sulphide gangue minerals consist mainly of pyroxene and feldspar along with minor quantities of talc, chlorite and chromite. Flotation is used to separate the valuable minerals from the siliceous gangue, with selective separation achieved by the adsorption of a collector onto the surface of the PGM and sulphide minerals. The aim is to maximise the recovery of PGM and sulphide minerals and minimise the amount of gangue minerals in concentrates, since the latter have an adverse effect on smelting.

The predominant gangue minerals reporting to the flotation concentrate are pyroxene and feldspar. They are characterised by a wide variation in chemical composition, crystal structure and content of isomorphous admixtures, which influence their behaviour in technological processes. It is believed that pyroxene and feldspar are naturally hydrophilic and thus when liberated they should report to the concentrate only by entrainment and entrapment. Previous studies carried out by colleagues at a PGM concentrator indicated that 61% of the total gangue in the concentrate was due to flotation and 34% due to entrainment. It is highly unlikely that xanthate collectors exhibit any affinity for siliceous gangue minerals to cause flotation. Therefore it is likely that activation of the mineral surface by metal ions is occurring, prior to xanthate adsorption. In terms of sulphide minerals, pentlandite is the most valuable base metal sulphide mineral in the Merensky Reef and it is the main source of nickel worldwide. There is scope for an improvement of pentlandite recovery at operating circuits treating Merensky Reef ore.

Due to a high percentage of gangue minerals reporting to the concentrate, particularly pyroxene, the objective of the thesis was to explain what can be done to minimise the

percentage pyroxene reporting to the concentrate and simultaneously maximise pentlandite recovery with the use of complexing agents.

Complexing agents have been recognised as potential reagents in mineral flotation for many decades. The proposed study focuses on the surface chemistry and interaction between valuable and gangue minerals as well as the interaction of complexing agents and reagents (xanthate, copper sulphate) in the system thereby gaining knowledge about the effect complexing agents have on mineral surface alteration and the distribution of ions on mineral surfaces and link these variables to flotation for pentlandite and pyroxene.

The key questions to be asked are whether the complexing agents improve pentlandite floatability and if so, what are the mechanisms contributing to this phenomenon. Do the complexing agents reduce pyroxene floatability and what are the mechanisms contributing to this fact.

Complexing agents will remove oxide and hydroxide layers from the mineral surfaces and reduce the concentration of ions that cause inadvertent activation of pyrrhotite mineral surfaces (Zhenghe et al. 1997 and Kelebek, 1996). It is hypothesised that this will also hold for siliceous gangue minerals since the complexing agent does not distinguish between gangue or sulphide mineral surfaces and only complexes with the hydrophilic oxide and hydroxide layers involving Cu(II) and Ni(II) ions.

This thesis presents the results of a study examining the effect of the addition of complexing agents, diethylenetriamine (DETA), ethylenediamine (EDA), triethylenetetramine (TETA) and ethylenediaminetetraacetic acid (EDTA), to pentlandite-pyroxene systems with a view to exploring the extent to which metal ion activation occurs and influences flotation and how this can be managed so as to increase the separation of pentlandite from pyroxene at pH 9. Specifically, the effect of sodium isobutyl xanthate, copper sulphate, DETA, EDA, TETA and EDTA on

pentlandite and pyroxene was evaluated. The mineral surface alteration was investigated using zeta potential, ToF-SIMS and XPS techniques.

CHAPTER 2

LITERATURE REVIEW

For many years, flotation has been used for concentrating sulphide minerals that are a primary source of base metals. With the depletion of high-grade ore deposits it has become necessary to treat low-grade complex polymetallic ores. This often involves processing of fine particles that are more difficult to float. Better understanding of surface oxidation, collector adsorption and distribution as well as ionic activation of mineral surfaces is needed to maximise valuable minerals recovery.

Platinum-bearing ores were first discovered in South Africa in 1923. Today, the Bushveld Igneous Complex is the world's largest deposit of platinum group minerals (PGM). The Bushveld ore contains platinum, palladium, rhodium, ruthenium, iridium, osmium, gold, as well as copper, nickel and cobalt in economically recoverable quantities. The predominant PGM mineral types as well as the mineral association vary significantly across the ore body.

A typical process circuit used across the South African PGM industry consists of two or three stages of milling. Each comminution stage is followed by flotation (Figure 2.1). Autogenous mills can be used in primary milling circuits while ball mills are employed in secondary milling stages.

A large variety of flotation circuits are currently used across the industry in South Africa as the primary method for the upgrading of valuable minerals. The roughing and scavenging stages are complemented by a number of cleaning circuits. In the new flotation plants, trends have leaned towards using larger cells. Lately, tank cells have been used more extensively. Typically, flotation is carried out at a pH of about 8.7. Various collectors, depressants and frothers are being used. The most common collectors utilised by the PGM industry appear to be xanthates and dithiophosphates. In terms of depressants, carboxymethyl cellulose and guar based reagents have been found to be effective in improving the flotation efficiency of separating valuable minerals

from siliceous gangue. In a number of operations, copper sulphate is used as an activator for pentlandite and pyrrhotite.

The major loss of PGM and base metal sulphides in the beneficiation of the Bushveld Igneous Complex occurs during the separation of the siliceous gangue from the PGM and sulphide minerals by selective flotation; therefore flotation remains the main metallurgical focus for the South African PGM producers.

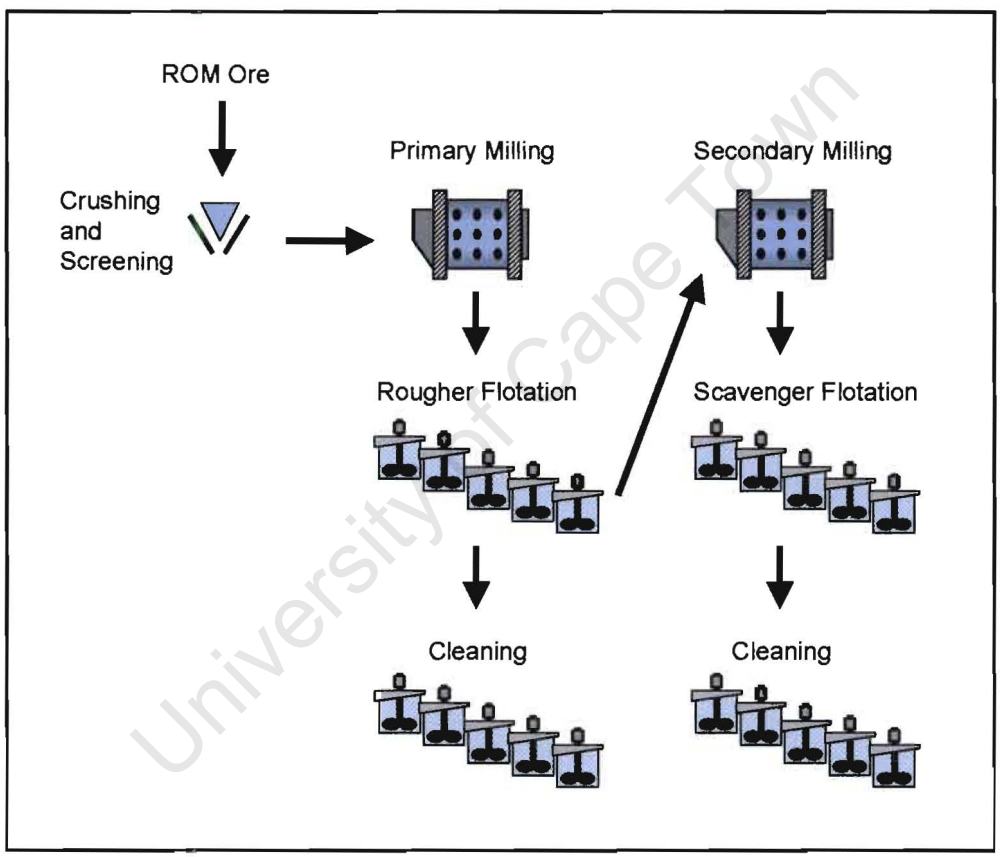

Figure 2.1: A typical concentrator flowsheet

A review of the available literature mainly of pentlandite (which is nearly always associated with pyrrrhotite) and pyroxene with particular reference to the surface chemistry is discussed. The areas reviewed are on the existing knowledge of the

mineralogy, flotation of ores, the chemistry of the reagents, as well as the speciation of the elements of interest.

2.1 Pentlandite

2.1.1 Mineralogy

Pentlandite is an iron nickel sulphide, which belongs to the sulphide mineral class. The sulphides form an important class of minerals that includes the majority of the ore minerals. Most of the sulphide minerals are opaque with distinctive colours and characteristically coloured streaks. The general formula for the sulphides is given as X_mZ_n in which X represents the metallic elements and Z the non-metallic elements. Pentlandite is an important ore of nickel and is commonly associated with other sulphides such as pyrite, chalcopyrite and pyrrhotite in basic igneous rock intrusions. Pentlandite's close association with the mineral pyrrhotite ($Fe_{1-x}S$) is believed to be the result of exsolution that occurs after magmatic segregation. Pyrrhotite is usually magnetic, although weakly so, and lacks the octahedral parting of pentlandite which provides the only good field tests for differentiation. Pentlandite's formula, $(Fe,Ni)_9S_8$, is believed to be composed of equal amounts of nickel and iron, but does show variation in tests. The structure of pentlandite is rather complex, with a face centered cubic arrangement and the metal ions in tetrahedral and octahedral coordination with the sulphurs. Coordination refers to the number and position of the sulphurs surrounding the metal ions. In the case of tetrahedral coordination, there are four sulphurs surrounding one metal ion and they are positioned at the four points of a tetrahedron. In the case of octahedral coordination, there are six sulphurs at the six points of an octahedron with a metal ion inside (Klein, C. and Hurlbut, Jr., C.S., 1985).

2.1.2 Surface and Flotation Studies

2.1.2.1 Self-induced (Collectorless) Flotation

The self-induced flotation of sulphide minerals has been known since the beginning of the last century. Pentlandite and pyrrhotite exhibit self-induced flotation, viz. flotation in the absence of collector, as a result of mild oxidation of the mineral itself. There have

been many studies published in the literature confirming this observation. Ishihara and Kagami (1964) showed that pyrrhotite is highly susceptible to oxidation as compared to other sulphide minerals. However, mild oxidation enhanced flotation due to the formation of elemental sulphur and Trahar (1983) has reported that pyrrhotite and pentlandite are strongly floatable.

Trahar (1984) also pointed out that there are at least three types of floatability displayed by sulphide minerals, which are not inherently floatable: self-induced, sulphur induced and collector induced. The floatability for each type is considered to be dependent on the oxidation-reduction state of the pulp.

The effect of pulp potential was investigated further by Heyes and Trahar (1984). They suggested that the collectorless floatability of pyrrhotite is dependent on the pulp potential. They pointed out that flotation occurs in mildly oxidising but not in reducing conditions. It was suggested that elemental sulphur might be responsible for collectorless flotation. They demonstrated that pyrrhotite shows self-induced flotation upon mild oxidation. In alkaline solutions, however, metal hydroxides form and when their solubility products are exceeded collectorless flotation is inhibited. Elemental sulphur oxidises to sulphur oxygen species and eventually to sulphate ions.

In 1987, Hayes et al. summarised that sulphide minerals which are amenable to collectorless flotation form metal-deficient sulphides and/or elemental sulphur on the mineral surfaces.

Healy and Trahar (1989) found that the potential at which self-induced flotation occurs (50% in the first minute) is at E_h values of -0.15 and 0.0 V for pentlandite and pyrrhotite, respectively. Ralston (1991) also reported that collectorless flotation is possible only under specific oxidation-reduction or E_h conditions in the flotation pulp.

Heiskanen et al. (1991) studied collectorless flotation of noritic and serpentinic nickel ores using batch flotation techniques. Only pH was varied from 3-12 during the tests.

Pyrrhotite (Noritic ore) floated markedly well at pH 3-5 but had a very low recovery at higher pH, which could be attributed to mechanical entrainment. Pentlandite gave a good recovery at low pH and a recovery of 40-60% at higher pH values. The results obtained showed that process iron had a marked effect on the collectorless flotation. Sulphides from samples ground in a ceramic mill floated better than those ground in a steel mill. The results demonstrated that either hydroxide and/or sulphate layers tend to build up during a long aeration time, thus hindering flotation. It was pointed out that the oxidation of pyrrhotite progressed more rapidly than that of pentlandite.

It can be deduced from the above observations that for collectorless flotation to take place the minerals should be exposed to some form of mild oxidation so that elemental sulphur, and/or metal deficient lattice, and/or polysulphide are present on the mineral surfaces, which would induce hydrophobicity. However, the identity and stability, both thermodynamic and kinetic, and the involvement of the hydrophobic species given above in collectorless flotation have been topics of considerable debate and there is still no single acceptable interpretation.

2.1.2.2 Collector Induced Flotation (Xanthates)

Xanthates are one of the major classes of collectors used in flotation of sulphide minerals. They have been successfully employed in the industry to separate sulphides from gangue minerals such as silicates.

Wang et al (1989) carried out thermodynamic calculations for the Fe-EX-H_2O system to study the stability of iron-xanthates. They showed that the formation and stability of insoluble iron-xanthate compounds depended critically on the xanthate concentration and on the pH and redox potential of the solutions. Ferric xanthate could be formed and was stable in acidic pH and in xanthate concentration ranges used in conventional flotation. It improved or caused the recovery of iron-sulphide flotation in this pH range. Insoluble hydroxyl ferric xanthate could be obtained and remained stable at very low xanthate concentrations in the pH range of weakly acidic to alkaline and under a wide

range of redox potentials. Ferric dihydroxo xanthate was only slightly hydrophobic. Liquid dixanthogen was formed at high redox potentials and high xanthate concentrations. No liquid dixanthogen could be obtained under conditions where ferric and hydroxyl ferric xanthates were formed. Ferrous xanthate could be obtained only with very high xanthate concentrations and under reducing conditions. Its role in the iron-sulphide flotation could be completely ignored.

Hodgson and Agar (1989) reported that xanthate adsorbs, at pH 9, on the pyrrhotite surface forming an $Fe(OH)_2X$ product. Unlike chemisorption, no electron transfer was considered to arise through the adsorption of xanthate on the surface. The collector was adsorbed through coulombic attraction with cationic iron (III) site generated through oxidation of the mineral surface:

$$FeS + 2H_2O \rightarrow Fe(OH)[S]^+ + 2H^+ + 2e \qquad (1)$$

$$Fe(OH)[S]^+ + X^- \rightarrow Fe(OH)[S]X \qquad (2)$$

Xanthate then oxidised to dixanthogen through the reduction of oxygen at the pyrrhotite surface

$$2X^- \rightarrow X_2 + 2e \qquad (3)$$

$$O_2 + 2H_2O + 4e \rightarrow 4OH^- \qquad (4)$$

Dixanthogen formation was considered to take place adjacent to the oxidised pyrrhotite surface and be physisorbed via the alkyl groups of the Fe(OH)[S]X complex. Dixanthogen was the species that conferred hydrophobicity on the surface of pyrrhotite and oxygen was required to promote the bubble contact. In the case of pentlandite it was concluded that the collector chemisorbed directly on to the nickel sites (pH 9). The addition of xanthate reduced the degree of oxidation of the pentlandite surfaces.

Dixanthogen is formed from chemisorbed xanthate on the pentlandite surface according to the following reactions

$$Ni + X^- \rightarrow NiX + e \qquad (5)$$

$$NiX + X^- \rightarrow Ni(X)_2 \rightarrow NiX_2 + e \qquad (6)$$

The formation of dixanthogen would occur concurrently with the adsorption of xanthate on the pentlandite during the oxidation process and enhances hydrophobicity.

The reaction of amyl xanthate in solution in the presence of pentlandite in a water-ethanol mixed solvent was studied by McNeil et al. (1994). Compared with water only, this solvent kept all products in solution while maintaining the same U.V. spectra, making it well suited to the study. Rapid oxidation of xanthate to dixanthogen was found, which appeared to be catalytic as no reaction products could be extracted from the pentlandite surface.

Bozkurt et al. (1997) investigated the effect Ni ions and pentlandite/pyrrhotite interaction has on adsorption of isobutyl xanthate using FTIR-ATR spectroscopy and open circuit potential measurements. Dixanthogen was the major surface product under all conditions on both minerals. From single mineral studies, dixanthogen concentration was greater on pentlandite than pyrrhotite and Ni ions always enhanced it. For mineral mixtures, dixanthogen concentration increased on pentlandite and decreased on pyrrhotite. The presence of Ni ions moderated this effect.

A year later, Bozkurt et al. (1998) reported on a similar study during which the interaction of isobutyl xanthate with pentlandite and pyrrhotite was investigated using ATR, FTIR and open circuit potential (rest potential) measurements. The study was performed with single and mixed mineral systems at pH 9.2. Mixing the minerals showed that dixanthogen formation on pentlandite was promoted while on pyrrhotite it was suppressed. A mixed potential model was used to explain this effect of mineral

interaction on dixanthogen formation. At the potential of the mixed mineral system, the anodic reaction (xanthate oxidation to dixanthogen) occurred preferentially on pentlandite and the cathodic reaction (reduction of oxygen to hydroxyl ion) occurred on pyrrhotite.

2.1.2.3 Surface Oxidation

A number of researchers have studied the problem of pentlandite alteration due to oxidation.

Broomhead and Lavers (1976) studied factors governing the dissolution of nickel and iron in pentlandite and pyrrhotite concentrates in aqueous solutions at normal temperatures and pressures. The direct reaction of oxygen in aerated water with pyrrhotite was much faster than with pentlandite and reaction rates were proportional to the dissolved oxygen concentration. The different reactivity can be explained by their different crystal structure. Pyrrhotite has vacancies and pentlandite does not. Divalent metal sulphates were produced initially for both minerals. The subsequent oxidation of iron(II) to iron(III) and its oxolation produced acid solutions, which rapidly attacked both minerals. Acidity increased with time.

The alteration in surface chemistry of pentlandite exposed to air was studied by Boyd (1979). If the mineral was cleaved in pure argon the only oxidation product formed was Fe_2O_3, if the mineral was cleaved in air, Fe_2O_3 and NiO were produced. Contacting the mineral with SIBX gave FeO, nickel xanthate, $Ni(IBX)_2$ and two unidentified species.

Thomber (1983) studied mineralogical and electrochemical stability of the nickel-iron sulphides, pentlandite and violarite. He pointed out that in a primary assemblage composed of pentlandite, pyrrhotite and pyrite, pentlandite reacted first at the lowest oxidation potential and it altered to violarite with nickel and iron released into solution according to the following reaction

$$Fe_{4.5}Ni_{4.5}S_8 \rightarrow 2FeNi_2S_4 + 0.5Ni^{2+}\ 2.5Fe^{2+} + 6e^- \qquad (7)$$

At the same time, the increased nickel activity caused the pyrrhotite to become unstable and it took up nickel from solution to form violarite

$$Fe_7S_8 + 4Ni^{2+} \rightarrow 2FeNi_2S_4 + 5Fe^{2+} + 2e^- \qquad (8)$$

Richardson and Vaughan (1989) used synthetic pentlandite to study the alteration of surfaces due to oxidation. The oxidants used were air, steam, ammonium hydroxide, hydrogen peroxide, and sulphuric acid. Electrochemical oxidation was also investigated. After oxidation the pentlandite surfaces were enriched in nickel in the subsurface. The subsurface is believed to restructure to violarite. The oxidised surfaces consisted of a range of iron oxides and hydroxides (Fe_3O_4, Fe_2O_3, FeOOH, $Fe(OH)_3$), nickel oxide (NiO) and iron sulphates ($FeSO_4$, $Fe_2(SO_4)_3$) of which the layer was approximately 10 Å in depth. The proportions of the phases present in the surface layer were dependent on the strength of the oxidant employed and the thermodynamic stability of the phases.

In 1991, Buckley and Woods used XPS and electrochemical techniques to investigate the surface oxidation of pentlandite. They found that on exposure to air, iron was removed from the pentlandite lattice to form a hydrated iron oxide overlayer, which left metal deficient pentlandite in addition to a restructured nickel-iron sulphide. Further oxidation resulted in some nickel being included in the oxide overlayer. The study in acetic acid (pH 2.9) showed that the oxide layer was largely soluble. Oxidation in basic media (pH 9.2) indicated that virtually all the iron and most of the nickel within the outermost few nanometres were bonded to oxygen. The voltammetric studies carried out at pH 4.6, 9.2 and 13 showed that the major process in the oxidation of pentlandite is the selective removal of iron. At pH 4.6 the sulphur product of oxidation process was mainly sulphur. At pH 9.2 and 13, the sulphur was again the major oxidation product but some sulphate was also formed, with a fraction of the mineral being oxidised to sulphate

(increasing with increasing potential). They pointed out that the oxidation products of pentlandite are similar to those of pyrrhotite.

Kelebek (1993) investigated the effect of oxidation on flotation behaviour of pyrrhotite and pentlandite using a nickel-copper ore sample of the Sudbury basin. In general, moderate oxidation promotes the floatability. Under oxidation deficient conditions the formation of hydrophobic surface species on pyrrhotite were restricted or at least retarded. Pyrrhotite requires higher redox potentials for reactions leading to its hydrophobisation. Pentlandite recoveries were practically the same in nitrogen and in air. Flotation selectivity increased in time towards higher pentlandite recovery. This indicates that pyrrhotite particles undergo a selective oxidation that renders the mineral more hydrophilic. They pointed out that an oxidation period of nearly six hours accounted for about 70% decrease in pyrrhotite recovery. The ferrous hydroxide that initially formed was subsequently converted to more stable ferric hydroxide and/or oxy-hydroxide thus contributing to the hydrophillic nature of pyrrhotite.

Smart (1994) pointed out that sulphide mineral surfaces undergo significant changes in the surface layers due to structural and chemical rearrangements after immersion in solutions. The iron-containing sulphide minerals are known to react in solution by the loss of iron ions from the sulphide lattice to form hydroxide overlayers. The removal of these hydroxide products from the surface during acid attack revealed a sulphur rich layer in which restructuring of $Fe_{1-x}S$ to a tetragonal Fe_2S_3 intermediate based on a defective pyrite lattice, is found. In this structure, the linear chains of Sn polysulphides have a S-S distance closely similar to that of elemental sulphur apparently conferring hydrophobicity on these surface layers.

Recently, near-pristine surfaces of natural pentlandite samples were studied by Legrand et al. (1997) using X-ray photoelectron spectroscopy. They found two major doublets in the S 2p spectrum, one with a S $2p_{3/2}$ binding energy of 161.44 eV and the other at 162.19 eV. These doublets were interpreted as being due to sulphur in a 4-coordinate and 5-coordinate environment, respectively. After exposure to de-ionised water for 1.5

hours, the results revealed that pentlandite surfaces were oxidised to give surfaces that were rich in iron oxyhydroxide species and depleted in nickel and sulphur.

In summary, surface oxidation is one of the most important factors that influence the flotation selectivity and recovery in the processing of complex sulphide ores. The degree of oxidation determines whether the surface film formed on a sulphide mineral will enhance hydrophobicity or hydrophilicity. The oxidation reaction suggested for pyrrhotite and pentlandite is

$$MS + xH_2O + 1/2xO_2 \rightarrow M_{1-x}S + xM(OH)_2 \qquad (9)$$

Where MS represents a metal sulphide.

Oxidation arises from the dissolution of minerals and grinding media. Dissolved metal ions hydrolyse and sulphide ions oxidise. These ions can re-adsorb on the mineral surfaces or react with each other or the dissolved gas molecules before precipitation (Clarke et al. 1995). It is well established that the surface products of excessive oxidation have a profound effect on surface hydrophobicity. Mild oxidation however, appears to be necessary for the flotation of sulphide minerals and is often a requirement for self-induced flotation. On the other hand, excessive oxidation inhibits flotation. The rate of oxidation of sulphide minerals depends on the surface area available for reaction, the partial pressure of oxygen, the type and composition of the sulphide mineral, solution pH and temperature (Ralston, 1991).

2.1.2.4 Heavy Metal Activation

The presence of metal ions in solution can have a major influence on the flotation and separation of sulphide minerals. Metal ion contamination of surfaces is frequently suspected of playing a detrimental role in selective flotation.

Forssberg and Jonsson (1981) carried out experiments that have shown that relatively large amounts of heavy metal ions can adsorb on both synthetic and natural pyrrhotite in an acidic pH. The possible cause is the presence of iron vacancies in the crystal lattice, as indicated by the chemical formula of pyrrhotite, $Fe_{1-x}S$. The vacancies can be filled by metal ions of suitable size. Pyrrhotite releases fairly large quantities of Fe^{2+} and Fe^{3+} ions under oxidising conditions. This can adversely affect the adsorption of heavy metals. Synthetic samples showed a higher specific adsorption, probably due to pores, which give them a higher adsorption rate.

Yoon et al. (1995) also showed that pyrrhotite can be activated by heavy metal ions present in the plant water. The pyrrhotite activation by Cu^{2+}, Ni^{2+}, and Ag^{+} ions was confirmed by XPS and LIMS analyses of the mineral specimens immersed in simulated plant water of pH 9.5 for 15 minutes. These ions can form more insoluble sulphides than Fe^{2+} ions therefore pyrrhotite can be activated by these heavy metal ions. When pyrrhotite is activated thiol collectors can adsorb on the surface at lower collector concentrations and lower potentials.

The influence of sulphur containing ions (several hundred mg/l) in recycled water on selective flotation of chalcopyrite, cubanite, pyrrhotite and pentlandite was investigated by Barskii et al. (1986). A study of the effect of pH on the potential of a mineral electrode showed that in the pH range 7-12, the pentlandite electrode was positive, while the pyrrhotite electrode potentials were negative. If the aqueous phase was saturated with thiosulphate ions, the oxidation of pentlandite and pyrrhotite was increased. If the aqueous phase was saturated with sulphate ions, the potential rapidly increased. The value of the surface charge on the sulphides was determined by the sulphate and thiosulphate ion concentrations in the pulp, and a change in their ratio caused a shift in the potential. The sorption of aerofloat on pentlandite increased significantly with increase in the sulphate ion concentration in the pulp. On pyrrhotite the sorption curve showed a discontinuity at $SO_4^{2-} = 0.4X10^{-2}M$, above which the sorption increased. The sorption of aerofloat was reduced with an increase in the thiosulphate ion concentration. Under highly reducing conditions, the collector was adsorbed

physically on the surface of pentlandite and pyrrhotite. They concluded that there is a close correlation between the selectivity of flotation complex copper-nickel sulphide ores and the sulfoxide ion concentration in pulp.

Hodgson and Agar (1989) carried out electrochemical studies to determine a possible effect of Ca^{2+}, $S_2O_3^{2-}$ and SO_4^{2-} ions on pentlandite and pyrrhotite floatability and xanthate interactions. It was found that these ions were significantly surface active at the normal process pH. It was concluded that these ions would influence the extent of X^- adsorption by the sulphide minerals as well as control the onset of hydrophobicity. $S_2O_3^{2-}$ and Ca^{2+} ions competed with xanthate for adsorption on the surface sites of pentlandite, whereas only Ca^{2+} increased the xanthate dosage required rendering pyrrhotite hydrophobic. The calcium ions adsorbed onto the surface sulphur sites, sulphate also being adsorbed onto the Fe sites. The $S_2O_3^{2-}$ ion was considered to be coordinated onto surface via the oxidised Fe sites or the Ca (S_2) product. Iron and polysulphides were considered to be surface-active forms, which form part of the pyrrhotite surface. Ca^{2+} cations can chemisorb onto the pentlandite surface, replacing metal ions at the pentlandite surface. The initial oxidation reaction for pentlandite is pH independent and to be of the following form

$$Fe_{4.5}Ni_{4.5}S_8 \rightarrow (Fe_{4.5-x}Ni_{4.5-x}S_8)+xFe^{2+}+xNi^{2+} + 4xe \qquad (10)$$

Presence of Ca ions modifies this reaction by replacing the metal cation at the surface.

A similar trend was observed by Agar et al. (1982) during the bench-scale testwork performed on the feed to the separation flotation circuit at INCO Metals' Copper Cliff Mill. They showed that lime addition caused desorption of xanthate from pentlandite, which raised the concentration of xanthate in solution.

Rao and Finch (1991), however, found that the presence of cationic species in water appeared to enhance the pyrrhotite xanthate-dixanthogen uptake at pH 8.4. This was noted especially with calcium ions, which do not oxidise, decompose and precipitate

xanthate, apparently due to the formation of $Ca(OH)^+$ species at the mineral surface thereby providing a greater number of positive surface sites. In the presence of Cu^{2+} ions xanthate uptake is much greater and there is dixanthogen formed in the solution even in the presence of nitrogen. This is explained by the oxidising action of Cu^{2+}. There is no dixanthogen on the mineral surface observed in the presence of nitrogen. It shows that dixanthogen is formed on the mineral surface by oxidation of adsorbed xanthate. Fe^{3+} ions can also oxidised xanthate to dixanthogen in solution, but the oxidation at the mineral surface occurs only in the presence of air.

Liu et al. (1993) carried out batch flotation tests on copper-zinc ore from Kidd Creek using recycle water, tap and distilled water. The results showed that recycle water containing up to 500ppm thiosalts and 300ppm calcium was not detrimental to flotation and appeared to enhance the depression of pyrite in copper rougher flotation.

Moreover, Kirjavainen et al. (2002) concluded that calcium and thiosulphate ions improved floatability of nickel and copper sulphides at the normal process pH (pH 9) after grinding in a steel mill. They pointed out that galvanic interaction between sulphides and mill iron is of major importance. When the galvanic effect of mill iron was effective, calcium activated nickel and copper sulphides and increased the adsorption of ethyl xanthate on the sulphides. Thiosulphate ions decreased the adsorption of xanthate, and it was concluded that thiosulphate reduced the effect of hydrophilic compounds on sulphide particles and thus improved their flotation.

Copper activation has been reviewed a number of times over the last thirty years by interalia Finkelstein and Allison (1976), Fuerstenau (1982) and Wang et al. (1989). More recently Finkelstein (1997) gave an in depth review of current theories on copper activation. The main emphasis of the review is the effect on sphalerite, with a few references to pyrrhotite. It appears that there has been no significant study of copper activation of pentlandite.

Wang et al (1989) carried out an investigation of the activation of natural pyrrhotite by Cu(II) in an acidic to neutral pH range. They deduced that the activation of pyrrhotite by Cu(II) ions involves a stochiometric replacement of iron in the lattice by Cu(II) from the solution. The reaction kinetics was characterised by two steps. The first very rapid step of the activation was controlled by the surface nucleation of copper sulphides. The second step was slower and controlled by the diffusion of Cu(II) into the lattice. The solubility of pyrrhotite was reduced significantly in the presence of Cu(II) ions, probably due to the formation of a copper sulphide layer on the pyrrhotite surface. Copper adsorption increased with an increase in the solution pH. Although oxygen reduced the adsorption of copper on pyrrhotite, the effect increased with a decrease of solution pH. The oxidation product of a pyrrhotite surface is thought to inhibit the surface conversion of copper hydroxide into copper sulphides.

Finkelstein and Allison (1976) suggested that in addition to ion exchange for copper activation, there is an oxidation - reduction reaction in which Cu(II) is reduced to Cu(I) and the sulphide of the mineral is oxidised. It has been demonstrated that activation of sulphide minerals at acid pH can result in collectorless flotation, which is not the case for alkaline conditions.

Most of the observations and conclusions made to date have been based on classical chemical methods of measuring adsorption. Recently more studies have been conducted using instrumental techniques (Auger, XPS, ToF-SIMS) to identify surface species before and after copper activation. One of the major concerns related to information from these techniques is that they are ex-situ techniques and the surface can be significantly altered depending on the methods used to prepare the sample prior to analysis. In particular hydrolysis and oxidation products that are reversibly adsorbed on the surface can easily be removed by washing procedures prior to analysis, and are alternatively easily deposited on the surface from the solution when the samples are dried prior to analysis.

The difference is sample preparation, which can lead to different results as is demonstrated by seemingly contradictory results from similar XPS studies. The studies have shown that after the activation of sphalerite at pH 9 Cu(II) is converted to Cu(I) with time. Opinions are divided over whether Cu(II) and Cu(I) are present under alkaline conditions. Kartio et al. (1996) did not detect Cu(II) on the surface (sphalerite pH 9.2), while Perry et al. (1984) noted that in some cases there was Cu(II) and Cu(I) on the surfaces. Prestidge et al. (1997) reported evidence for Cu(II) on the surface in excess of a monolayer. The Cu(II) species had been attributed to cupric oxide and copper hydroxides. The one difference in the two studies has been the method used for preparing the samples. Perry et al. (1984) and Kartio et al. (1996) rinsed the samples in de-ionised water, while Prestidge et al. (1997) rinsed the sample with an alkaline solution, transferred the sample as a slurry to the instrument and removed the water under vacuum. The first procedure may have removed the majority of the hydroxides. The second procedure while reducing dissolution could result in hydroxides being deposited from the solution onto the surface.

There is further controversy with regards to the form of the oxidised sulphide generally refered to as COS (complex oxidised sulphide) which is formed as a result of the oxidation – reduction reaction involved in copper activation. Is it a polysulphide or a metal deficient lattice? Finkelstein (1997) argues that the difference between the two forms is not merely about semantics, but rather about the difference between a localised increase in sulphur concentration (polysulphide) and a homogeneous distribution over an entire lattice. Finkelstein (1997) concludes that depending on the conditions either or both can be formed.

Ralston et al. (1981) found that as the pH of the solution increased, the amount of elemental sulphur on the surface of sphalerite decreased with no elemental sulphur being detected above pH 7.5. Under normal flotation conditions employed, which are alkaline, elemental sulphur species are not expected, and the oxidation of the sulphide surface would result in the formation of sulphoxy compounds.

Perry et al. (1984), using Auger spectroscopy, found for copper activation of sphalerite that patches of copper rich islands are formed only after a few monolayers of evenly distributed copper has been adsorbed. Prestidge et al. (1994) using XPS found that the copper is not evenly distributed for the same mineral.

Finkelstein (1997) discusses the kinetics and reaction mechanisms in depth. It is generally accepted that the reaction takes place in two stages, a rapid stage where a few monolayers are deposited on the surface and then a slower stage where the rate is controlled by diffusion into the sulphide lattice.

One of the findings highlighted by Finkelstein (1997) as being of importance for the application of metal activation to flotation is the extent to which the "lattice cations, the adsorbed cations and the induced acceptor states are mobile". Activation and oxidation of the surfaces results in a surface layer that is significantly different in chemical composition from the bulk. The surface is described as being metastable and alters significantly with time. The implication of this is that the surface, which defines floatability, may change significantly during the passage through the flotation circuit. The time between activation and collector adsorption could therefore be used to improve the selectivity of flotation. With time the copper adsorbed on, say, pyrrhotite may diffuse into the bulk, leaving a surface without copper.

An important component in understanding copper activation is a thorough knowledge of the ionic species in the water used. The temperature, pH, E_h and ions present in the aqueous environment will dictate the chemistry of activation.

Wang et al. (1989) reviewed the aqueous and surface chemistry in the flotation of sulphide minerals. It is well known that heavy metal ions undergo a series of pH-controlled hydrolysis reactions in a binary metal cation-water system. For example in the case of Cu(II), the following reactions occur spontaneously:

$$Cu^{2+} + OH \leftrightarrow Cu(OH)^{+} \quad \text{(initial hydrolysis)} \quad (11)$$

$$2Cu^{2+} + 2OH \leftrightarrow Cu_2(OH)_2^{2+} \quad \text{(dimer formation)} \quad (12)$$

$$Cu^{2+} + 2OH \leftrightarrow Cu(OH)_2(aq) \quad (13)$$

$$Cu^{2+} + 2OH \leftrightarrow Cu(OH)_2(s) \quad \text{(precipitation)} \quad (14)$$

$$Cu^{2+} + 3OH \leftrightarrow Cu(OH)_3^{-} \quad (15)$$

$$Cu^{2+} + 4OH \leftrightarrow Cu(OH)_4^{2-} \quad (16)$$

The distribution of these species at varying pH values can be calculated from their equilibrium constants. Numerous log concentration versus pH diagrams are available in the literature (Figure 2.2). The only concern is that most of this data is produced at 25°C rather than the higher temperatures often typical of flotation circuits.

Note that free metal ions dominate only at very acidic pH values. At highly alkaline pH, they will precipitate as metal hydroxides. In medium pH range, the systems are highly complicated by the formation of soluble hydroxyls and even dimers and polynucleas. Thus, different interactions between the mineral surface and metal ions should be expected, depending on the solution pH and total metal ion concentration.

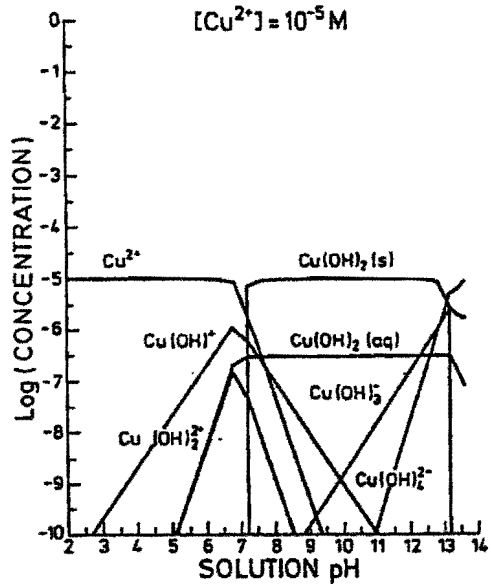

Figure 2.2: Log(Conc.)-pH Diagram for metal-water system of Cu(II) activator at a total metal concentration of $1x10^{-5}$M

From Figure 2.2 it is evident that at the pH typical of Merensky ore flotation circuits, namely pH 9, the Cu species present in decreasing order are $Cu(OH)_2$ (s) >>$Cu(OH)_2$ (aq) > $Cu(OH)_3^-$> $Cu(OH)^+$> $Cu(OH)_4^{2-}$> $Cu_2(OH)_2^{2+}$. The addition of copper sulphate at pH 9 is therefore expected to produce a copper hydroxide precipitate.

Wang et al. (1989) have studied the stability of the ternary Fe(III)-OH-EX complexes and have shown that the intermediate pH depression of pyrite in its flotation with xanthate is very strongly correlated with the presence of ternary compounds. They have also shown that these ternary compounds are not strongly hydrophobic, however, if excess collector is present, they will be associated on the mineral surfaces and make the mineral particle sufficiently hydrophobic for flotation. The stability of Cu(OH)EX(s) would be expected to lie between that of $Cu(EX)_2$(s) and that of $Cu(OH)_2$(s). The equilibrium potential (pE) vs. pH diagram of the Cu-EX-H_2O system at a total concentration of $1x10^{-4}$ M copper and ethyl xanthate is shown in Figure 2.3.

Low pE values represent a reducing environment while high pE values an oxidising environment. The pE scale is intended to represent the concentration of the standard

reducing agent (the e^-) analogously to the pH scale representing the concentration of standard acid (H^+). The pE values are obtained from reduction potentials by dividing E° by 0.059.

The stability constants were taken from Kakovskii (1957) and Kakovskii and Arashkevich (1968) and that of Cu(OH)EX(s) was estimated. From Figure 2.3 it can be seen that there is a large area of stability for Cu(OH)EX(s), thus if the redox potential of the system falls into this area flotation will be inhibited.

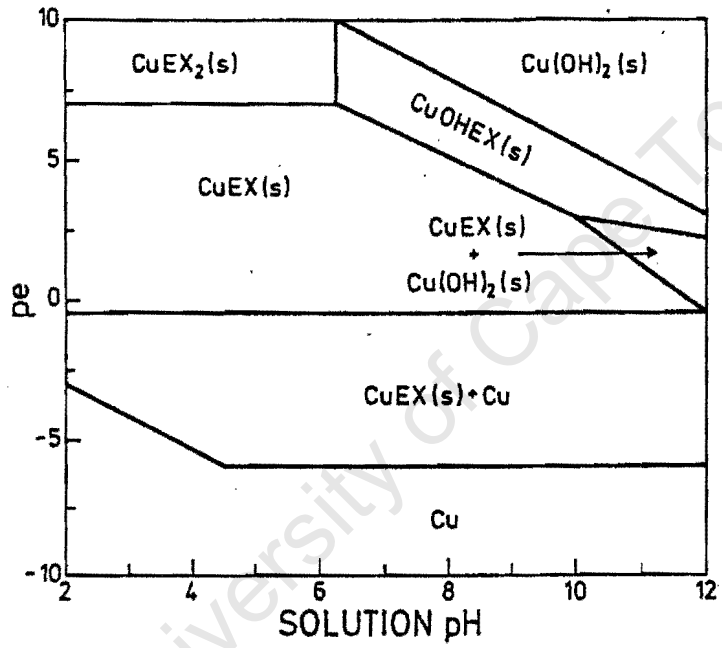

Figure 2.3: pE-pH Diagram for Cu-Ex system at a total concentration of Cu = $1x10^{-4}$M and EX = $1x10^{-4}$M, showing possible stability area of the compound Cu(OH)EX.

Notwithstanding the literature review above, many questions remain regarding the issue of copper activation. In particular, little attention has been paid to pentlandite in terms of copper activation as well as the application of this knowledge to improve selectivity in flotation of Merensky Reef ore.

2.2 Pyroxene

2.2.1 Mineralogy

The pyroxene minerals belong to the silicate mineral class and approximately 30% of all minerals are silicates. With a few exceptions all the igneous rock-forming minerals are silicates, and they thus constitute well over 90% of the Earth's crust. The basic chemical unit of silicates is the SiO_4 tetrahedron shaped anionic group with a negative four charge. The central silicon ion has a charge of positive four while each oxygen has a charge of negative two and thus each silicon-oxygen bond is equal to one half the total bond energy of oxygen. This condition leaves the oxygen with the option of bonding to another silicon ion and therefore linking one SiO_4 tetrahedron to another and another, etc. The silicate tetrahedrons can form as single units, double units, chains, sheets, rings and framework structures. A pyroxene structure is shown in Figure 2.4.

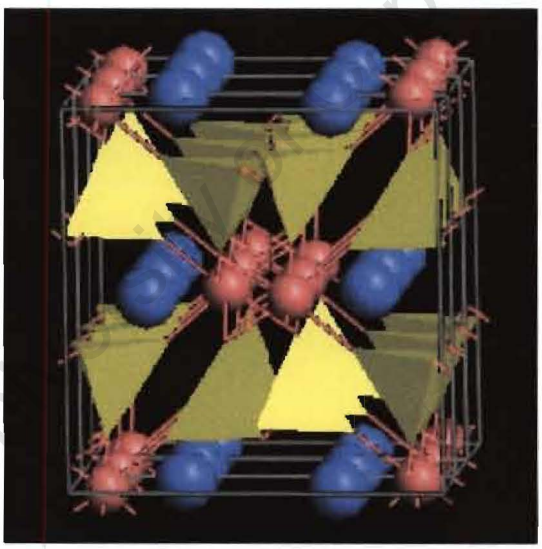

Figure 2.4: Pyroxene structure, viewed obliquely along z.
Yellow: SiO_4 tetrahedra; Blue: Larger *X* Cation Sites
Red: Smaller *Y* Cation Sites.

The pyroxene minerals are inosilicates of the general formula $XY(Si, Al)_2O_6$. The *X*, represents ions such as Ca^{2+}, Na^{+}, Fe^{2+} and Mg^{2+} and more rarely zinc, manganese and lithium. The *Y*, represents ions of generally smaller sized such as Cr^{3+}, Al^{3+}, Fe^{3+},

Mg^{2+}, Mn^{2+}, scandium, titanium, vanadium and even Fe^{2+}. Aluminium, while commonly substituting for silicon in other silicates, does not often substitute for silicon in a pyroxene. The typical pyroxene structure contains chains of SiO_3 tetrahedrons that every other one alternates from the left side to the right side of the chain. Each of the tetrahedrons has one flat edge that lies on the "base" of the structure as if the entire chain were a chain of connected three sided pyramids on a flat desert. The orderliness of the tetrahedrons means that they repeat every three tetrahedrons, ie. left-right-left. The chain structure explains the general prismatic to fibrous character of the members of this group. The slope of the tetrahedral pyramids helps to determine the cleavage angle of the pyroxenes at nearly 90° degrees (actually 93° and 87°). The pyroxenes are closely related to a group of inosilicates called the pyroxenoids. The pyroxenes are an important group among the single chained inosilicates. They are common rock forming minerals and are represented in most igneous and many metamorphic rocks (Klein, C. and Hurlbut, Jr., C.S., 1985).

2.2.2 Surface and Flotation Studies

Deju and Bhappu (1965) studied surface properties of silicate minerals in terms of correlating the oxygen-silicon ratio for various silicate minerals to the adsorption of hydrogen ions. Upon the fracturing of a silicate mineral crystal, the oxygen-metal bond, which is almost entirely ionic in character, should break more easily than the oxygen-silicon bond, resulting in a negative charge on the surface. They concluded that the reaction between the silicate mineral particles and the acidified water involves mainly an exchange of metal ions for hydrogen ions on the surface of the solid, leading to an increase in pH of the aqueous phase. The degree of reaction depends directly on the oxygen-silicon ratio of the silicate structure and on the total surface area of the solid; i.e. on the number of exchange sites available. The reaction also seems to be greatly influenced by the amount of iron present on the solid; more iron increases the degree of reaction.

In 1966, Deju and Bhappu reported that the point of zero charge of silicate minerals increases as the oxygen-silicon ratio increases. Also, since specific gravity is approximately directly proportional to the oxygen silicon ratio, it follows that the point of zero charge is directly proportional to the specific gravity for very pure silicate minerals. This relationship, however, will not be valid for impure minerals. If the silicate sample is leached and purified, a large number of the M^+ ions may leave the surface and an equivalent amount of H^+ ions will replace them. The number of M^+ ions present on the surface will then be substantially less than for the unleached sample and the amount of OH^- ion formed as an end product will also be much less. For this reason, the point of zero charge of the leached and purified sample may be less than that of the impure sample.

From other published studies worth mentioning is the investigation by Mackenzie and O'Brien (1969). They used zeta potential determinations to investigate the adsorption of nickel and cobalt ions from aqueous solution onto the quartz surface. They concluded that Ni^{2+} and Co^{2+} are only weakly adsorbed onto the quartz surface and that $NiOH^+$ and $CoOH^+$ were the main Ni(II) and Co(II) ionic species adsorbed. They suggested that the adsorption of these ions might involve a combination of coulombic forces between the negative $Si\text{-}O^-$ sites at the quartz surface and the positive $NiOH^+$ and $CoOH^+$ ions as well as hydrogen bonding between the OH groups of the hydroxide complex and the Si-OH and $Si\text{-}O^-$ groups at the quartz surface; i.e. the latter being the dominant mechanism. They also pointed out that positively charged $Ni(OH)_2$ and $Co(OH)_2$ colloids could attribute to the positive zeta potential values at high pH values (less than 11).

Fuerstenau (1975) investigated the role of metal ion hydrolysis in oxide and silicate flotation systems. Electrophoretic data showed that a greater charge was left at the surface after hydroxy complex adsorption than was present prior to adsorption. Either of the two mechanisms could account for this phenomenon, namely, hydrogen bonding between the hydroxy complex and an oxide site, or water formation from the hydroxyl of the hydroxy complex and adsorbed hydrogen ions. In the case of water formation, he suggested that the hydrogen ion could adsorb onto oxide sites while hydroxyl ion could

adsorb onto silicon sites. Adsorption of hydroxy complexes, such as $CuOH^+$, could occur by splitting out water. In the presence of collector, this could lead to collector adsorption onto this site.

Fuerstenau et al. (1977) also studied the mechanism of pyroxene (augite, diopside) flotation with potassium oleate. Electrophoretic data indicated that the hydroxy complexes $FeOH^+$, $MgOH^+$, and $CaOH^+$ were responsible for the flotation of these pyroxenes.

More recently, Nagaraj and Brinen (1995) have shown how SIMS and XPS were used to study copper ion adsorption, and its effect on subsequent sulphide collector adsorption, on pyrite and pyroxene minerals under flotation related conditions at pH 9. The analysis of pyroxene and pyrite treated with iso-butyl ethoxycarbonyl thionocarbamate indicated no evidence of collector adsorption in the absence of copper activation. Copper was found to adsorb on both minerals, which caused sulphide collector adsorption. It was also found in this study that in the absence of collector, copper on pyroxene was in the Cu^{2+} form, whereas after collector treatment it was in the Cu^{1+} form suggesting the formation of a copper-collector complex. Unfortunately, they did not carry out flotation tests and thus link the surface coverage to floatability.

A year later, Nagaraj and Brinen (1996) reported on a similar study as described above. During this investigation, amyl xanthate in addition to iso-butyl ethoxycarbonyl thionocarbamate was used as a sulphide collector. SIMS and XPS techniques were employed to investigate the adsorption of sulphide collectors on pyroxene in the absence and presence of copper sulphate at pH 9. No collector adsorption could be detected on pyroxene. Once pyroxene was treated with Cu^{2+} ions, washed and then treated with collector, XPS measurements showed that Cu on pyroxene was reduced from cupric to cuprous upon collector adsorption. SIMS imaging suggests that collector adsorption occurs on copper sites on the surface. Once again, no flotation tests were carried out.

2.4 Complexing Agents (Chelates)

2.4.1 Chemistry

Metal chelate compounds may be defined simply as complexes in which donor atoms are attached to each other as well as to the metal (Chaberek and Martell, 1959). A chelate has two or more donor atoms, with adjacent donors linked together by a short chain of atoms. These links are often carbon atoms but they could also be other non-metals, as in the oxyacids. The bound ligand and the metal ion form a 'ring' of atoms referred to as the 'chelate ring'. The optimal size for a chelate ring depends on the type of functional group(s) containing the donor atoms, and on the size and binding preference of the metal ion. For the majority of metal ions a 5-membered chelate ring is favoured: *i.e.* metal ion plus two donor atoms plus two linking atoms. By sharing a common donor atom or a common atom in a chelate ring, ligands can have several donor atoms or donor functional groups linked together into a chain or cluster. The ligands formed are *poly*-dentate and will occupy 2 or more coordination sites on the metal ion. The linking together of two or more chelate rings introduces the possibility of ligands with rings of different size and/or different donor atoms.

An example is the polyamines: $NH_2(CH_2)_nNH(CH_2)_mNH_2$

where n = 2 or 3 and m = 2, 3 or 4.

All properties of metal ions in aqueous solution become altered when they are combined with chelating agents. The solubility product of the chelating agent determines whether the metal chelate will precipitate or remain in solution. If the metal chelate is quite stable, the reactivity's of the metal toward various reagents may be greatly altered or completely blocked. Even when weak, highly dissociated metal chelates are formed, some of the common properties of the metal ion, such as colour, oxidation potential and solubility may be altered considerably.

Metal ions have characteristic coordination numbers, which indicate the number of groups that normally become associated with the metal ion through the formation of coordination bonds. The crystal structures of the Cu(II) compounds have been thoroughly investigated and show that only four donor atoms surround each copper ion. The stable complex ammines of Cu(II) have all been found to contain four basic nitrogen atoms per metal ion. In the presence of an excess of ammonia or amine, there is evidence for a relatively weak association between the complex and additional basic nitrogen atom. Therefore it is possible to conclude that, while the characteristic coordination number is 4, the coordination number may be 5 or 6 under special conditions.

Formation of single metal chelates, MA, occurs when a chelating agent contains a sufficient number of electron donor groups that the subsequent coordination with the given metal ion results in a saturation of its coordinating positions, a single stable chelate is generally formed. A good example is EDTA. Metal chelates may also combine with hydroxyl ions to form hydroxo metal chelate compounds in which both the ligand and hydroxyl ion are coordinated with the metal ion. The tendency to form hydroxo species would depend on the affinity of the metal for the donor atom of the ligand as well as the hydroxyl ion concentration and consequently the hydrolysis of relatively stable metal chelates occurs only in alkaline solutions if at all. The interaction of a metal ion with a chelating agent results in the successive formation of more than one stable chelate species in aqueous solution. Bidentate and in many cases terdentate ligands form stable complex compounds containing one, two and even three moles of chelating agent per mole of metal ion. A good example is the reaction of Cu(II) ions and ethylenediamine (EDA) as reported by Jonassen and Dexter (1949)

Selectivity, applied to ligands, refers to a ligand's ability to preferentially bind to one metal ion, or a group of metal ions, in the presence of others. This is thermodynamically driven and is expressed by the relative stability constants for complex formation. Selectivity could also be based on the relative rate constants for complex formation (kinetic selectivity). Selectivity is a key factor in ore enrichment,

since the dissolution from minerals, grinding media and/or ions occurring in process water could alter the recovery and selectivity in the flotation process.

2.4.2 Applications of Complexing agents in the Mineral Processing Industry

Complexing agents have been recognised as potential reagents in mineral flotation for many decades. For example, complexing agents, in particular diethylenetriamine (DETA, NH_2-CH_2-CH_2-NH-CH_2-CH_2-NH_2), have been used in the selective flotation of pentlandite-pyrrhotite and copper-nickel ores. Investigations have mainly focused on the depressing mechanism of pyrrhotite by DETA. No investigations appear to have been reported on systems containing siliceous gangue minerals.

Marticorena et al. (1995) identified DETA as an effective pyrrhotite depressant, which has become a standard reagent in INCO's Sudbury area milling complex. DETA forms stable complexes with cuprous, nickelous and ferrous ions in mildly alkaline pH. DETA, as compared to EDTA, is a selective complexing agent and will readily complex with Cu^{2+} and Ni^{2+}, but not with Fe^{3+}, Ca^{2+} and Mg^{2+}. The complexing strength of DETA is sufficient to desorb copper and nickel species from pyrrhotite regardless of whether they are present as hydroxide or xanthate (Xu, et al., 1997).

Yoon et al. (1995) has also shown that DETA is a selective depressant for nickeliferous pyrrhotite during pentlandite flotation. The flotation of pyrrhotite was attributed to the inadvertent activation of the mineral by heavy metals ions, such as Ni^{2+}, Cu^{2+} and Ag^{+} that are present in process water. Pyrrhotite rejection was greatly improved by small additions of DETA, especially when the mineral was oxidised. It was also shown that both dixanthogen and iron xanthate are formed on the surface of pyrrhotite when contacted with amyl xanthate, the latter becoming more prominent at higher potentials. In the presence of DETA, only a small amount of xanthate is absorbed on the mineral at potentials ~200mV higher that the case without DETA. It should also be noted that DETA is most effective when the process water is saturated with Ca^{2+} ions, the mechanism and role of the Ca^{2+} ions is not as yet known.

Kelebek (1996) reported on testwork where collectorless flotation tests were carried out in the absence and presence of DETA. Copper and nickel ions are known to adsorb onto pyrrhotite surfaces and promote flotation of this mineral whether a collector is present or not. DETA involves the sequestration of copper and nickel ions from surfaces under a wide range of redox conditions. Analysis of filtrate samples taken during the tests confirmed the sequestering action. Once deactivated (copper and nickel ions removed) pyrrhotite acquires a surface state characterised by a greater hydrophilic/hydrophobic ratio due to the formation of iron hydroxide(s) and/or the lack of kinetic capability to form elemental sulphur. The results also indicated that pentlandite recoveries were unaffected by the presence of DETA yet nickel grades were much higher in the presence of DETA. Thermodynamic calculations for the Ni-Fe-S-DETA-water, Cu-FE-S-DETA-water and Fe-DETA-water systems indicate that the action of DETA involves the sequestration of metal ions under a wide range of redox potentials. Thus it appears that DETA may enhance the self-hydrophobicity of chalcopyrite and pentlandite by exposing more of the sulphur-rich surface sites for bubble contact in flotation.

Kelebek et al. (1996) also describes similar findings as highlighted above for the differential flotation of chalcopyite, pentlandite and pyroxene in Ni-Cu sulphide ores. DETA controls the metal ions, which are responsible for inadvertent activation of pyrrhotite.

One possible function of DETA, the complexation and removal of potential activating ions, e.g. copper and nickel known to be present on the surface of pyrrhotite under plant conditions, has also been explored by Zhenghe et al. (1997). DETA was found to remove copper and nickel ions from the surface and leave on it hydrophilic ferric species. The metal: DETA molar ratio was 1:2. Copper was more readily removed than nickel. Certain combinations of nickel ions, xanthate, dithionite (S_2O_4) or dithionate (S_2O_6) and DETA produced hydrophilic precipitates. DETA adsorption on pentlandite surface was negligible indicating that DETA complexes readily with nickel when it is in the hydroxide and xanthate form. It does not, however, compete with the surface lattice

Ni-S bond. Similar observations were reported by Rao et al. (1995) and Forward et al. (1960).

There are also reports of studies carried out on the effect DETA has on xanthate adsorption. Bozkurt et al. (1999) described the effect depressants have on xanthate adsorption on pentlandite and pyrrhotite. Xanthate interaction with pentlandite and pyrrhotite in the presence of DETA showed that dixanthogen was the main adsorption product on both minerals, higher on pentlandite compared to pyrrhotite. The presence of DETA reduced the dixanthogen adsorption on both minerals. Similar observations were concluded for the study of the formation and charaterisation of nickel-DETA complexes related to flotation systems (Vreughenhil et al., 1997). These authors studied the soluble species and precipitates generated by mixtures of nickel ions with DETA and xanthate, in the presence of CO_3^{2-} or SO_3^{2-}, by IR and UV-visible spectroscopy. They found that DETA could coordinate metal ions with either two or three of its nitrogen atoms. In the case of two-fold coordination, the unattached nitrogen atom can replace one of the coordinated nitrogen ions. This process causes a flexible arrangement of the ligands around the metal atom. The complex formed depends on the relative molar ratio of nickel to DETA and the presence of other ligands. DETA is capable of rapidly dissolving many solid nickel salts, which suggests that the formation of bis-DETA nickel or DETA-aquo nickel is an important mechanism by which nickel ions are removed from mineral systems. Ni-DETA in the presence of CO_3^{2-} or SO_3^{2-}, results in this case in a neutral complex, $[Ni(DETA)(L)]^{n+}$, where n depends on the charge of the ligand, L. The formation of this species indicates that the presence of other ligands could play a role in the action of DETA depression of pyrrhotite. The Ni-DETA-ethylxanthate precipitation formation indicates that xanthate is not coordinated to the nickel ion but is acting as a counter ion for the charged bis-DETA nickel complex. Ethylxanthate thus does not displace the DETA ligands to form the much less soluble xanthato-nickel complexes. The inhibition of xanthate nickel formation could also be an effective means by which DETA acts as a depressant. When half the amount of ethylxanthate is added then ethylxanthate coordinates to nickel and the results suggest that when nickel is coordinated by only one DETA ligand, it is susceptible to attack by

xanthate to form a metal complex containing both xanthate and DETA. This species is much less soluble than the species formed when nickel is coordinated with two molecules of DETA. It could, however, allow the formation of a hydrophobic coating on mineral surfaces.

Figure 2.5 shows the chemical structure of DETA and corresponding 1:1 copper(II)-DETA complex (Chaberek and Martell, 1959).

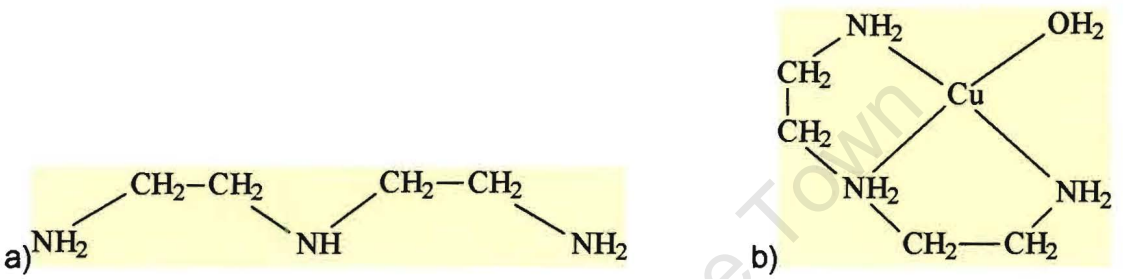

Figure 2.5: a) DETA structure and b) 1:1 Cu(II)-DETA structure

Ethylenediamine (EDA, NH_2-CH_2-CH_2-NH_2) has been tested as a potential ligand for complexing copper and nickel ions, Hubbard et al. (1996). EDA and DETA are ligands that complex Ni^{2+} ions between the pH of 6-7. Ligands that complex Cu^{2+} are EDA between the pH of 4-6 and DETA at a pH of <4. There does not seem to have been any testing of EDA using flotation conditions.

Figure 2.6 indicates the chemical structure of EDA and 1:1 copper(II)-EDA complex (Chaberek and Martell, 1959).

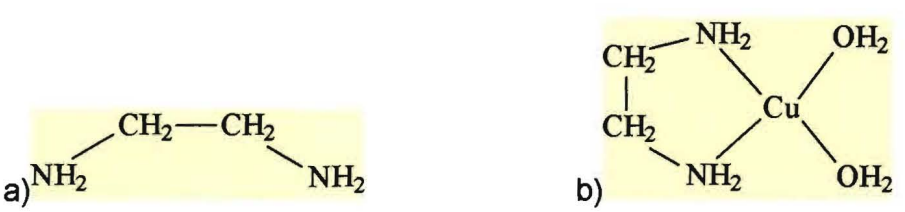

Figure 2.6: a) EDA structure and b) 1:1 Cu(II)-EDA structure

Triethylenetetramine (TETA, NH_2-CH_2-CH_2-NH-CH_2-CH_2-NH-CH_2-CH_2-NH_2) is a more powerful chelating agent (and less volatile) compared to DETA for the control of metal ions that cause inadvertent activation and catalytic oxidation in flotation, Kelebek et al (1999). TETA like DETA is capable of forming stable complexes (chelates) with a great number of metal ions. The study evaluated the effect TETA has on the depression of hexagonal pyrrhotite using a massive copper-nickel sulphide ore. The flotation rate for pentlandite and pyrrhotite were reduced with TETA alone. The pentlandite-pyrrhotite flotation selectivity obtained with TETA and sodium metabisulphite was similar to base line conditions, however excellent separation of the two minerals resulted in a higher concentrate grade.

Figure 2.7 below, displays the chemical structure of TETA and 1:1 copper(II)-TETA complex (Chaberek and Martell, 1959).

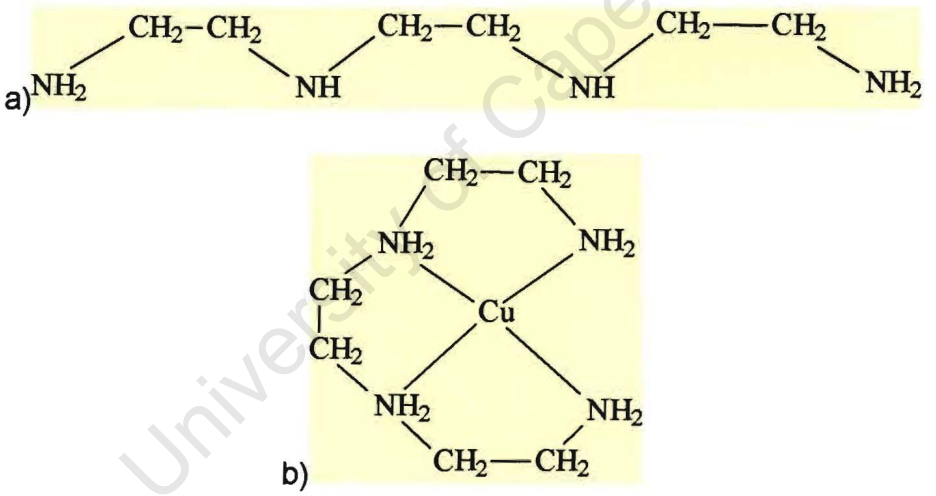

Figure 2.7: a) TETA structure and b) 1:1 Cu(II)-TETA structure

Ethylenediaminetetraacetic acid (EDTA, $(HOOCCH_2)_2NCH_2CH_2N(CH_2COOH)_2$) has mainly been used to dissolve oxidation products from sulphide minerals, but only weakly attached metal species such as hydroxides can be dissolved, Clarke et al. (1995). The dissolution of iron hydroxides in EDTA has been investigated extensively and EDTA has also been shown to improve flotation response. EDTA may also be used to selectively leach, not only metal oxides and hydroxides but also carbonates and sulphates, away

from sulphide minerals. More recently EDTA has been used in a semi quantitative study, Kant et al. (1994).

Figure 2.8 displays the chemical structural formulas for EDTA and corresponding 1:1 chelates with Cu^{2+} ions (Chaberek and Martell, 1959).

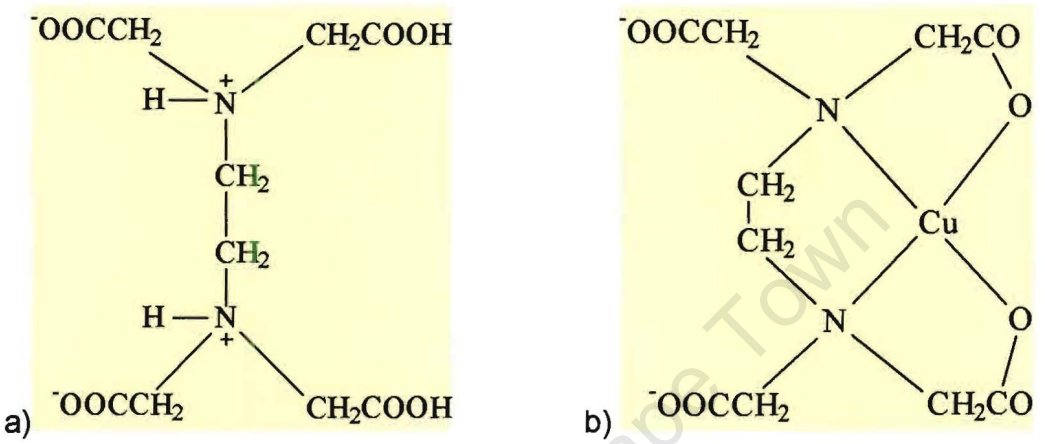

Figure 2.8: a) EDTA structure and b) 1:1 Cu(II)-EDTA structure

2.5 Comments Regarding the Literature Review

The mechanisms involved in pentlandite surface alteration due to oxidation in air and solution at various pH values have been studied extensively by many researches over the years. A range of iron oxides and hydroxides (Fe_3O_4, Fe_2O_3, FeOOH, $Fe(OH)_3$), nickel oxide (NiO) and iron sulphates ($FeSO_4$, $Fe_2(SO_4)_3$) were observed to form in the immediate oxidised surface. It was also found that the oxide and hydroxide layers were largely soluble in acid environment. Pentlandite hydrophobicity in the absence and presence of collectors in aqueous phase has also been studied at length. It has been shown that xanthate chemisorbs directly onto the pentlandite nickel sites and, subsequently, dixanthogen forms from the chemisorbed xanthate.

However, there is not much information available in the literature about pyroxene in terms of inadvertent activation and subsequent flotation due to the adsorption of xanthate ions onto inadvertently activated silicate mineral surfaces. The mechanisms contributing to true flotation of pyroxene are of primary interest at operating circuits treating Merensky Reef ore. The use of complexing agents as well as the mechanisms involved has been described in the literature, however, to the author's knowledge the application to deactivate siliceous gangue minerals has not been studied.

CHAPTER 3

EXPERIMENTAL METHODS

3.1 Minerals

Natural pyroxene from the Merensky Reef in the Northern Province, South Africa, was crushed to 2mm and selected by hand-picking. Chemical analysis indicated that pyroxene consisted of 13.2% Mg, 11.0% Fe, 3.7% Ca, 2.7% Al, 25.1% Si. Pentlandite was synthesised at Anglo Platinum Research Centre using a method developed by Johnson Matthey, Sonning. After hydrogen desorption, reduced iron (11.0g) and reduced nickel (11.86g) were mixed with sulphur flake (11.41g) and transferred to a quartz ampoule. The evacuated, sealed ampoule was heated in a furnace to 1150°C then cooled to ambient temperature.

The pentlandite produced is not always homogeneous even though the methods for the preparation and thermal treatment of the material are followed meticulously. The final product is sent for mineralogical analysis to verify the homogeneity of the sample. Unfortunately there are always impurities present and those samples with the least amount are used for testwork. An example of an inhomogeneous and homogeneous pentlandite sample is shown in Figures 3.1 and 3.2 respectively. A sample of around 35 grams of pentlandite is produced in each batch, which allows approximately 21 microflotation tests, so testwork is planned in such a manner that one batch is used per set of experiments. Standard flotation tests are performed on each batch so that a comparison can be drawn between batches of material.

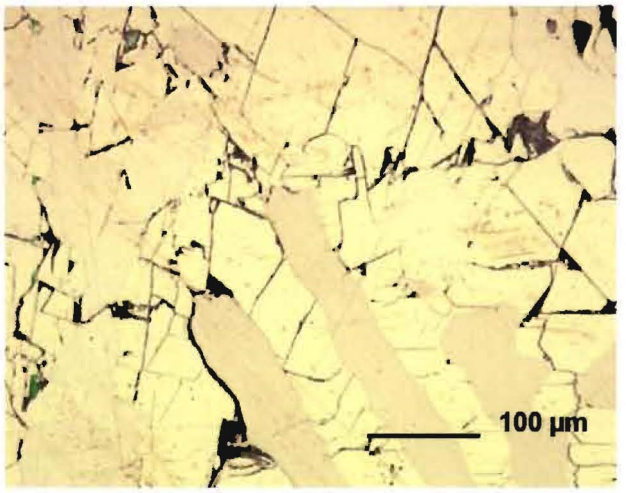

Figure 3.1: Pentlandite – Inhomogeneous sample. The pinkish-brown areas are nickeliferous pyrrhotite/troilite and cream areas are pentlandite.

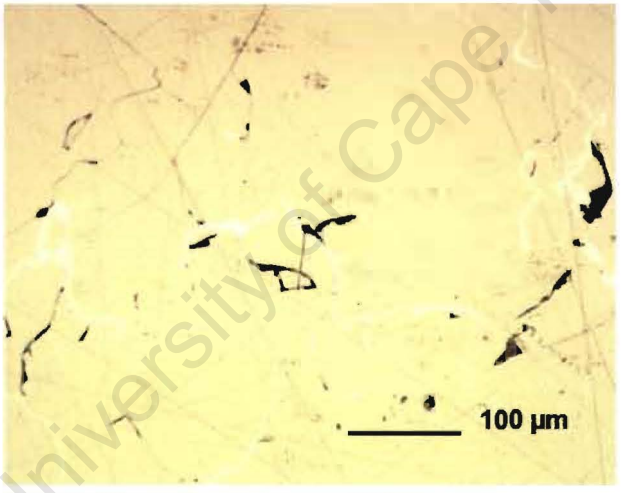

Figure 3.2: Pentlandite – Homogeneous sample. The brighter phase is iron-nickel alloy, and the darker phase is iron-rich pentlandite.

All mineral samples were stored under argon in a freezer and freshly ground in an agate mortar under argon in a glove box just prior to each experiment. The products were screened to obtain size fractions of –25µm for zeta potential determinations and +38 – 106µm for microflotation tests. Using the BET method, the surface area of the +38 – 106µm size fraction of pyroxene and pentlandite was found to be approximately 0.59m^2/g and 0.30m^2/g, respectively.

3.2 Reagents

During the study, water with a specific conductance of 0.7µS cm^{-1} with a surface tension of 72.8 mN m^{-1} at 20°C, produced by a MILLI-RO PLUS apparatus, was used to prepare synthetic water (*I* = 2.0E-02). All experiments were carried out in aerated solutions. High purity argon (Afrox) was used during storage to minimise pentlandite oxidation.

Purified collector, sodium isobutyl xanthate, was obtained from SENMIN and a commercial grade of depressant IMP 4 and frother DOW 200 from Trohall and Cytec, respectively. Other chemicals were of analytical grade quality. Copper sulphate (Saarchem) was used as activator. Diethylenetriamine, ethylenediamine and triethylenetetramine (Riedel-de Haen) and ethylenediaminetetraacetic acid (Sigma Aldrich) were utilised as complexing agents. Sodium carbonate (Saarchem) and hydrochloric acid (Riedel-de Haen) were used for pH adjustment.

3.3 Synthetic Water Composition

Water with a specific conductance of 0.7µS cm^{-1} was modified by the addition of various chemical compounds of analytical grade quality (Table 3.1) to produce synthetic process water (*I* = 2.0E-02). The synthetic water contained amounts of key ions similar to those typically found in circuit water (Ca^{2+} 80ppm, Mg^{2+} 80ppm, Na^{+}135ppm, Cl^{-} 270ppm, SO_4^{2-} 250ppm, NO_3^{-} 135ppm, NO_2^{-} 40ppm, CO_3^{2-} 40ppm, TDS 1030).

Chemical Compound	Formula	Mass(g) in 1 litre	Mol/dm^3
Calcium chloride (BDH Chemicals)	$CaCl_2.2H_2O$	0.147	0.001
Calcium nitrate (BDH Chemicals)	$Ca(NO_3)_2.4H_2O$	0.236	0.001
Magnesiun sulphate (Saarchem)	$MgSO_4.7H_2O$	0.615	0.0025
Magnesium nitrate (BDH Chemicals)	$Mg(NO_3)_2.6H_2O$	0.107	0.0004
Sodium chloride (Saarchem)	NaCl	0.356	0.0061
Sodium carbonate (Saarchem)	Na_2CO_3	0.058	0.0005

Table 3.1: Synthetic water composition, I = 2.0E-02.

3.4 Microflotation Tests

Mineral recovery by flotation can be used as an indicator of hydrophobicity in a given chemical and electrochemical system. Small-scale flotation experiments have been found to be a useful tool to investigate flotation behaviour of the various constituents of the ore. A study of the effect of reagent adsorption on a specific mineral can be carried out, since the influence of froth phase and cell dynamics in the pulp phase are not present.

3.4.1 Microflotation Cell Description

The cell consists of a conical tapered cylindrical tube with air introduced through a needle at the base of the cell. Mineral loaded bubbles rise through the cell and are deflected off the cone at the top of the cell, after which they burst, resulting in the minerals dropping into the concentrate launder. After a set time the needle is removed and the particles in the launder are collected as a concentrate. During the study, flotation was carried out by introducing air at a flowrate of 5 cm^3/min. The mean bubble size diameter was 0.957mm (Bradshaw and O'Connor, 1996). The peristaltic pump speed was kept constant and set to maintain a good particle suspension. The microflotation apparatus used during the study is shown in Figure 3.3.

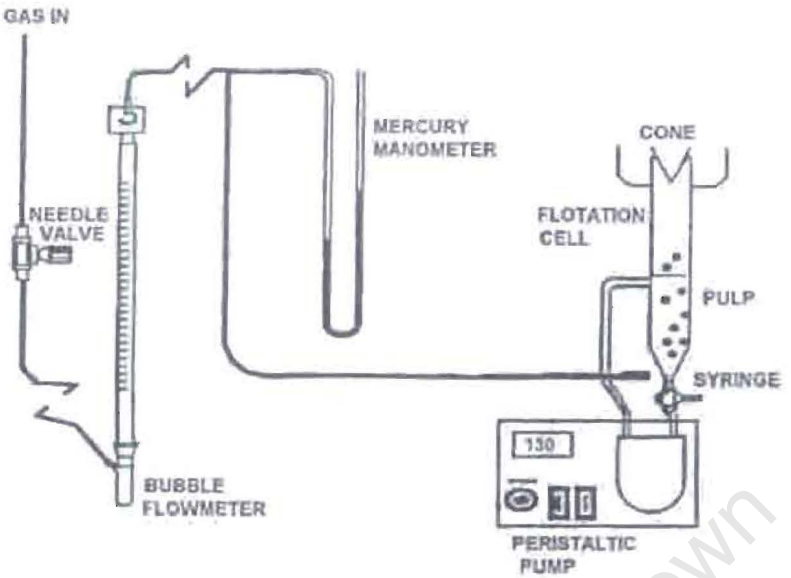

Figure 3.3: Microflotation apparatus (Wesseldijk et al., 1999)

3.4.2 Experimental Testwork

Microflotation tests were conducted in synthetic water. A 2g sample (1g of each mineral for mineral mixtures) was added to 250ml of the required solution, which had been adjusted to the desired pH. The desired pH was maintained throughout flotation by adjusting with either sodium carbonate or hydrochloric acid. Concentrates were collected at time intervals of 3, 10 and 20 minutes. The floated and non-floated fractions were allowed to dry in air and weighed. The microflotation products were analysed for sulphur using the Leco analyser, thus enabling the recovery of each individual mineral to be determined.

The reagents used during the study are listed in Table 3.2, which includes the reagent abbreviations.

Chemical Reagent	Abbreviation
Copper Sulphate	$CuSO_4$
Sodium isobutyl xanthate	SIBX
Diethylenetriamine	DETA
Ethylenediamine	EDA
Triethylenetetramine	TETA
Ethylenediaminetetraacetic acid	EDTA

Table 3.2: Chemical reagents and abbreviations used during the study.

During the tests, various combinations of reagents were investigated. These were SIBX, [$CuSO_4$ + SIBX], [$CuSO_4$ + DETA + SIBX], [$CuSO_4$ + EDA + SIBX], [$CuSO_4$ + TETA + SIBX], [$CuSO_4$ + EDTA + SIBX], [EDA +$CuSO_4$ + SIBX] and [$CuSO_4$ + SIBX + EDA]. The sequence of reagent addition was as indicated by the sequence of reference in brackets. Conditioning periods for the reagents tested were 2 minutes for SIBX and 5 minutes for $CuSO_4$ and the complexing agents.

3.5 Surface Techniques

3.5.1 Zeta Potential Determinations

Zeta potential determinations are used to study the electrokinetic phenomena at mineral-collector interfaces. This information can thus be used to assist in predicting flotation behaviour of a mineral in an aqueous system.

Electrokinetic measurements are of considerable interest for the study of electrical double layers. The double layer model is used to visualise the ionic environment in the vicinity of a charged particle. The double layer is formed in order to neutralise the charged particle and, in turn, causes an electrokinetic potential between the surface of the particle and any point in the mass of the suspending liquid. It is customary to interpret electrokinetic data in terms of ζ-potential. This is the potential of the slipping

plane between the moving and stationary phase, when the liquid far away from the interface is considered to be at zero potential.

When an electrical field is applied across an electrolyte, charged particles suspended in the electrolyte are attracted towards the electrode of opposite charge. Viscous forces acting on the particles tend to oppose this movement. When equilibrium is reached between these two opposing forces, the particles move with constant velocity and this phenomenon is called electrophoretic mobility. The velocity of a particle is related to the dielectric constant and viscosity of the suspending liquid and to the electrical potential at the boundary between the moving particle and the liquid (Malvern Instruments Training Manual, 1996).

Zeta potential is related to the electrophoretic mobility by the Henry equation:

$$U_E = \varepsilon \times \zeta \times \kappa_a / 6 \times \pi \times \eta \qquad (17)$$

where U_E is the mobility, ε the fluid dielectric constant, ζ the zeta potential, η the viscosity and κ_a is the ratio of particle radius to double layer thickness (1.0 for non-polar media, 1.5 for large particles in polar media). Electrophoretic determinations of zeta potentials are most commonly carried out in aqueous media and moderate electrolyte concentration. Since $\kappa_a << 1$, Von Smoluchowski equation can be used to calculate the zeta potential (Hunter, 1993):

$$\zeta = U_E \times 4 \times \pi \times \eta / \varepsilon \qquad (18)$$

At 25°C this reduces to:

$$\zeta = 12.85 \times U_E \text{ (mV)} \qquad (19)$$

3.5.1.1 Experimental Testwork

During the study described in this thesis, the zeta potential determinations were carried out on dilute dispersions of the individual minerals studied using a Malvern Zetasizer 4. The instrument gives the electrophoretic mobility from which the zeta potential was calculated using the Smoluchowski equation (18). The zeta potential determinations were carried out at pH 4, 6, 8 and 10 at 25°C. During the experiments, the effect of SIBX (5.00E-05M), $CuSO_4$ (5.00E-05M), DETA (6.98E-05M), EDA (4.00E-05M), TETA (4.93E-05M) and EDTA (4.93E-05M) on the mineral surface alteration was investigated. A mineral sample weighing 0.075g was dispersed in $60cm^3$ of synthetic water and the pH was adjusted to the desired value. Conditioning of the mineral for zeta potential determinations was carried out for 20 minutes. The pH was checked prior to taking the reading. The E_h was allowed to vary naturally.

3.5.2 Time of Flight Secondary Ion Mass Spectrometry (ToF-SIMS)

ToF-SIMS analysis is known to be a technique used to determine the occurrence of atomic/molecular species on the surface of mineral samples.

The basic concept of time of flight secondary ion mass spectroscopy is fairly simple. A pulsed primary ion beam bombards the sample surface, causing the emission of atomic and molecular secondary ions. The term "secondary ions" is used to distinguish them from the primary bombarding ions. A small percentage of the secondary ions are charged and can therefore be extracted by an electric field (accelerating field) into a mass spectrometer. The kinetic energy of the ions can be expressed as

$$E_{kin} = eV_o = \frac{1}{2}mv^2 \qquad (20)$$

where V_o is the accelerating potential, m the mass of the ion and e its charge. Lighter ions have higher velocities than the heavier ions and will therefore arrive at the detector

first. The mass separation is obtained by the flight time (t) from the sample to the detector. This can be determined using equation 21.

$$t = L_o/v = L_o\,(m/2eV_o)^{1/2} \qquad (21)$$

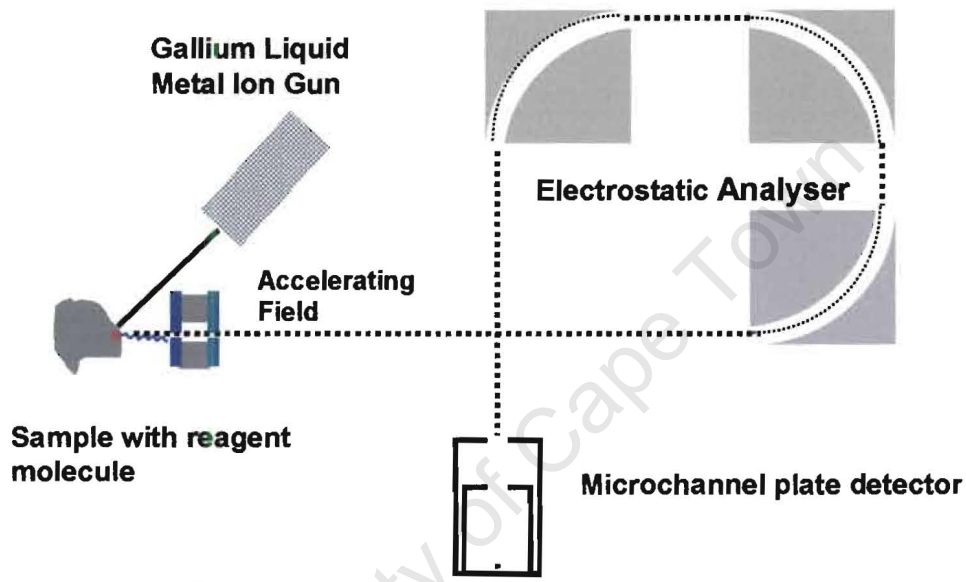

where L_o is the effective length of the spectrometer.

Figure 3.4: ToF-SIMS layout (de Vaux, 1997)

The mass spectra are recorded by measuring the time difference between pulsing the primary ion gun and the arrival of secondary ions on a fast dual microchannelplate detector at the spectrometer by means of a multistop time-to-digital converter (TDC) (Figure 3.4). Neighbouring masses m_o and $m_o+\Delta m$ can only be resolved if the relationship between time width and separation are correct. Using equation (21) it can be shown that for small mass differences the relationship between flight times and mass resolution is given by

$$m/\Delta m = t_o/2\Delta t \qquad (22)$$

From equation (22) it can be seen that in order to obtain high mass resolution, a short primary ion pulse (t_o) has to be used (Figure 3.5).

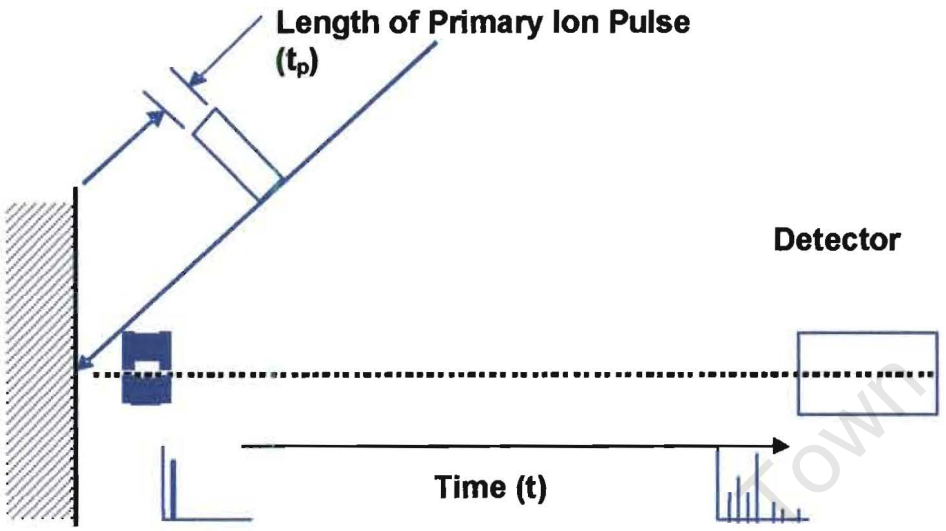

Figure 3.5: The separation of ions by Time of Flight (de Vaux, 1997)

The energy transferred when a primary ion impacts with the sample surface results in fragmentation of the original surface in the vicinity of the impact, resulting in the release of atomic species. Further away from the impact site, higher mass molecular species are released as a result of the energy transferred by the impact throughout the substrate. A heavy energetic primary ion cannot be stopped immediately by the first atoms it encounters and will therefore continue into the surface until it has lost all its energy due to elastic scattering off atomic cores and inelastic scattering off electronic shells and free electrons. The ions that are collided with will recoil and displace other atoms, which will in turn collide with other atoms, setting up a complex sequence of collisions. Some atoms will be permanently displaced from their positions while others will return elastically to their original lattice positions. The collision cascade will eventually result in the surface atoms being displaced (Schueler, 1992, Reich, 1997).

The PHI TRIFT II^{NT} instrument operates in the static SIMS regime. The term static refers to the number of primary ions impacting the surface per unit area. The static

SIMS regime is accepted to be about 10^{12}–10^{13} primary ions/cm^2. The density of a silicon surface is approximately 10^{15} atoms/cm^2. The PHI TRIFT II^{NT} ToF-SIMS features state of the art primary ion gun technology, including a focused liquid metal ion gun with three orders of magnitude range of beam current, from 20 nA (fast spectroscopy) to 20 pA (high lateral resolution, 0.1 μm analytical probe). The ToF-SIMS is capable of analysing small features of interest on both conducting and insulating samples due to automatic electron charge compensation (Reich, 1997).

3.5.2.1 Experimental Testwork

During the study, microflotation products as well as mineral mixtures, which were conditioned in synthetic water in the presence of the desired reagents for 20 minutes, were analysed using ToF-SIMS instrument operating in the static SIMS regime. The procedures for the preparation of the conditioned samples were identical to those used for the microflotation tests. The samples were filtered and washed with water (conductivity 0.7μmS cm^{-1}), adjusted to the desired pH, to remove any physically attached ions. All samples were dried in an argon atmosphere at ambient temperature. The 15 kV, 600pA gallium beam was used throughout the investigation. 30 grains or more of each mineral were imaged and analysed for Ca, Mg, Al, Si, Fe, Na, Cu and Ni during positive ion analysis and O, OH, S and xanthate during negative ion analysis. The data obtained were evaluated using Statistica. The intensities obtained are normalised for the elements of interest and presented as a relative percent surface coverage.

3.5.3 X-ray Photoelectron Spectroscopy (XPS)

Surface analysis by X-ray Photoelectron Spectroscopy (XPS) involves irradiating a solid *in vacuo* with monoenergetic soft x-rays and analysing the emitted electrons by energy. The spectrum is obtained as a plot of the number of detected electrons per energy interval versus their kinetic energy. Each element has a unique spectrum. The spectrum from a mixture of elements is approximately the sum of the peaks of the individual constituents. Because the mean free path of electrons in solids is very small,

the detected electrons originate from only the top few atomic layers. Quantitative analysis can be obtained from peak heights or peak area, and identification of chemical states often can be made from the exact measurement of peak positions and separations, as well as from certain spectral features (Moulder et al. 1995).

3.5.3.1 Experimental Testwork

Samples were prepared as described for ToF-SIMS analyses, the only exception being that different size fractions of pentlandite and pyroxene were used so that the minerals could be separated into single phases after treatment; this enabled better statistical data to be obtained during XPS analysis. Identification of the spectral regions of interest was performed using the NIST X-ray Photoelectron Spectroscopy Database, Version 3.0 (Web Version).

CHAPTER 4

RESULTS

This section incorporates only the results and observations obtained, any interpretation related to mechanisms and speciation will be discussed in detail in Chapter 5.

4.1 Microflotation Testwork

4.1.1 Reproducibility

The objective of the reproducibility tests was to evaluate the reliability of the procedure and apparatus used for the microflotation testwork. Any possible error includes the variability of the mineral samples and the operator's ability to be consistent.

In order to determine the reproducibility and standard deviation, the microflotation tests were carried out on a 1:1 mixture of pentlandite and pyroxene in the presence of copper sulphate followed by sodium isobutyl xanthate in synthetic water. Concentrates were collected at 3, 10 and 20 minute intervals and the results are displayed in Tables 4.1 and 4.2 for pentlandite and pyroxene, respectively. The results are also graphically represented in Figures 4.1 and 4.2 for pentlandite and pyroxene, respectively.

Time (mins)	*Pentlandite Recovery (%)*			*Mean*	*Std Dev*	*Relative Std Dev (%)*
	1	2	3			
3	37.39	32.05	35.62	34.98	2.70	7.72
10	84.39	75.36	77.48	79.07	4.73	5.90
20	96.76	89.02	94.70	93.49	4.00	4.28

Table 4.1: Pentlandite recovery (in mixture with pyroxene) for microflotation tests and standard deviations for concentrates collected at 3, 10 and 20 minute intervals in synthetic water, I = 2.0E-02.

Time (mins)	Pyroxene Recovery (%)			Mean	Std Dev	Relative Std Dev (%)
	1	2	3			
3	15.84	16.60	12.35	14.93	2.27	15.2
10	53.14	55.69	48.98	52.60	3.39	6.44
20	75.30	72.62	71.18	73.04	2.09	2.86

Table 4.2: Pyroxene recovery (in mixture with pentlandite) for microflotation tests and standard deviations for concentrates collected at 3, 10 and 20 minute intervals in synthetic water, *I*= 2.0E-02.

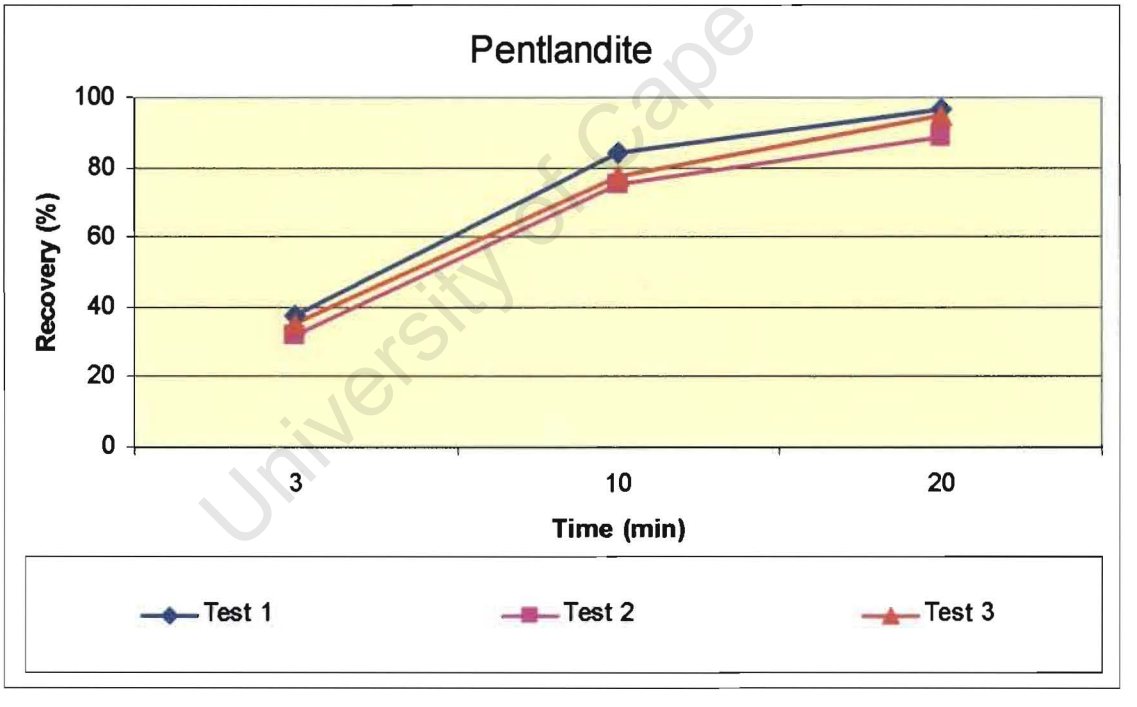

Figure 4.1: Pentlandite reproducibility recovery-time curves (in mixture with pyroxene) for concentrates collected at 3, 10 and 20 minute intervals in synthetic water, *I* = 2.0E-02.

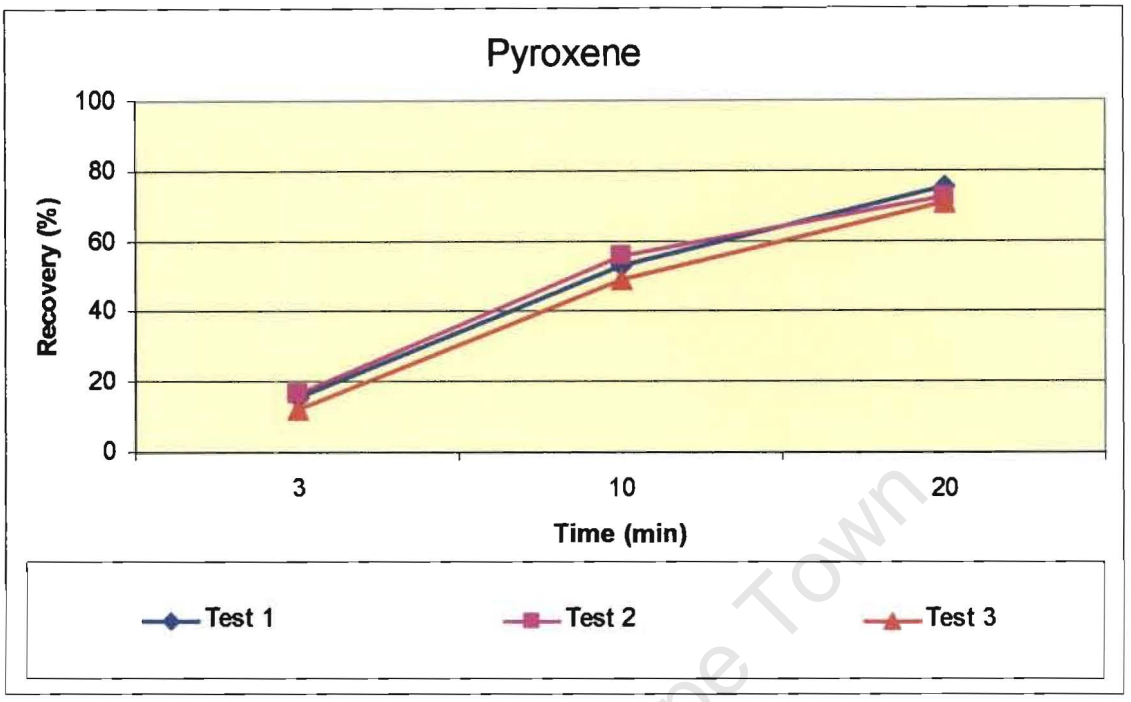

Figure 4.2: Pyroxene reproducibility recovery-time curves (in mixture with pentlandite) for concentrates collected at 3, 10 and 20 minute intervals in synthetic water, I = 2.0E-02.

As demonstrated by the recovery-time curves and the low standard deviation for each concentrate collected, the procedure and apparatus used gave consistent results.

4.1.2 Dosage Curves

The aim of this testwork was to determine the optimal dosages to be used for the complexing agents being tested at pH 9. E_h was allowed to vary naturally and was measured to be ~0.1 V for the testwork. These trials were performed in the presence of copper sulphate (5.00E-05M) and sodium isobutyl xanthate (5.00E-05M). Figures 4.3 - 4.6 show the dosage trends for each complexing agent (DETA, EDA, TETA and EDTA). The dosages chosen were based on gram per ton values and converted to molarities; these figures vary between complexing agents due to the different molecular masses.

In Figure 4.3 the optimal dosage for DETA can been seen to be 6.98E-05M (900g/t). This dosage was chosen since it gave better selectivity between pentlandite and pyroxene without significantly reducing the pentlandite recovery. Although selectivity appears to improve with an increase in dosage the recovery of pentlandite drops off to below 80% and the aim is to increase the pentlandite recovery and simultaneously reduce the pyroxene recovery. The ultimate recovery achieved at the optimal dosage was 96 and 74% for pentlandite and pyroxene, respectively.

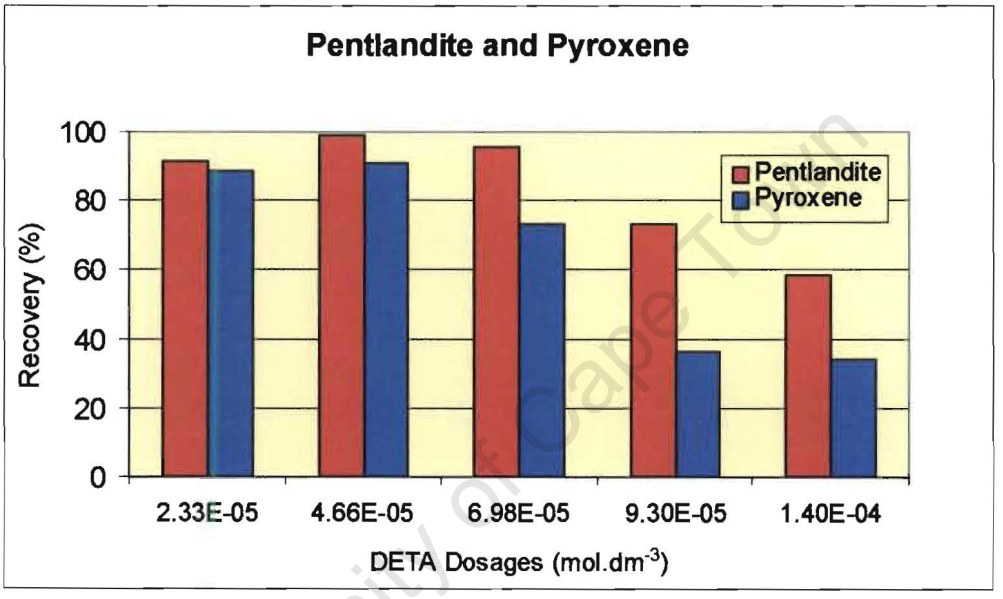

Figure 4.3: Dosage data for DETA at pH 9.

Figure 4.4 shows the dosage trends for EDA. The results indicate that the optimal dosage is 4.00E-05M (300g/t). Ultimate recoveries achieved for pentlandite and pyroxene is 90 and 45%, respectively. Any higher dosage reduces the pentlandite recovery to below 60%.

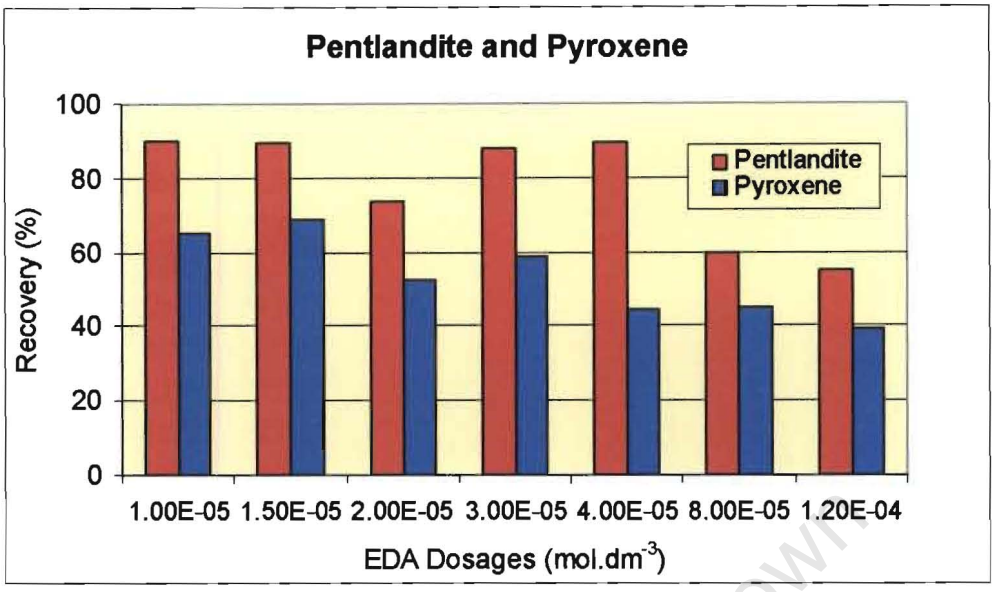

Figure 4.4: Dosage data for EDA at pH 9.

The optimal dosage for TETA, seen in Figure 4.5, is 4.93E-05M (900g/t). This dosage offers the best selectivity and any higher dosage compromises the pentlandite recovery. The ultimate recoveries obtained for pentlandite and pyroxene is 95 and 70% respectively.

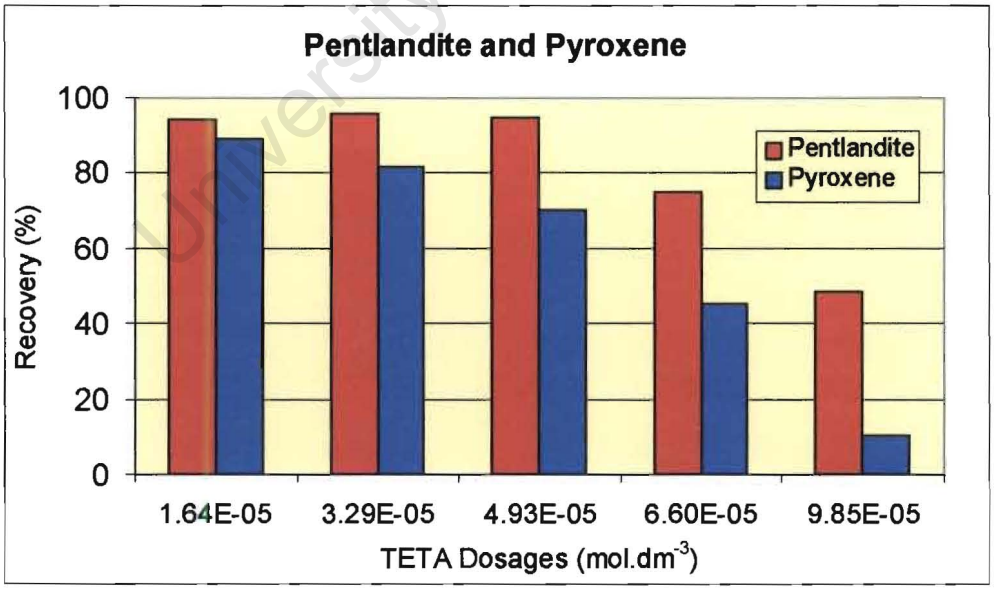

Figure 4.5: Dosage data for TETA at pH 9.

EDTA shows the least selectivity out of all the complexing agents tested. The optimal dosage appears to be 4.93E-05M (1800g/t), Figure 4.6. From the trend observed any further (higher) dosage would reduce the pentlandite recovery. The ultimate recovery obtained for pentlandite and pyroxene is 92 and 79% respectively.

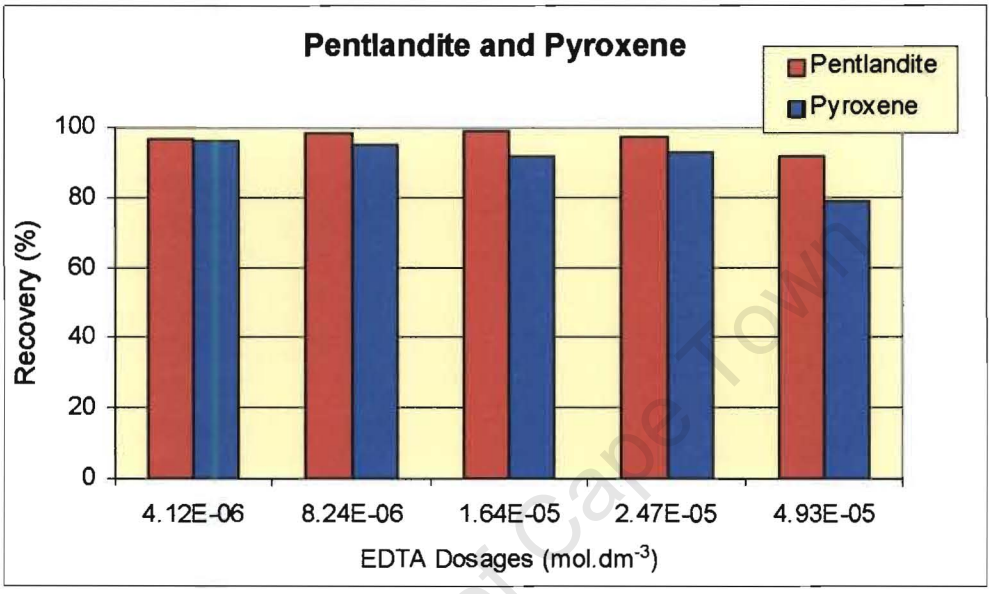

Figure 4.6: Dosage data for EDTA at pH 9.

It is apparent from the data given above that there are differences between the complexing agents tested with respect to pentlandite and pyroxene recovery and selectivity at pH 9. The results indicate that EDA offers the best selectivity between pentlandite and pyroxene with a high recovery of pentlandite.

From the results obtained above the following dosages for each complexing were used for the comparative trials:

- DETA 6.98E-05M
- EDA 4.00E-05M
- TETA 4.93E-05M
- EDTA 4.93E-05M

In Table 4.3, the optimal dosages determined for the complexing agents and the dosages used for copper sulphate and xanthate have been converted into grams, moles and psuedo-monolayers for the active ingredients of the reagents. All the complexing agents' complex with copper in a 1:1 ratio except EDA, which complexes with copper in a 1:2 ratio and this has been taken into account for the calculations of the pseudo-monolayers.

Chemical Reagent	Gram of Reagent	Moles of Reagent	Psuedo-monolayer of Reagent
***Copper Sulphate,* (CuSO$_4$)**	0.0008	1.26E-05	3.5
***Sodium isobutyl xanthate,* (SIBX)**	0.0019	1.28E-05	6.3
***Diethylenetriamine,* (DETA)**	0.0018	1.23E-05	4.8*
***Ethylenediamine,* (EDA)**	0.0006	1.00E-05	5.6*
***Triethylenetetramine,* (TETA)**	0.0018	1.75E-05	3.4*
***Ethylenediaminetetraacetic acid,* (EDTA)**	0.0036	1.23E-05	3.4*

* = Atom size of the complexing agents is based on the copper atom size (20.8 Å^2, Gaudin et al. 1959)

Table 4.3: Reagent concentrations in grams, moles and pseudo-monolayers for all the active ingredients of the chemicals used during the study.

The gram / mole values in Table 4.3 show that DETA, TETA and EDTA dosages were 2 – 5 times higher compared to that of copper, however, EDA gave the best results with the lowest dosage. The pseudo-monolayers is an approximation and show that when comparing the complexing agents there are more monolayers of EDA and DETA compared to TETA and EDTA, which may explain why better results are obtained with respect to pentlandite and pyroxene recovery and selectivity.

Figures 4.7 and 4.8 show recovery-time curves for:

- Each complexing agent at the optimal dosages determined
- In the absence of reagent
- In the presence of xanthate (5.00E-05M)
- In the presence of copper sulphate (5.00E-05M) and xanthate (5.00E-05M)

The results indicate that EDA is probably the best complexing agent offering the highest selectivity between pentlandite and pyroxene without a loss in pentlandite recovery. The results also show the need for a complexing agent when compared to the standard copper sulphate and xanthate case. Also worth noting is that the addition of copper sulphate, prior to xanthate addition, improved the flotation kinetics, particularly for pentlandite.

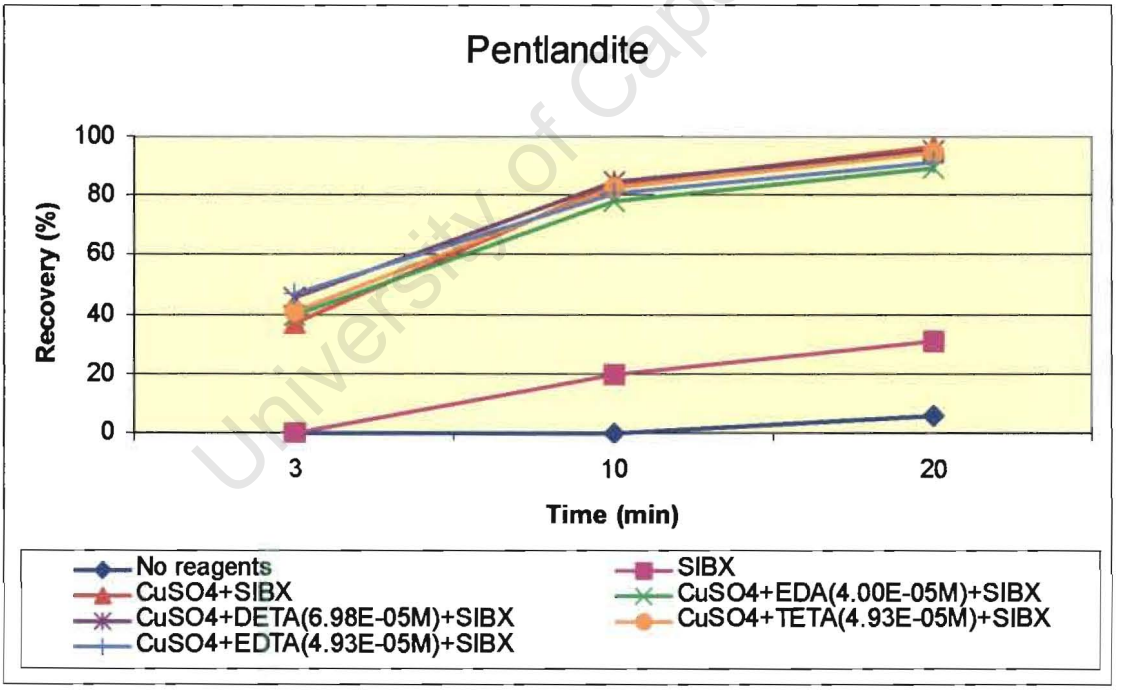

Figure 4.7: Comparative pentlandite (in mixture with pyroxene) recovery-time curves at pH 9.

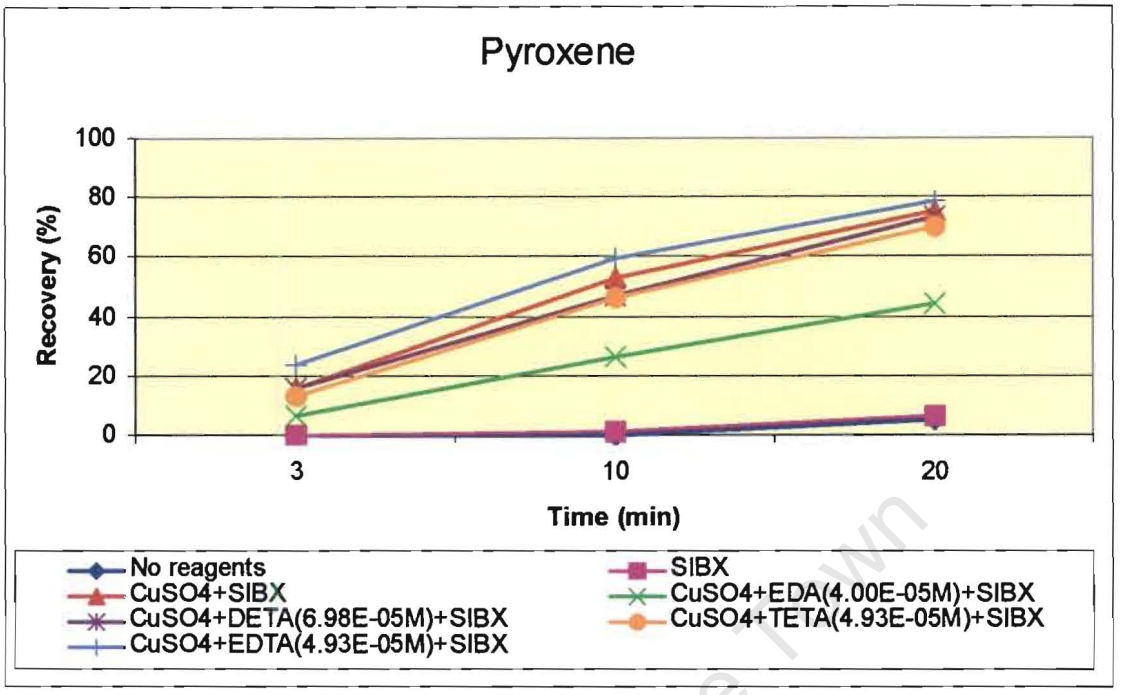

Figure 4.8: Comparative pyroxene (in mixture with pentlandite) recovery-time curves at pH 9.

4.1.3 Sequence of Reagent Additions

The variations in the sequence of the addition of reagents tested were carried out to determine whether the order of addition had any effect with respect to pentlandite and pyroxene recovery and selectivity. The conventional order of addition was copper sulphate; to activate the mineral surfaces, followed by the complexing agent; to limit the copper activated effect from the pyroxene surfaces and xanthate: as collector.

The variations investigated included:

- Adding ethylenediamine (EDA) initially, before the copper sulphate (5.00E-05M) and xanthate (5.00E-05M) additions.
- Adding ethylenediamine in between the copper sulphate (5.00E-05M) and xanthate (5.00E-05M) additions.

- Adding ethylenediamine after the copper sulphate (5.00E-05M) and xanthate (5.00E-05M) additions.

The results of the microflotation tests are shown in Figures 4.9 and 4.10 for pentlandite and pyroxene, respectively. The results at pH 9 show that no added benefit is achieved with respect to pentlandite recovery and selectivity, and thus the reasoning chosen for the conventional sequence of reagent addition is valid.

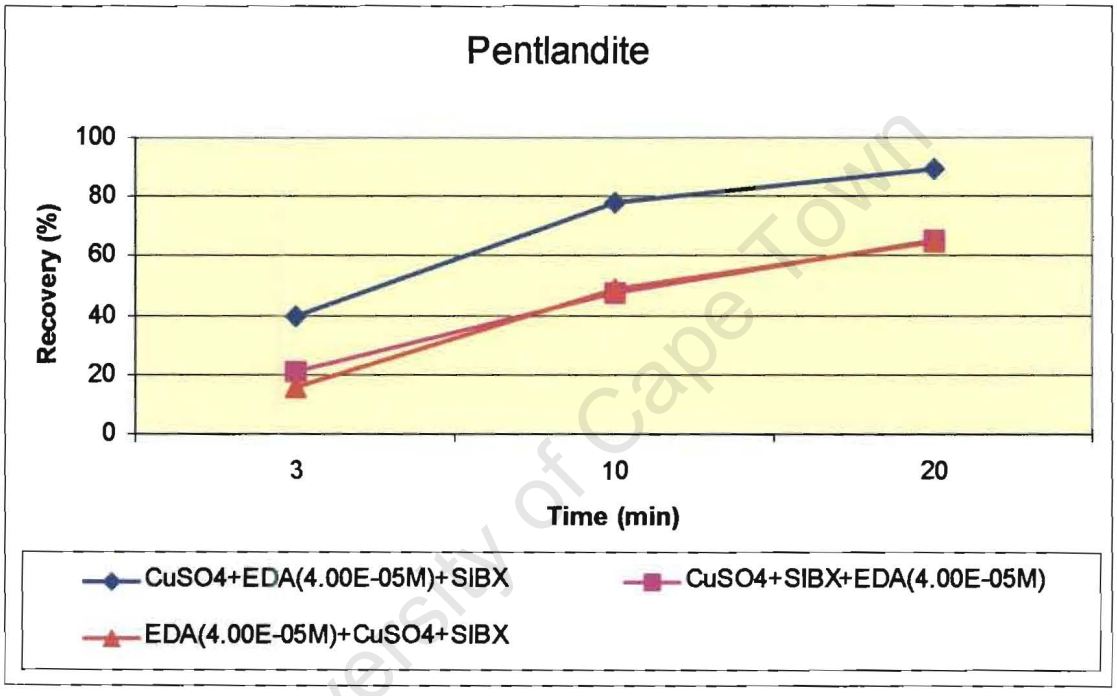

Figure 4.9: Pentlandite (in mixture with pyroxene) recovery-time curves at pH 9 comparing various sequences of EDA addition.

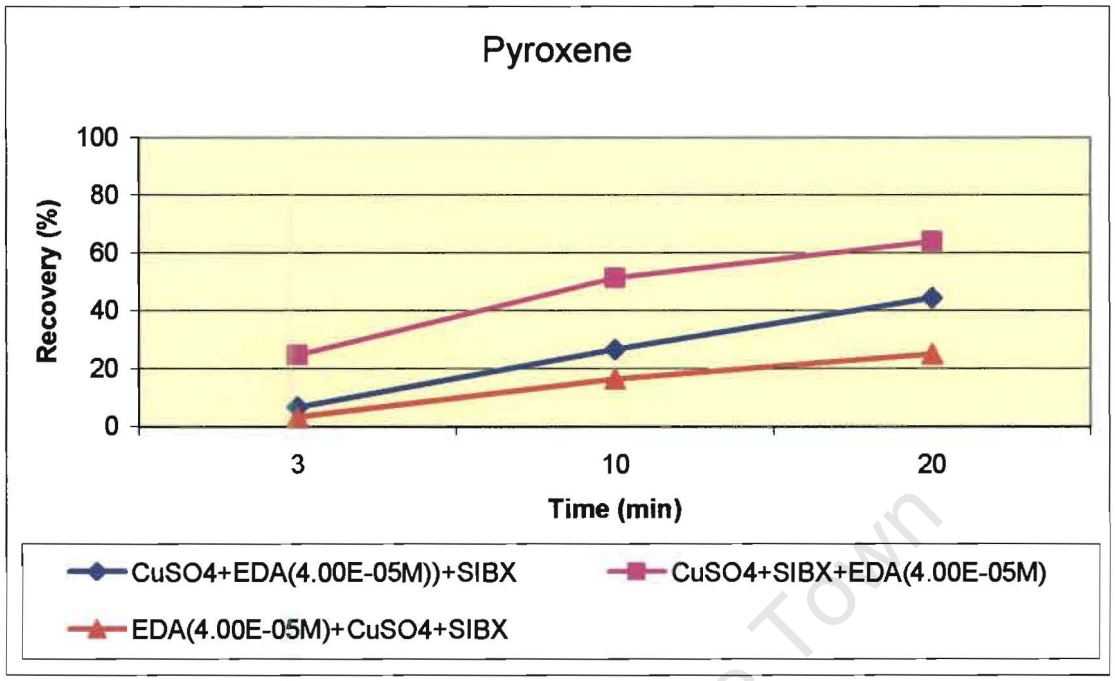

Figure 4.10: Pyroxene (in mixture with pentlandite) recovery-time curves at pH 9 comparing various sequences of EDA addition.

4.1.4 Variation of Copper Sulphate and Xanthate Concentrations

Microflotation testwork was performed to determine the effect that reducing the copper sulphate and xanthate concentrations would have on the flotation response and selectivity of pentlandite and pyroxene at pH 9. The sequence of reagent addition was unchanged and in the order as depicted in the Figures. The concentrations for copper sulphate and xanthate were reduced from 5.00E-05M to 5.00E-06M. The results are shown in Figures 4.11 and 4.12 and indicate that lowering the copper sulphate concentration 10 times reduced the pentlandite recovery significantly. However, the addition of the complexing agent increased the ultimate recovery by around 20% relative to the 10 times lower copper sulphate followed by xanthate recovery-time curve (Figure 4.11). When the concentration of xanthate was reduced 10 times, the results showed that it had no effect on the flotation response or selectivity compared to the corresponding copper sulphate, EDA and xanthate trial.

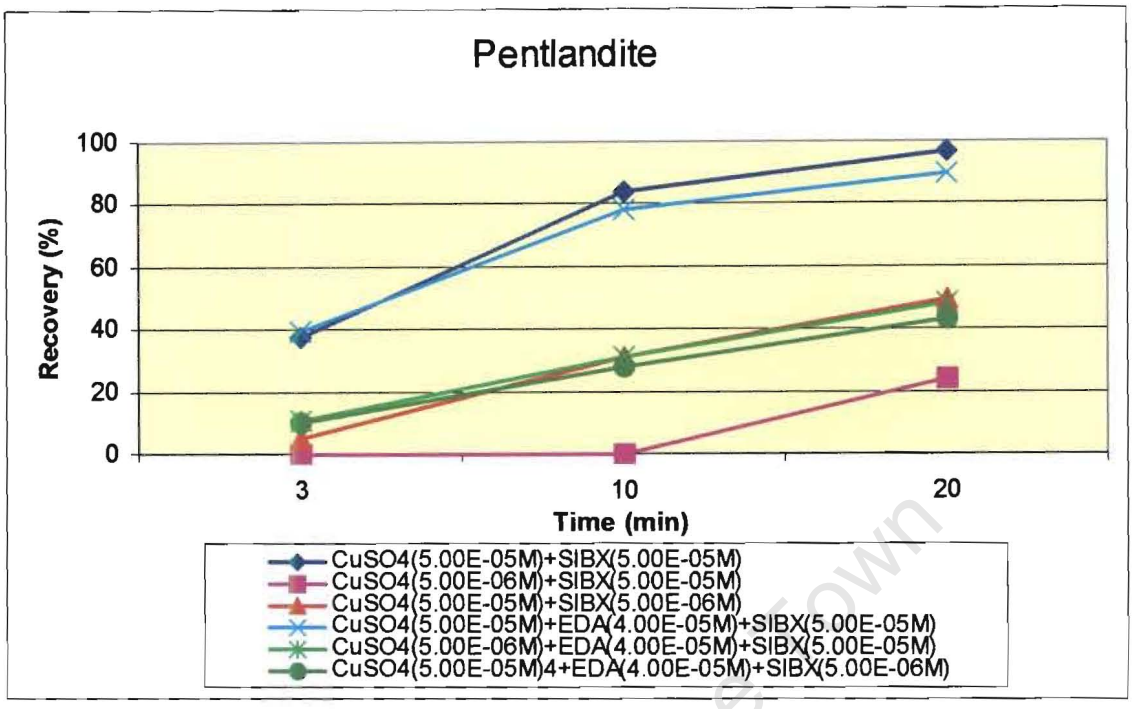

Figure 4.11: Pentlandite (in mixture with pyroxene) recovery-time curves at pH 9 comparing different copper sulphate and xanthate concentrations.

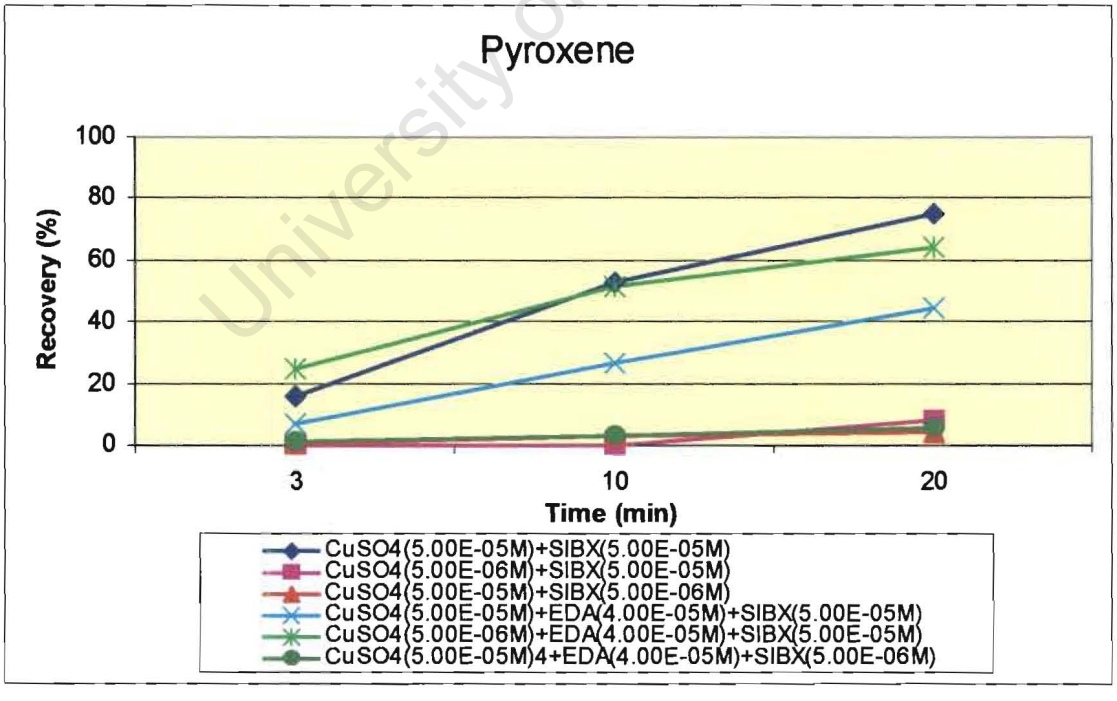

Figure 4.12: Pyroxene (in mixture with pentlandite) recovery-time curves at pH 9 comparing different copper sulphate and xanthate concentrations.

It is interesting to note that as in the case of the pentlandite recovery, the pyroxene recovery also significantly increased with the addition of EDA in the presence of lower copper sulphate concentrations.

4.2 Surface Techniques

4.2.4 Zeta Potential Determinations

4.3.1.1 Reproducibility

The aim of the reproducibility tests was to establish the reliability of the zeta potential determination procedure used during the study. Any possible error includes the variability of the mineral samples, the consistency of the Malvern Zetasizer operation as well as the operator's ability to be consistent.

In order to determine the reproducibility and standard deviation, zeta potential determinations were carried out on a sample of pyroxene, in the absence of any reagent addition. The zeta potential determinations and standard deviations for each pH investigated are given in Table 4.3. The results obtained are graphically summarised by zeta potential-pH curves in Figure 4.13.

pH	*Zeta Potential Determinations (mV)*						*Mean*	*Std Dev*	*Relative Std Dev (%)*
	1	2	3	4	5	6			
4	-16.8	-17.3	-18.6	-18.2	-18.8	-18.6	-18.0	0.81	4.50
6	-19.1	-20.3	-20.3	-21.1	-20.4	-20.3	-20.3	0.64	3.16
8	-19.4	-19.2	-18.6	-20.2	-19.8	-18.6	-19.3	0.63	3.26
10	-15.3	-16.3	-17.8	-14.9	-17.7	-17.8	-16.6	1.31	7.89

Table 4.4: Zeta potential determinations and standard deviations for pH 4, 6, 8, and 10 in synthetic water, I = 2.0E-02.

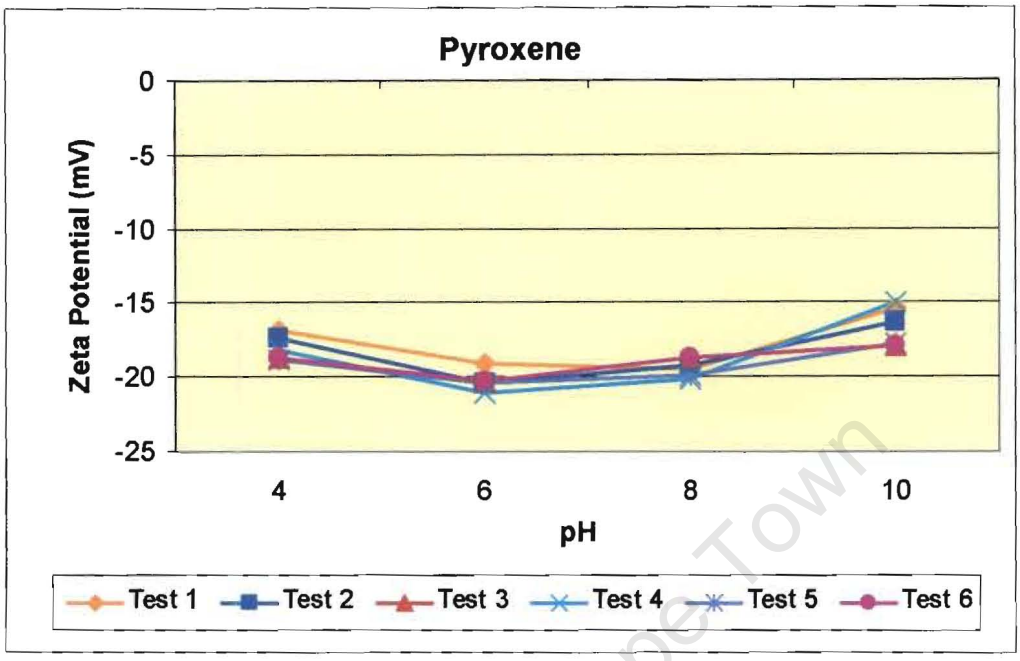

Figure 4.13: Zeta potential determination reproducibility curves for pH 4, 6, 8 and 10 in synthetic water, I = 2.0E-02.

As demonstrated by the zeta potential-pH curves and the low standard deviation for each pH measured, the technique and the procedure used gave reproducible results.

4.3.1.2 Zeta Potential Determinations for the Individual Reagents used in the study

Zeta potential results are given in Figures 4.14 and 4.15 and show the results obtained for the individual reagents added on their own for pentlandite and pyroxene, respectively.

As seen in Figure 4.14, two pH_{iep} (isoelectric point pH) were observed for pentlandite in the absence of reagents, namely 5.2 and 10. The results also show that the zeta potential / pH curve shifts from a negative to a more positive charge with the addition of copper(II) ions particularly from pH 6 - 10 indicating the adsorption of copper species.

For the addition of xanthate, the data obtained clearly showed that SIBX on its own readily adsorbs onto the pentlandite surfaces between pH 5 and 9 when compared to the zeta potential / pH curve in the absence of reagents. At pH 4, a colloidal precipitate forms with the addition of xanthate, which interferes with the zeta potential reading; no attempt will be made to interpret the results.

The addition of DETA, EDA and TETA gave similar results at pH 4 and 6, showing a positive shift in the zeta potential / pH curve compared to the zeta potential / pH curve in the absence of reagents. From pH 6, the DETA and TETA curves remained unchanged until pH 10 where TETA causes the pentlandite zeta potential / pH curve to shift to more positive values. EDA shifts the curve to more negative values from pH 6 - 9 indicating a higher affinity for iron and nickel oxide and hydroxide species compared to DETA and TETA. EDTA shifts the pentlandite surface charge to more negative values for the entire pH range studied.

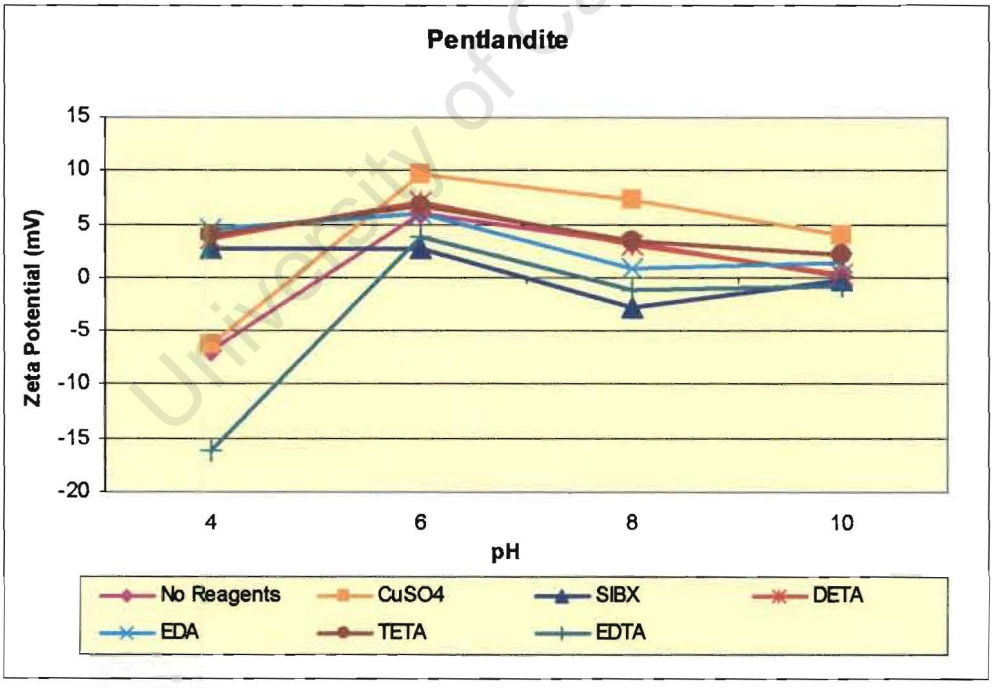

Figure 4.14: Zeta potential determinations of pentlandite in synthetic water, I = 2.0E-02, for the individual reagents used during the study.

The zeta potential determinations for pyroxene are given in Figure 4.15.

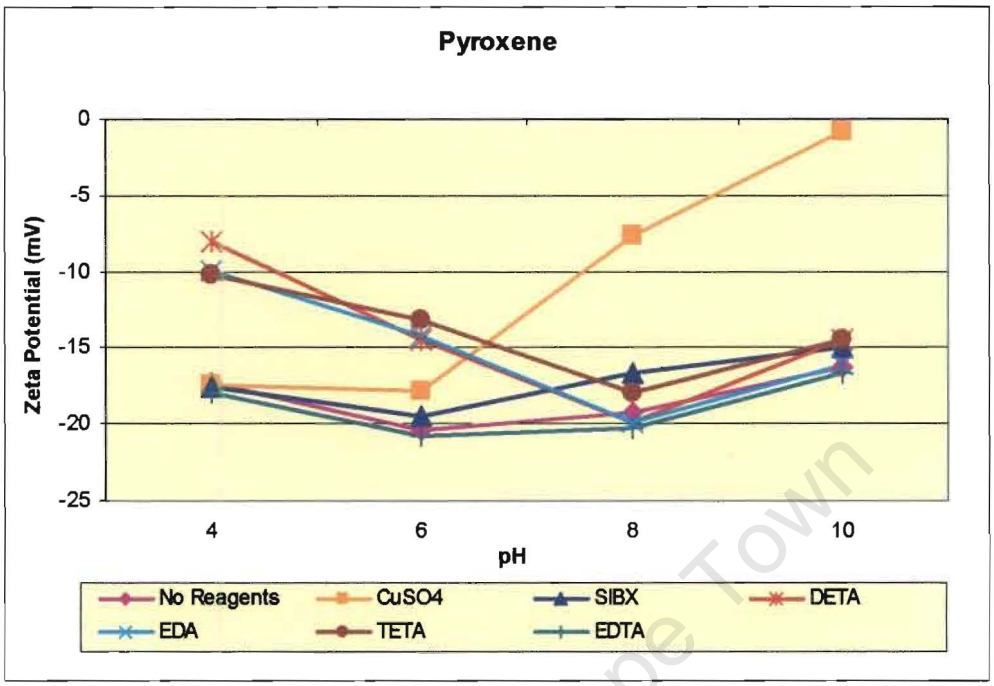

Figure 4.15: Zeta potential determinations of pyroxene in synthetic water, I = 2.0E-02, for the individual reagents used during the study.

The results indicate that the pyroxene surface charge in synthetic water is between –15mV and –20mV without any reagent added at the pH range of interest. It is evident that, in the presence of copper(II) ions, the pyroxene surface became more positively charged above pH 6, which indicates an adsorption of various positively charged copper species. The data obtained clearly showed that SIBX on its own does not readily adsorb onto the pyroxene surfaces. The results for DETA, EDA and TETA are all very similar indicating a shift of the zeta potential / pH curve to more positive values in the pH range of 4 – 7 compared to the zeta potential / pH curve in the absence of reagents. From pH 8 - 10 the shift is negligible. EDTA does not alter the position of the zeta potential / pH curve in the absence of reagents, indicating no interferences with pyroxene mineral surfaces. As observed for pentlandite, DETA, EDA and TETA increased the pyroxene surface charge in an acid environment (pH 4 - 6).

4.3.1.3 Zeta Potential Determinations of Copper Activated Mineral Surfaces in the Presence of Complexing Agents

The next set of zeta potential results show the effect the addition of a complexing agent has on copper activated mineral surfaces. The results are displayed in Figures 4.16 and 4.17 for pentlandite and pyroxene, respectively.

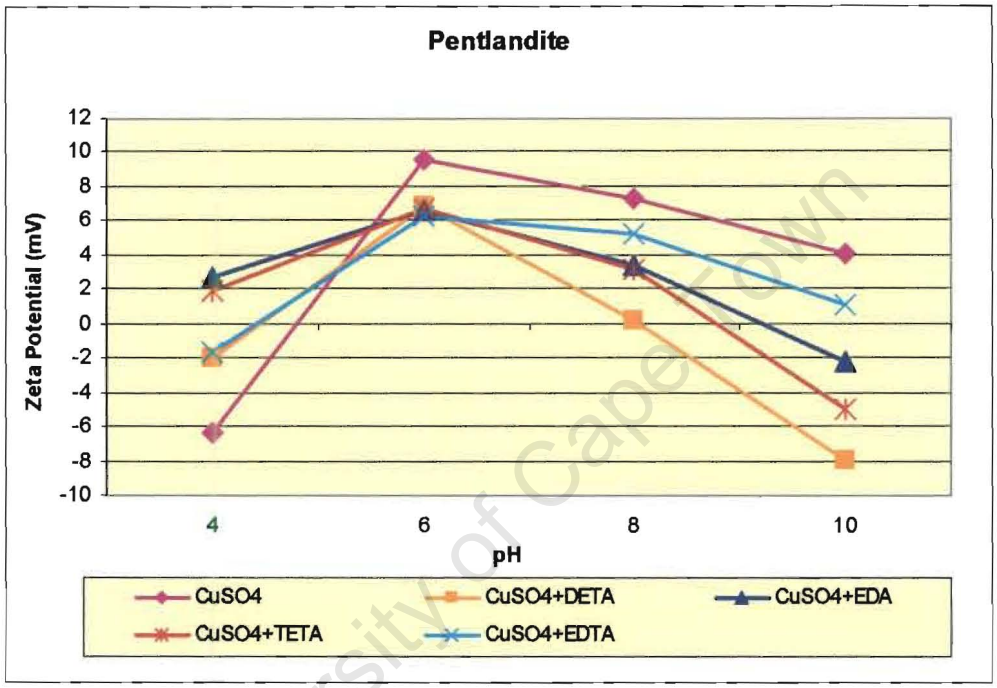

Figure 4.16: Zeta potential determinations for copper activated pentlandite in synthetic water, I = 2.0E-02, in the presence of the complexing agents.

In Figure 4.16 a small change in the zeta potential / pH curves of the complexing agents was observed at pH 6 compared to the copper sulphate zeta potential / pH curve. However, from pH 6 the addition of DETA, EDA and TETA shifts the copper sulphate curve to more negative zeta potential / pH values indicating the removal of copper species, probably copper oxide and hydroxide, from the pentlandite surfaces. EDTA has the least effect with respect to copper removal from the mineral surface. At pH 4 all the curves are more positive compared to the copper sulphate curve indicating the formation of positively charged copper and nickel species on the pentlandite surfaces.

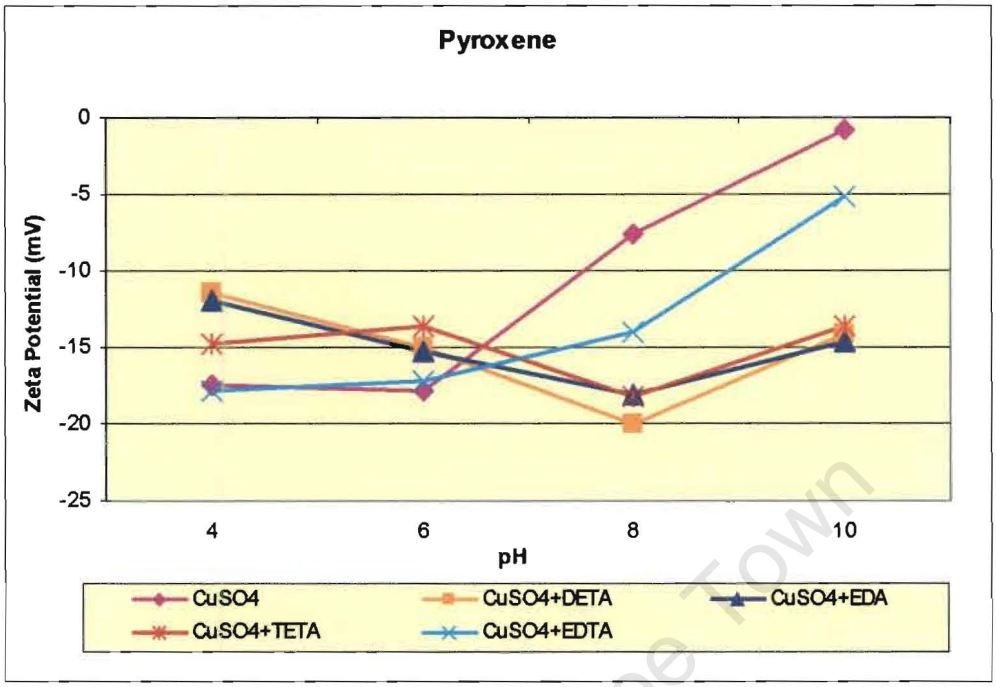

Figure 4.17: Zeta potential determinations for copper activated pyroxene in synthetic water, *I* = 2.0E-02, in the presence of the complexing agents.

The results for pyroxene (Figure 4.17), in the presence of the complexing agents are very similar to those observed for pentlandite. When DETA, EDA and TETA are added to the copper sulphate system at alkaline pH, the zeta potential / pH curves move to more negative values when compared to the copper sulphate curve. This indicates that copper(II) ions are being removed as oxide and hydroxide species thereby reducing the activating effect of copper sulphate on the pyroxene mineral surface. A comparison of the EDTA, DETA, EDA and TETA zeta potential / pH curve indicates that EDTA is less selective for copper species.

4.3.1.4 Zeta Potential Determinations of Copper Activated Mineral Surfaces in the Presence of Complexing Agents and Xanthate

Further experiments investigated the effect xanthate has on the copper activated mineral surface in the presence and absence of a complexing agent.

The results are shown in Figures 4.18 and 4.19 for pentlandite and pyroxene, respectively. The results for pentlandite indicated that when xanthate was added in the presence of copper sulphate and the complexing agents tested, the zeta potential / pH curve shifted to more negative potentials indicating xanthate adsorption onto pentlandite surfaces.

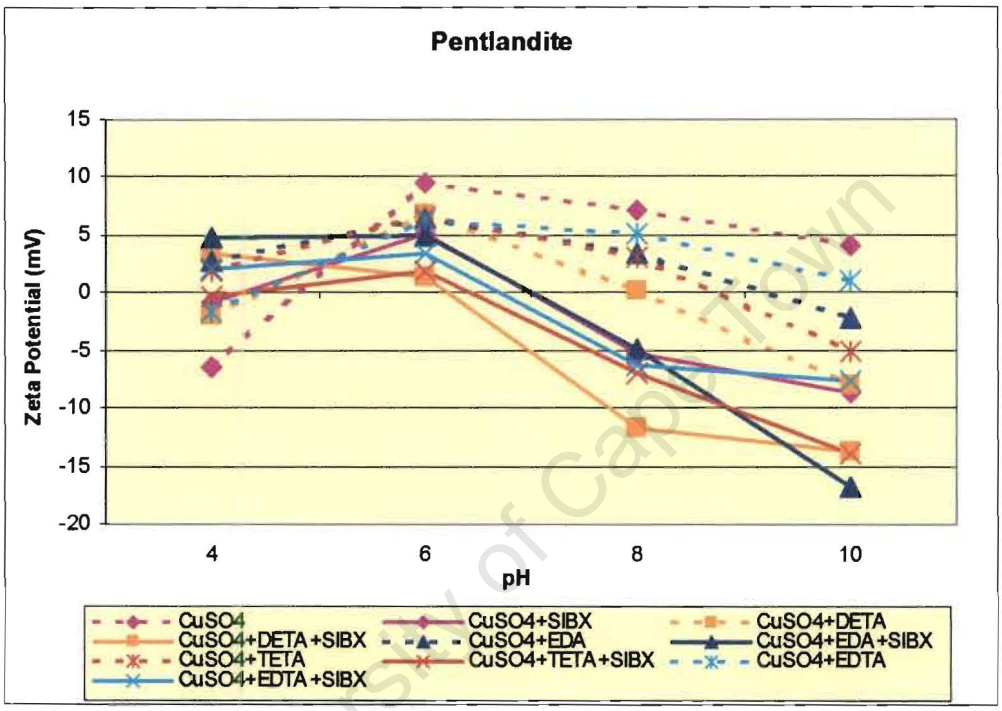

Figure 4.18: Zeta potential determinations for copper activated pentlandite in synthetic water, I = 2.0E-02, in the presence of the complexing agents and xanthate.

As seen in Figure 4.19, the introduction of xanthate ions in the presence of copper(II) ions shifted the zeta potential / pH curve to more negative values, compared with the curve for copper sulphate on its own, showing that xanthate adsorption on copper activated mineral surfaces is occurring. The addition of the complexing agents has shown that copper species are removed from the pyroxene surfaces to varying degrees depending on the complexing agent used (Figure 4.17). In the presence of xanthate the results show a low degree of xanthate adsorption onto the copper activated pyroxene surfaces in the presence of DETA, EDA and TETA, thereby introducing selectivity

between pentlandite and pyroxene. This, however, was not observed for the EDTA addition, where the zeta potential / pH curve shift was significantly more negative clearly demonstrating the adsorption of xanthate ions onto copper-activated pyroxene grains.

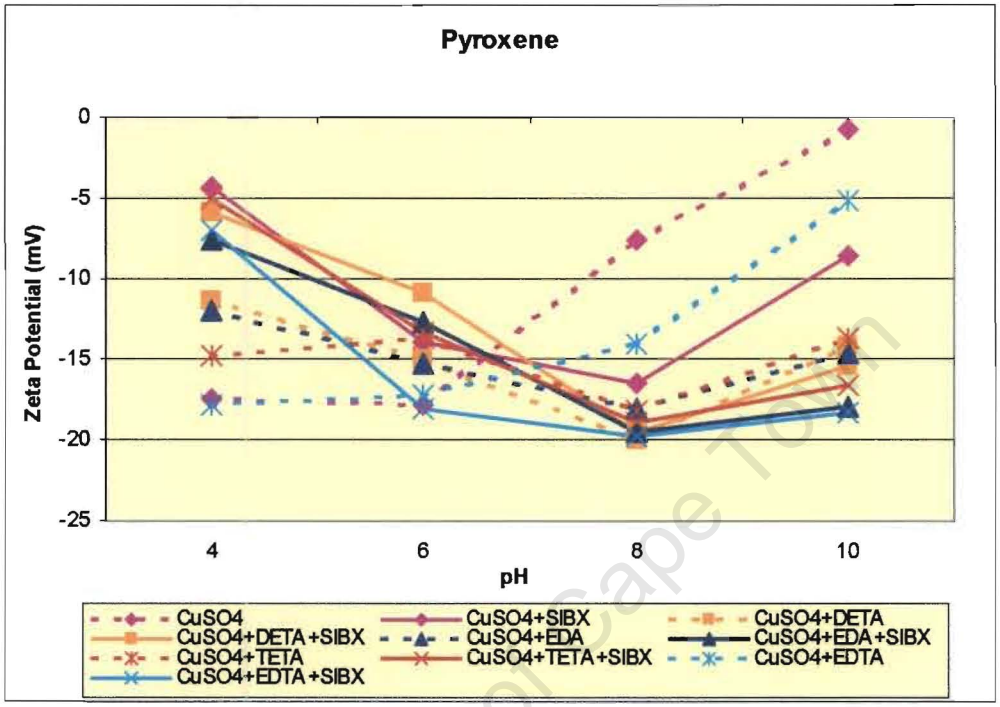

Figure 4.19: Zeta potential determinations for copper activated pyroxene in synthetic water, *I* = 2.0E-02, in the presence of the complexing agents and xanthate.

4.2.2 ToF-SIMS Analyses

ToF-SIMS analyses were carried out with the aim of gaining an understanding of mineral surface alterations and link those to flotation recovery. It has to be noted that the ToF-SIMS technique is qualitative; hence the trends obtained are compared, rather than the absolute values.

4.2.2.1 Comparative Surface Analysis of Reagent Additions Determined for the Microflotation Testwork

The ToF-SIMS data for pentlandite is displayed in Figures 4.20 – 4.25 and the data for pyroxene is shown in Figures 4.26 – 4.28. The sequence of reagent addition is the same as depicted in the Figures.

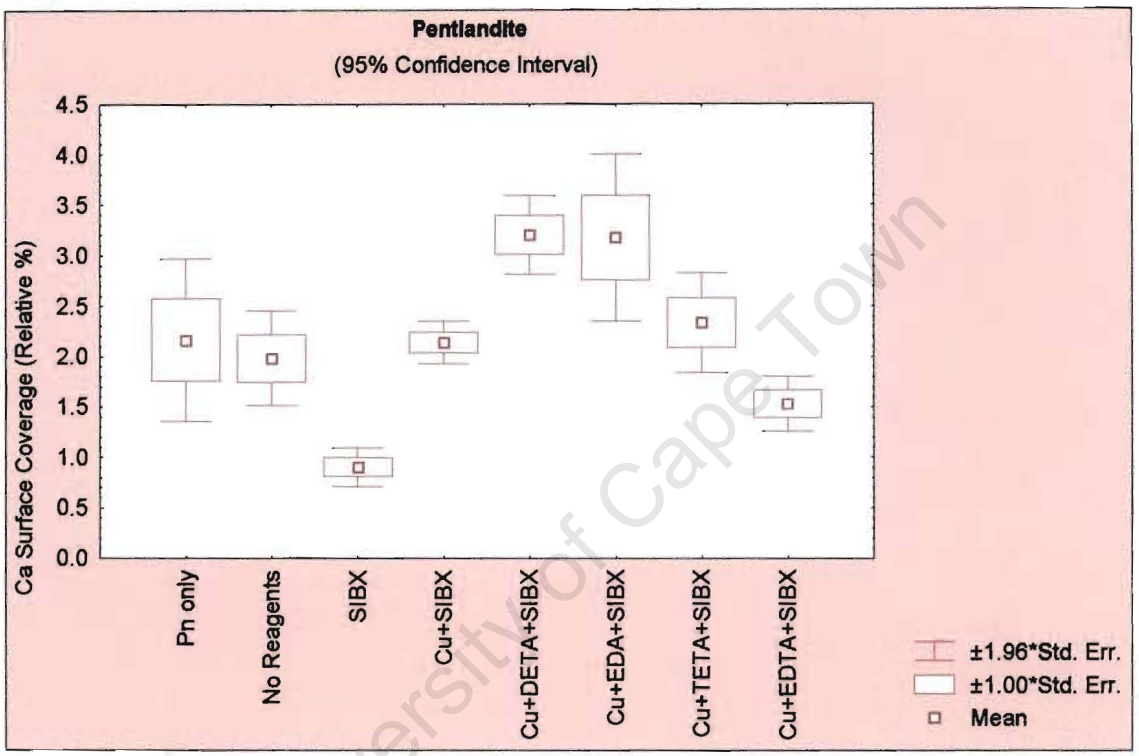

Figure 4.20: Calcium ions relative percent surface coverage for pentlandite in synthetic water, I = 2.0E-02.

Figures 4.20 and 4.21 shows the surface coverage of calcium and magnesium ions on pentlandite surfaces, these ions are present in the synthetic water, which was used during the study. The results for calcium surface coverage (Figure 4.20) on pentlandite indicate that the lowest calcium surface coverage was observed in the presence of xanthate. In addition, it shows the difference in selectivity of the complexing agents tested with respect to calcium ions. EDTA is known to complex with calcium ions and shows the lowest concentration of calcium on the pentlandite mineral surfaces compared to the other complexing agents tested (Skoog and West, 1982).

The opposite is true for the magnesium ion where it was observed that EDTA has the highest coverage of magnesium compared to the other complexing agents tested. All the complexing agents appear to remove magnesium from the mineral surface compared to the trials without the addition of a complexing agent (Figure 4.21). However, DETA, EDA and TETA as compared to EDTA, are selective complexing agents and will readily complex with Cu^{2+} and Ni^{2+}, but not with Fe^{3+}, Ca^{2+} and Mg^{2+} ions. The formation constants for the various EDTA-metal complexes show that Fe^{3+} (25.1), Fe^{2+} (14.2), Cu^{2+} (18.3) and Ni^{2+} (18.4) should be complexed before Ca^{2+} (10.7) and Mg^{2+} (8.7) ions (Chaberek and Martell, 1959).

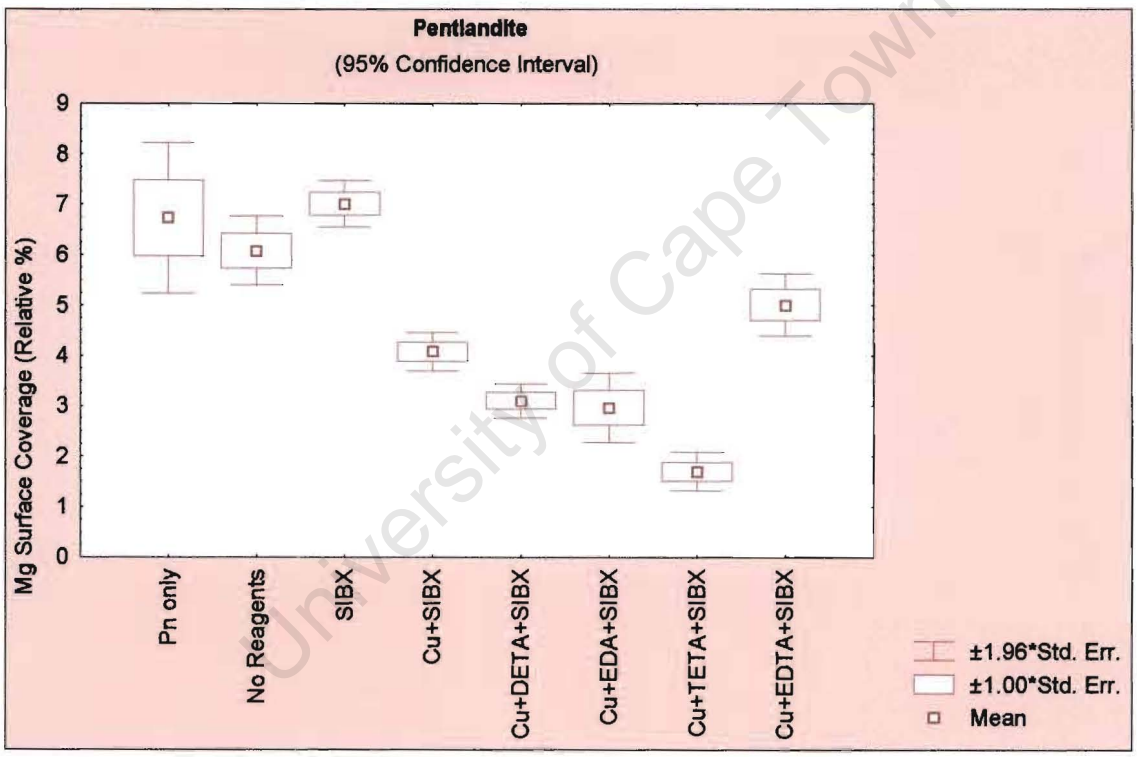

Figure 4.21: Magnesium ions relative percent surface coverage for pentlandite in synthetic water, I = 2.0E-02.

Figure 4.22 shows the copper surface coverage on pentlandite and indicates that EDA removes the least amount of copper from the pentlandite mineral surface compared with the other complexing agents, this could probably be attributed to a trade-off between the calcium and magnesium surface coverage.

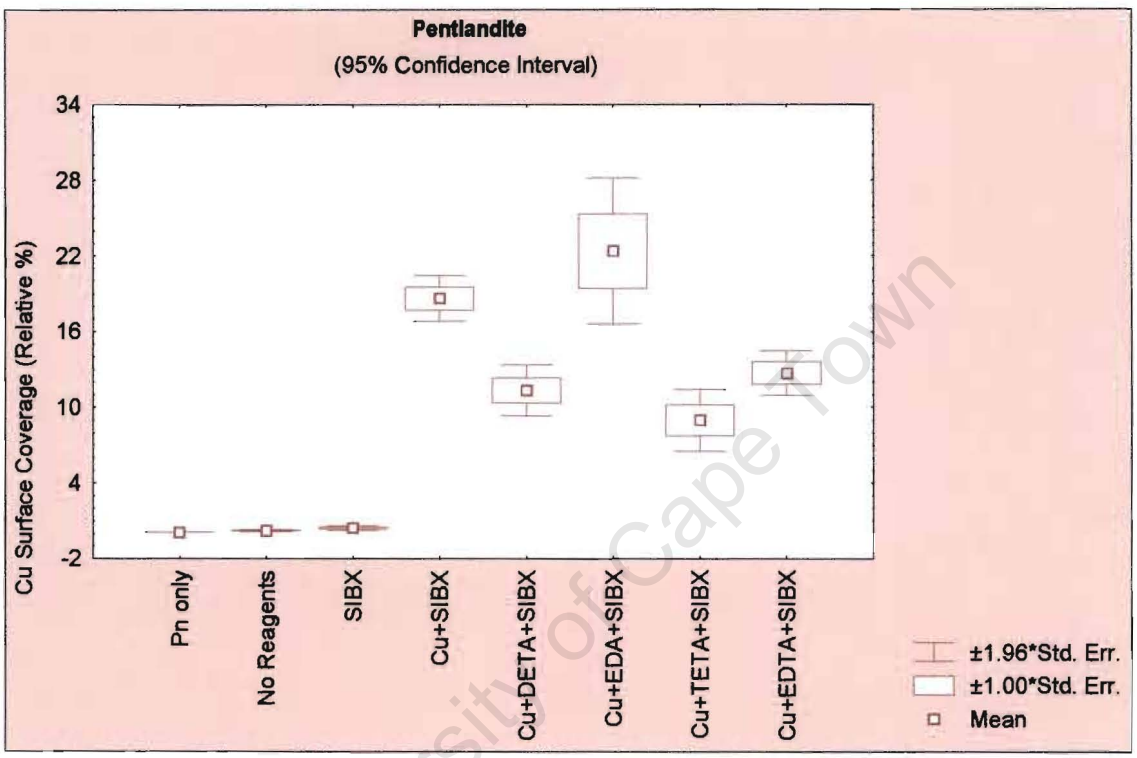

Figure 4.22: Copper ions relative percent surface coverage for pentlandite in synthetic water / = 2.0E-02.

The results in Figure 4.23 display the nickel surface coverage for pentlandite. The results show that the lowest nickel coverage is observed with the addition of EDA and this could be due to the high copper coverage, which masks the nickel surface of the pentlandite mineral. Figure 4.24 displays the iron / nickel ratio in the pentlandite surface layer and indicates a higher iron surface coverage when EDA is added compared to the other complexing agents. EDTA shows the highest iron removal indicating its strong complexing ability with iron species, particularly Fe^{3+} ions.

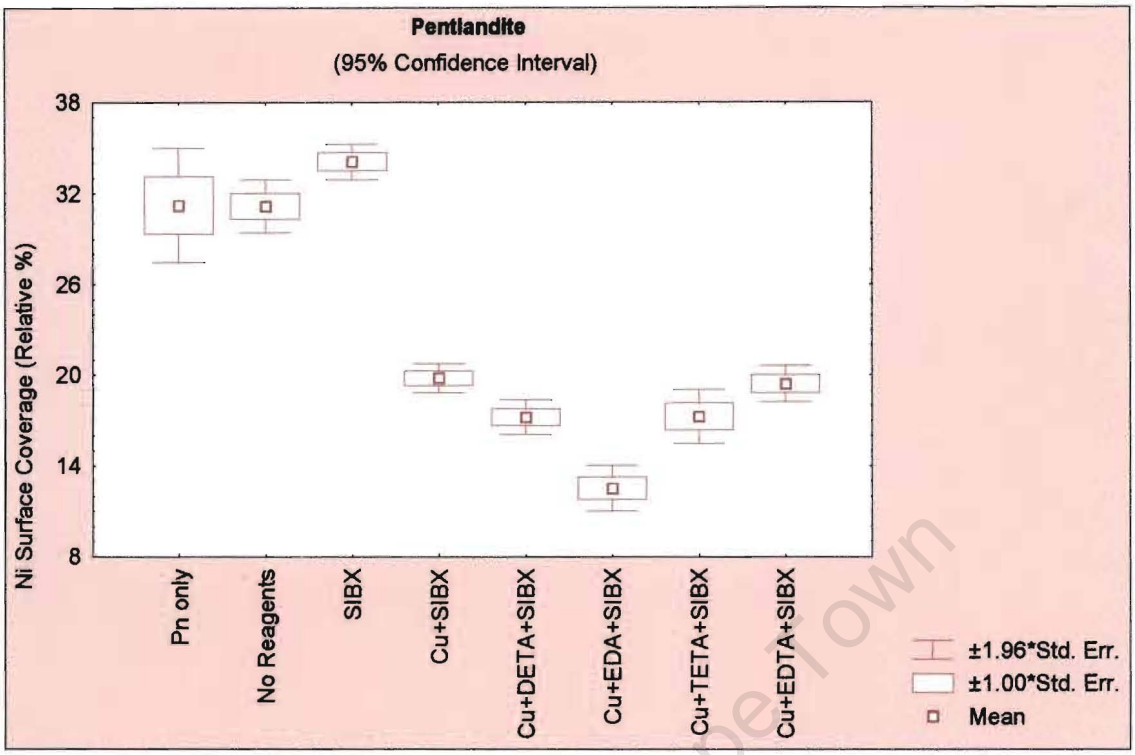

Figure 4.23: Nickel ions relative percent surface coverage for pentlandite in synthetic water, *I* = 2.0E-02.

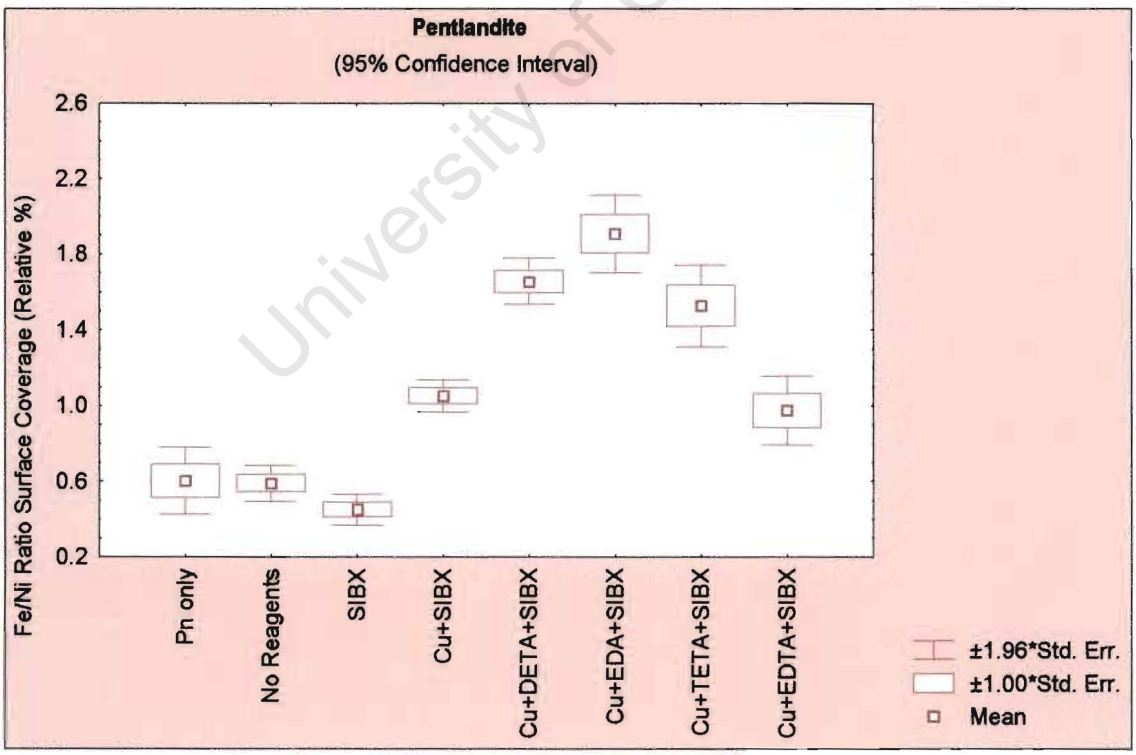

Figure 4.24: Fe/Ni Ratio relative percent surface coverage for pentlandite in synthetic water, *I* = 2.0E-02.

Figure 4.25 gives the sulphur surface coverage on pentlandite. The results indicate that the highest sulphur ion concentration was obtained in the presence of EDA, which would introduce hydrophobicity and enhance true flotation.

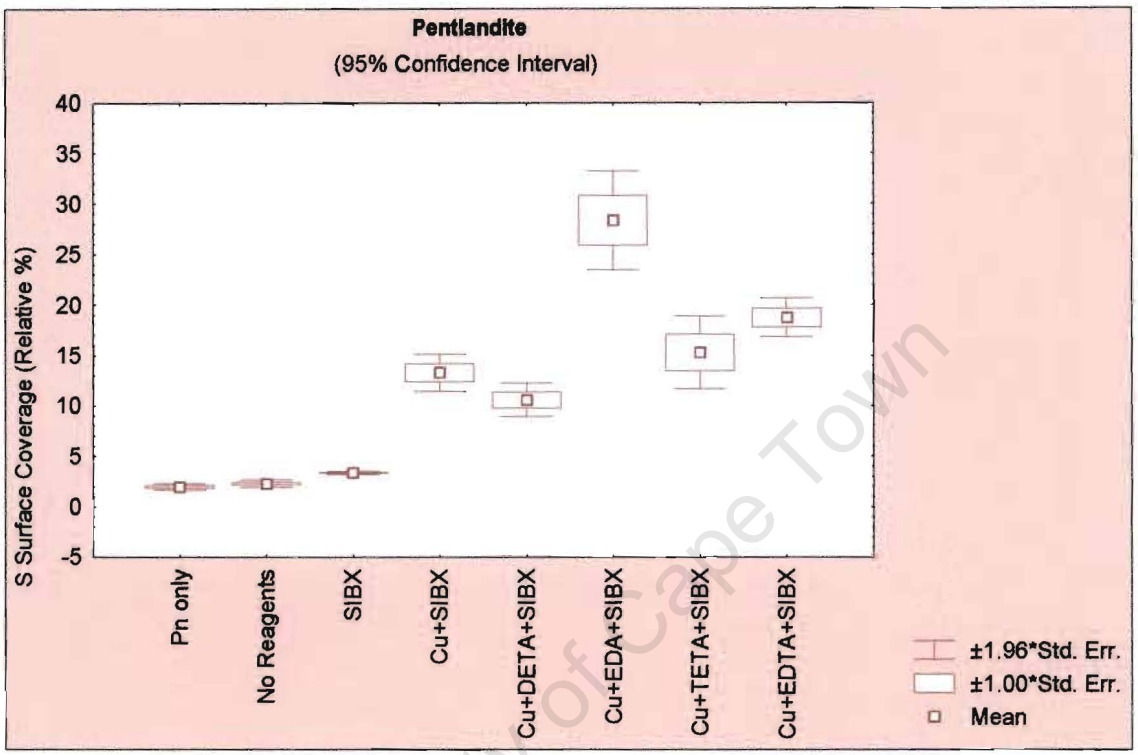

Figure 4.25: Sulphur ions relative percent surface coverage for pentlandite in synthetic water, I = 2.0E-02.

The surface coverage of copper on pyroxene mineral surfaces is shown in Figure 4.26. The results revealed that the addition of EDTA does not alter the copper surface coverage compared with the [$CuSO_4$ + SIBX] trial indicating a low degree of copper removal. The addition of DETA, EDA or TETA gives a similar relative % abundance of copper ions on pyroxene surfaces. The same trends are displayed for nickel surface coverage (Figure 4.27), where EDTA did not lower the nickel ion concentration compared with the other complexing agents, which reduced the nickel surface concentration to less than that observed when no reagents are added.

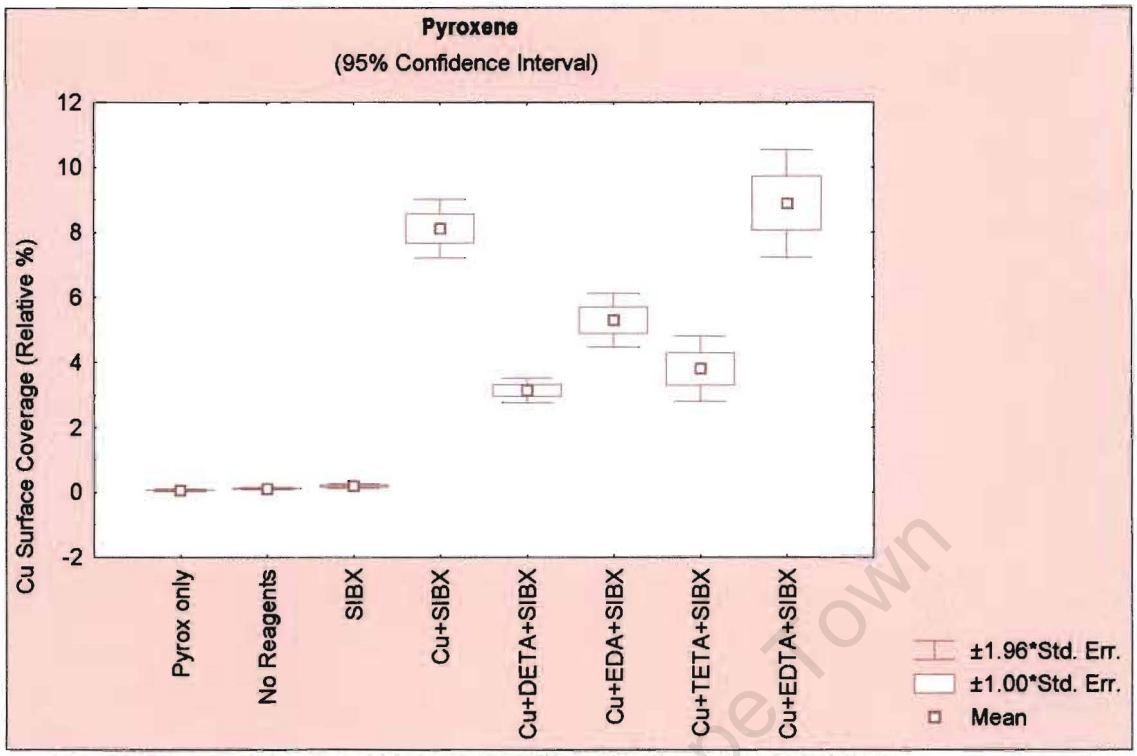

Figure 4.26: Copper ions relative percent surface coverage for pyroxene in synthetic water, I = 2.0E-02.

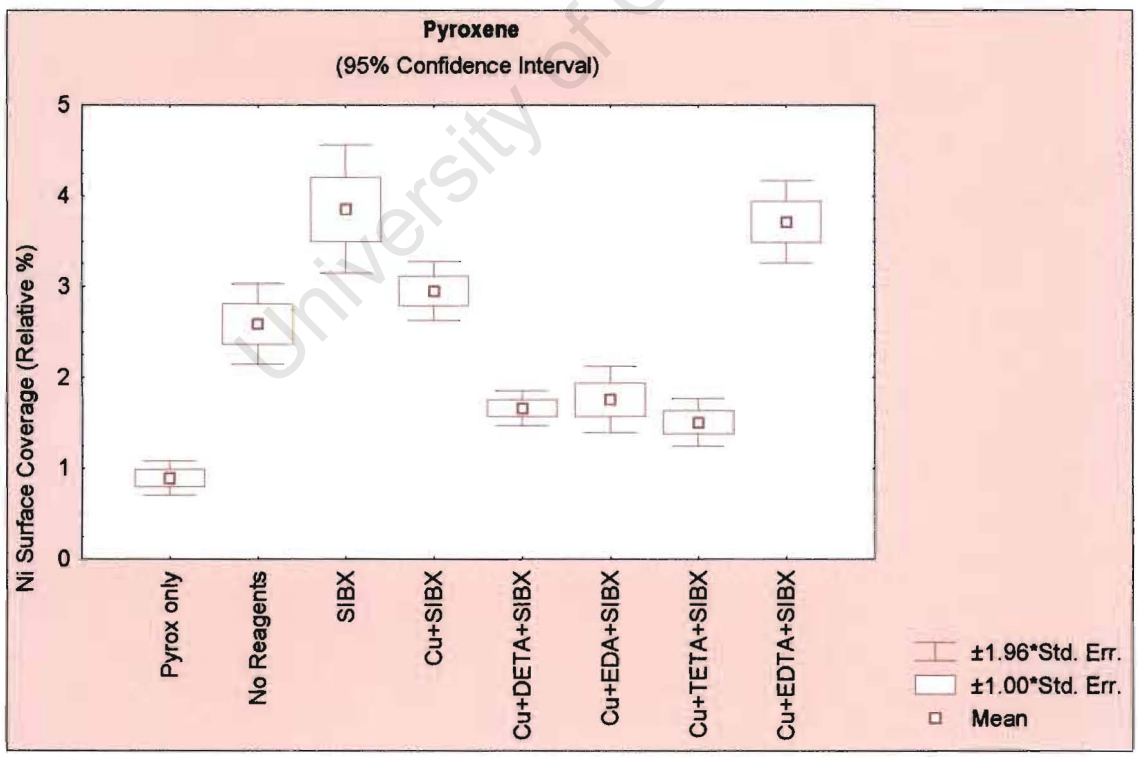

Figure 4.27: Nickel ions relative percent surface coverage for pyroxene in synthetic water, I = 2.0E-02.

An interesting observation was the sulphur surface coverage for pyroxene (Figure 4.28) where the highest sulphur ion concentration was shown with the addition of EDTA. EDTA displayed the lowest selectivity between pentlandite and pyroxene and visually the flotation products were extremely "oily" which introduces hydrophobicity and resulted in a recovery of close to 100% for pentlandite and 80% for pyroxene.

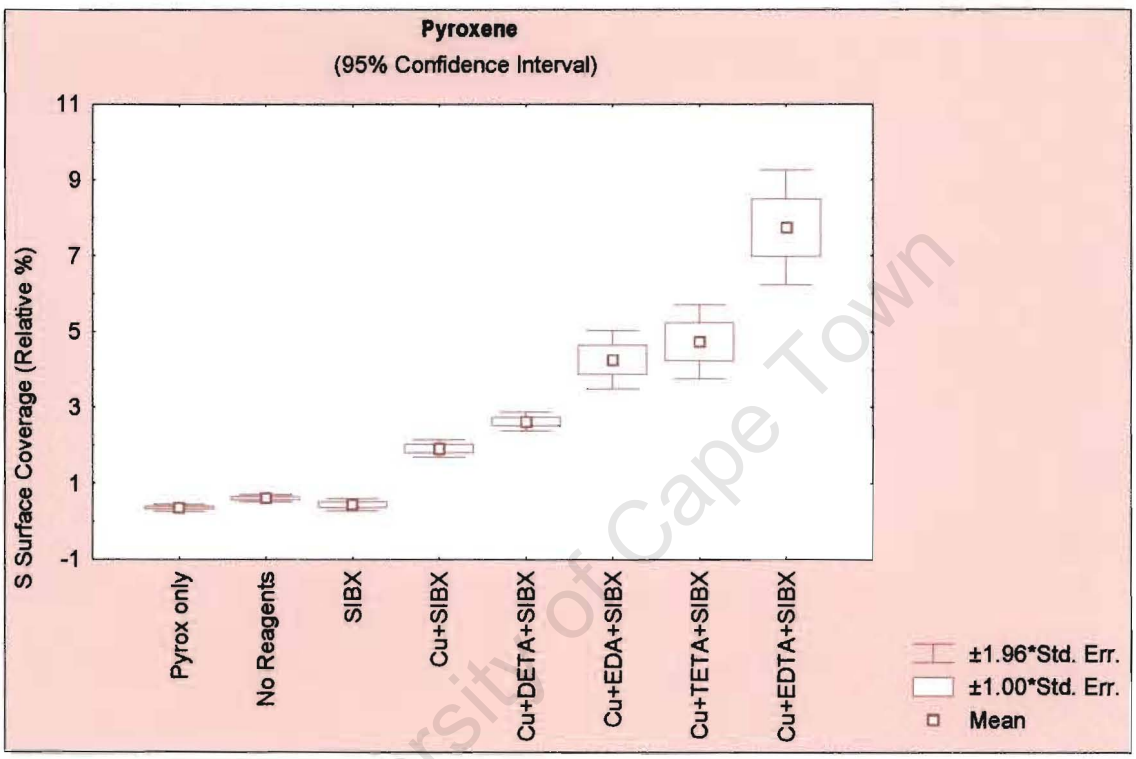

Figure 4.28: Sulphur ions relative percent surface coverage for pyroxene in synthetic water, I = 2.0E-02.

The surface coverage for xanthate on both pentlandite and pyroxene surfaces were very low and showed no significant difference between the complexing agents, however, the surface coverage of xanthate on pentlandite was around 10 times higher compared to that on pyroxene.

4.2.2.2 Sequence of Reagent Additions

The variations in the sequence of the addition of reagents tested were carried out to determine whether the order of addition had any effect with respect to pentlandite and

pyroxene recovery and selectivity. Microflotation results showed that no added benefit was gained by varying the EDA addition points. ToF-SIMS analyses of these pentlandite and pyroxene surfaces for the various cases were compared with the aim of gaining an understanding of mineral surface alterations and link them to the flotation recovery obtained.

The variations investigated included:

- Pentlandite on its own in synthetic water.
- 1:1 pentlandite-pyroxene mixture with xanthate addition.
- 1:1 pentlandite-pyroxene mixture with copper sulphate addition.
- 1:1 pentlandite-pyroxene mixture with copper sulphate followed by xanthate.
- 1:1 pentlandite-pyroxene mixture with copper sulphate followed by EDA and xanthate.
- 1:1 pentlandite-pyroxene mixture adding copper sulphate initially followed by xanthate and finally EDA.
- 1:1 pentlandite-pyroxene mixture adding EDA initially followed by copper sulphate and finally xanthate.

The results for pentlandite and pyroxene mineral surface alteration are given in Figures 4.29 - 4.32. The results in Figure 4.29 show the copper ions surface coverage for pentlandite surfaces and indicate that the copper concentration is similar for all cases where copper sulphate was added, however, when a copper/nickel ratio is calculated, it can be seen in Figure 4.30 that the case where EDA is added in between the copper sulphate and xanthate additions has the higher ratio and therefore improved floatability as shown in the microflotation testwork (Figure 4.9).

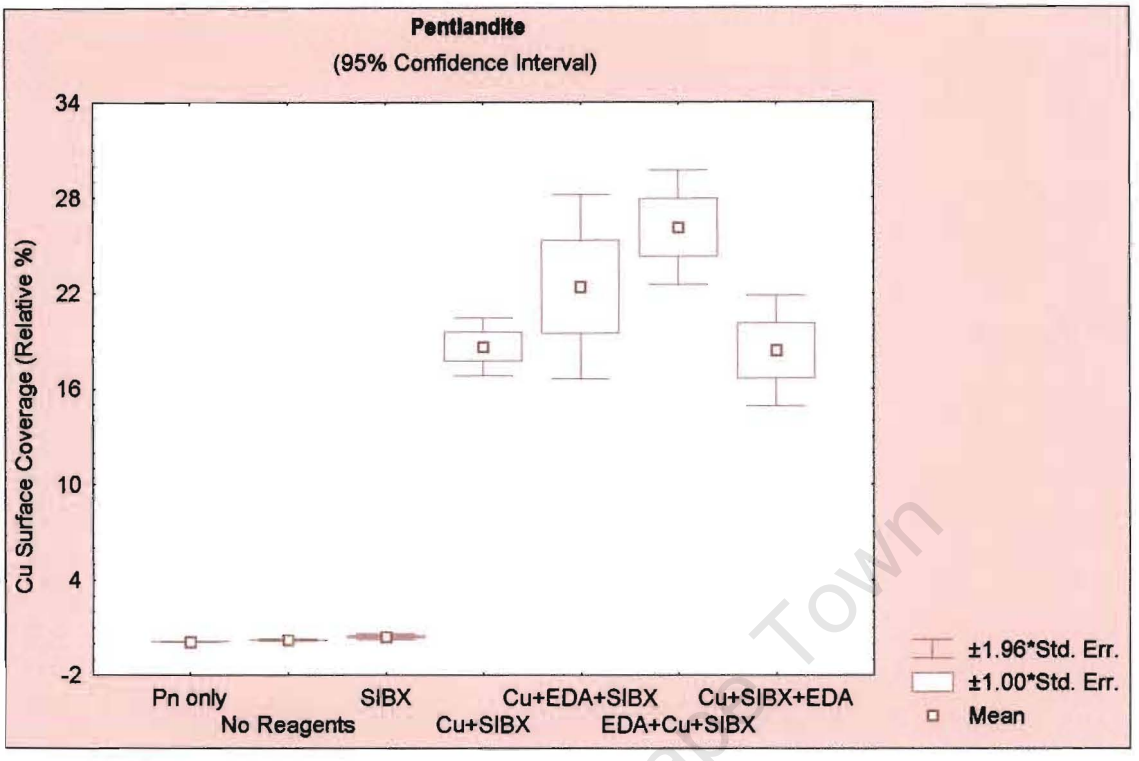

Figure 4.29: Copper ions relative percent surface coverage for pentlandite in synthetic water, *I* = 2.0E-02.

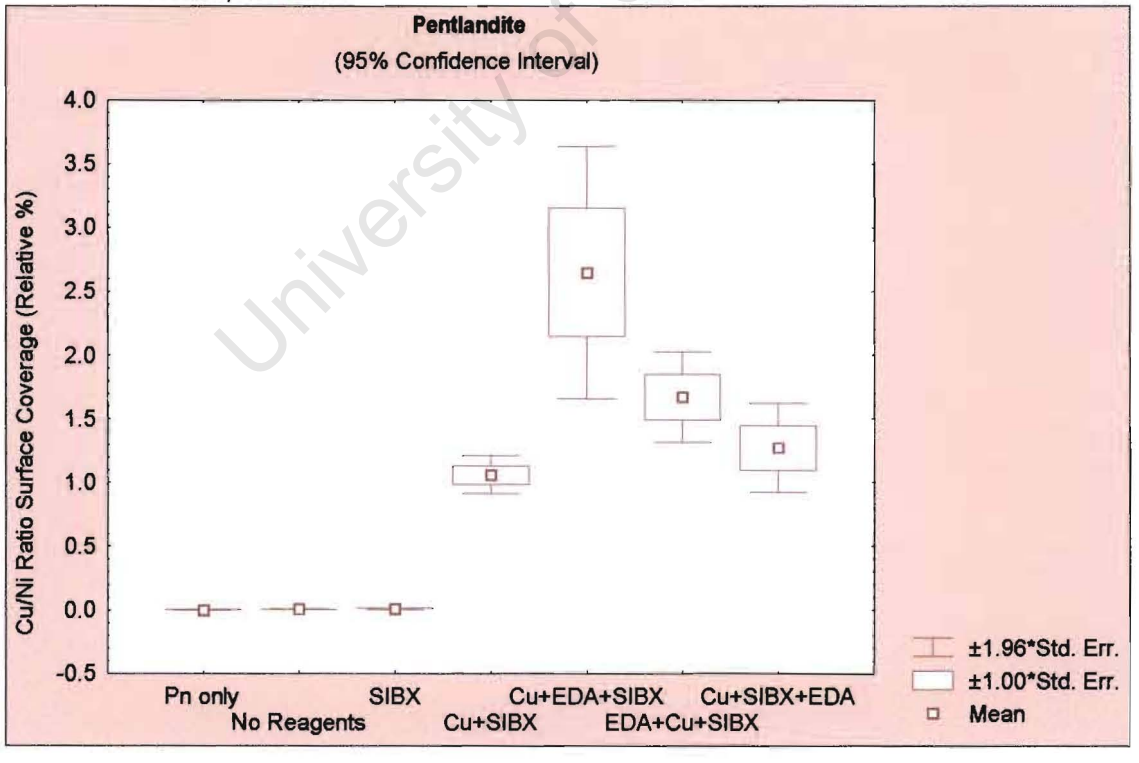

Figure 4.30: Copper/Nickel ratio relative percent surface coverage for pentlandite in synthetic water, *I* = 2.0E-02.

The copper surface coverage for pyroxene (Figure 4.31) shows that the lowest copper concentration is obtained when EDA is added in between the copper sulphate and xanthate additions.

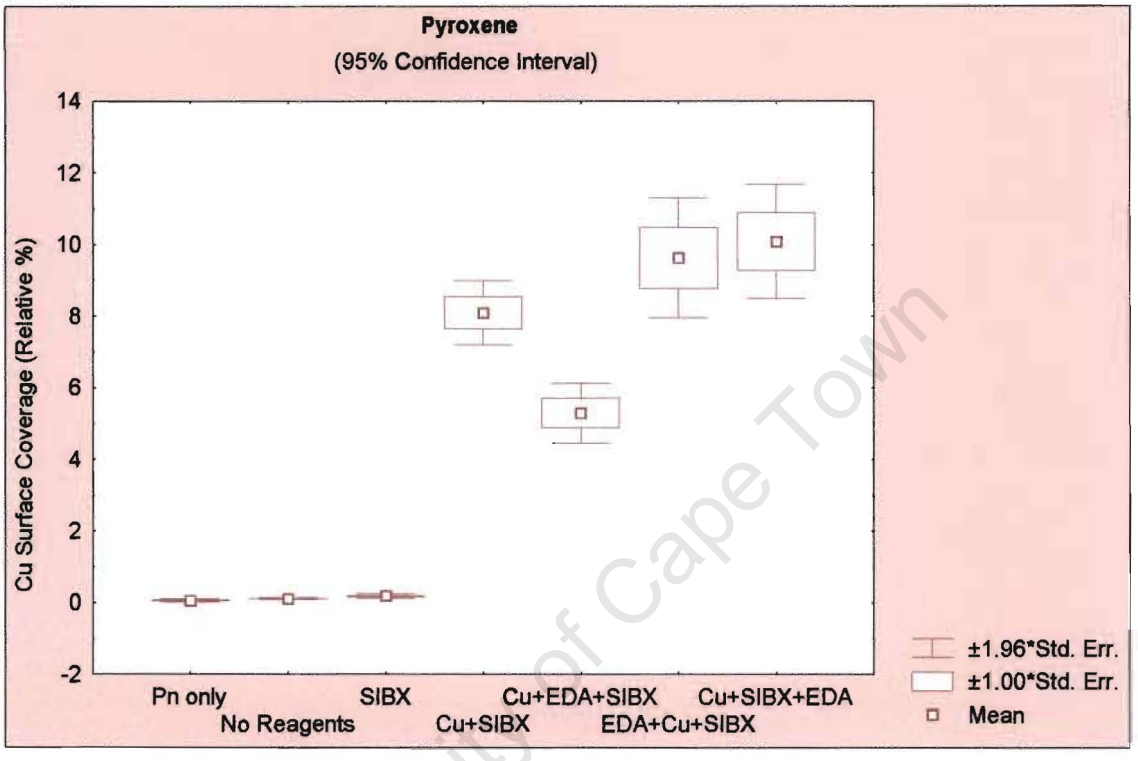

Figure 4.31: Copper ions relative percent surface coverage for pyroxene in synthetic water, I = 2.0E-02.

The results also show that any inadvertent activation by nickel ions is also reduced when EDA is added (Figure 4.32) relative to the copper sulphate and xanthate case. The lowest nickel concentration on the pyroxene surfaces is observed when EDA is added prior to copper sulphate and xanthate. This is attributed to complexing of nickel ions present on the mineral surface from pentlandite dissolution products. Nickel ions will be chelated first with this order of reagent addition since no copper is present in solution yet.

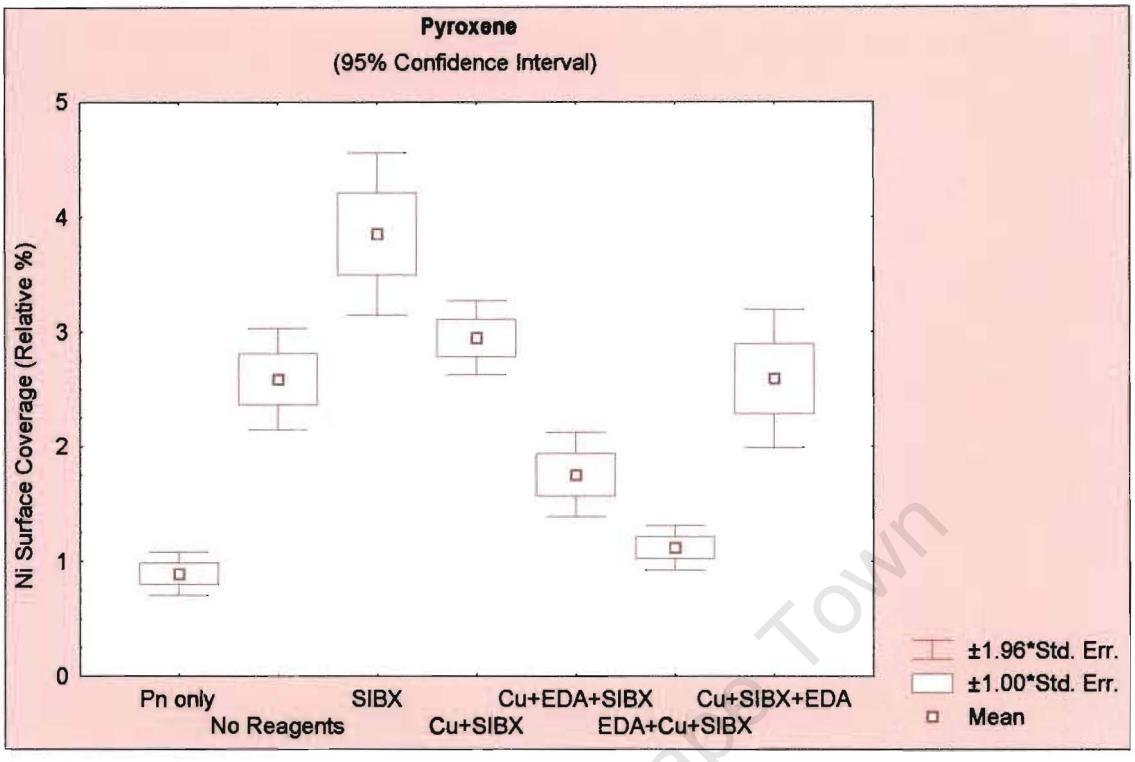

Figure 4.32: Nickel ions relative percent surface coverage for pyroxene in synthetic water, I = 2.0E-02.

The results clearly demonstrate that the order of reagent addition resulted in surface alteration, which affects the pentlandite and pyroxene recovery as well as selectivity.

4.2.3 XPS Analyses

A comparison of pentlandite and pyroxene surfaces with the addition of $CuSO_4$, [$CuSO_4$ + EDA] and [$CuSO_4$ + EDTA] was carried out in an attempt to identify copper species present on the mineral surfaces and quantify the percentage removal of these species due to the addition of complexing agents. EDA and EDTA were chosen since they gave the highest and lowest selectivity between pentlandite and pyroxene during the microflotation tests.

The XPS data with respect to copper coverage for pentlandite and pyroxene at pH 9 is displayed in Figure 4.33, a-f. The results for pentlandite (Figure 4.33, a-c) show that the addition of EDA and EDTA removes around 55 and 27% of the copper present on

the mineral surface, respectively. The binding energy of the Cu $2p_{3/2}$ and Cu $2p_{1/2}$ photoemission lines is 952.5 (+/- 0.2) eV for Cu_2S, which correlates with the binding energy obtained during the XPS analysis of pentlandite. These results indicate that most of the copper is bound to the sulphur atom in the lattice of the mineral which will not be removed by the addition of a complexing agent. The pyroxene results (Figure 4.33, d-f) indicated that the addition of EDA and EDTA removes around 75 and 11% of the copper present on the mineral surface, respectively. The species that was removed is most likely to be copper(II) oxide, which correlates with a binding energy of 933.3 (+/- 0.2) eV for pyroxene. The Cu 2p spectrum of the divalent $Cu(OH)_2$ shows well-defined satellites on the high binding energy sides of the core peaks. In contrast, there is no clear satellite in the spectra of the copper activated pentlandite and pyroxene minerals.

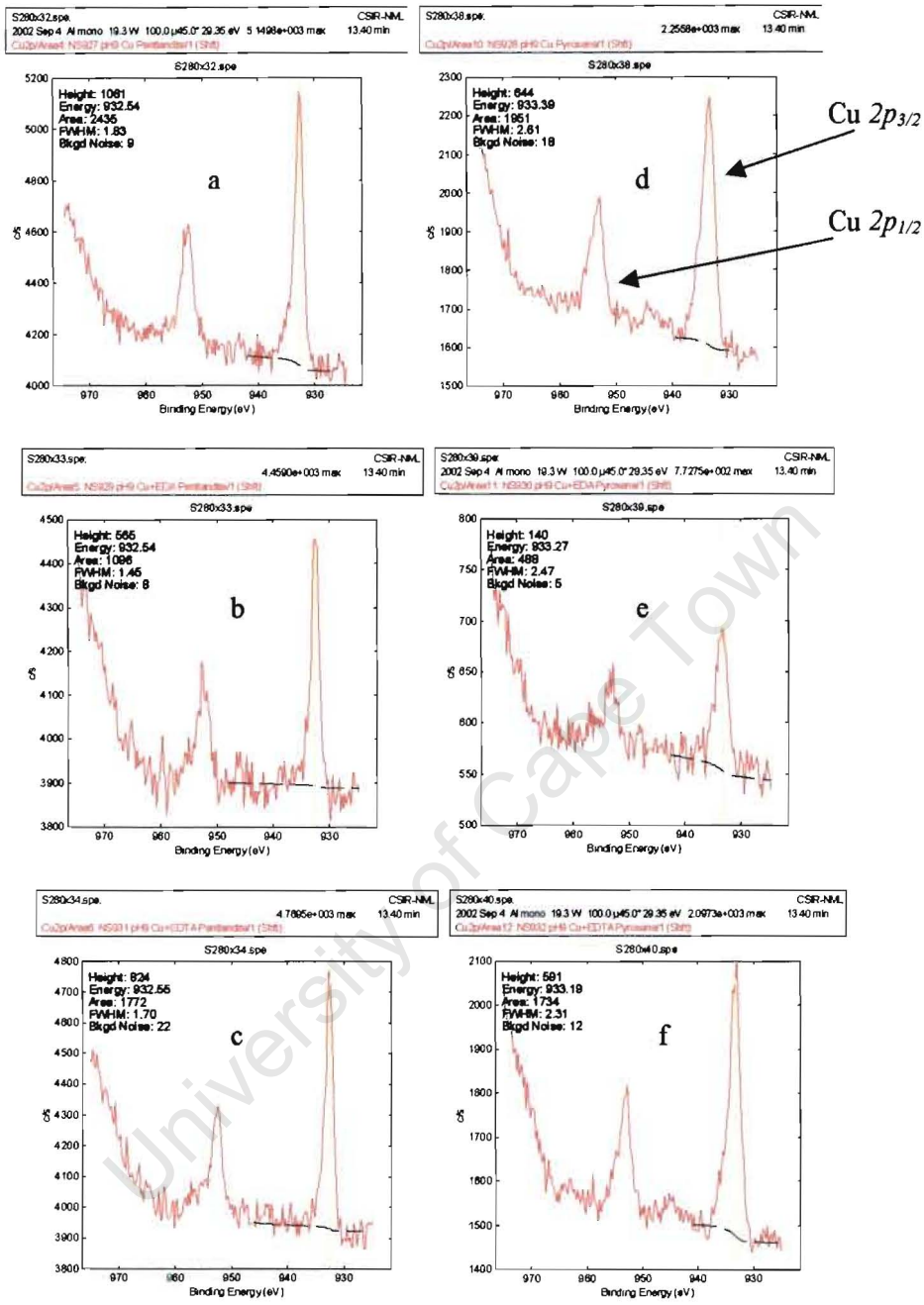

Figure 4.33: Cu 2p spectral region for pentlandite and pyroxene 1:1 mixture in synthetic water, *I* = 2.0E-02, a and d) addition of copper sulphate (5.00E-05M), b and e) addition of copper sulphate (5.00E-05M) and EDA (4.00E-05M), c and f) addition of copper sulphate (5.00E-05M) and EDTA (4.93E-05M).

4.2.4 Summary

The microflotation data have indicated:

- A high flotation response for pentlandite and pyroxene in the presence of copper sulphate and xanthate.
- The need for the use of a complexing agent to reduce the pyroxene recovery by removing the activating metal ions from the mineral surface.
- EDA has proved to be the best complexing agent for the system studied at pH 9 with respect to pentlandite recovery and selectivity over pyroxene.
- Variation in the sequence of reagent addition and copper sulphate and xanthate concentrations showed no added benefit.

The zeta potential determinations have shown:

- Pentlandite and pyroxene become copper activated in the presence of copper sulphate.
- Xanthate adsorption was observed on copper activated mineral surfaces.
- The addition of the complexing agents reduces the concentration of copper species from pentlandite and pyroxene minerals surfaces but predominantly from pyroxene surfaces.
- EDTA showed the least ability to reduce copper and nickel species from pyroxene mineral surfaces.

The ToF-SIMS data has shown:

- Pentlandite and pyroxene are copper activated in the presence of copper sulphate.
- The addition of the complexing agents, DETA, EDA and TETA reduce the concentration of copper and nickel ions on pyroxene mineral surfaces.
- Xanthate adsorption on pyroxene surfaces is approximately 10 times lower compared to that of pentlandite, which reduced further in the presence of the DETA, EDA and TETA.

- EDTA once again showed the least ability to reduce copper and nickel species from pyroxene mineral surfaces.
- The variation in the addition point of EDA to a copper sulphate and xanthate trial affects the concentration of copper on both pentlandite and pyroxene mineral surfaces.

The XPS data has shown:

- Pentlandite and pyroxene are copper activated in the presence of copper sulphate.
- EDA reduces the copper concentration on pentlandite and pyroxene surfaces by 55 and 75%, respectively compared to EDTA, which reduced the copper concentration by 27 and 11%, respectively.

CHAPTER 5

DISCUSSION

Evaluation of the complexing agents, DETA, EDA, TETA and EDTA, for use in the flotation of pentlandite and pyroxene systems, has revealed differences as well as similarities with respect to floatability, selectivity and surface alteration for the system studied. In order to understand the way complexing agents function in flotation systems one must first understand their solution chemistry and how they interact with metal ions.

5.1 Chelate Chemistry

5.1.1 Chelate Chemistry Fundamentals

The choice of a chelating agent is made on the basis of its function in well-known analytical metal separations. The major donor atoms are S, N, O and P. The basic requirements chelating agents must satisfy to form a chelate are that the ligand molecules should have suitable functional groups and that the functional groups must be situated to permit the formation of a ring with a metal as a closing member. These two conditions are necessary but not sufficient for the formation of a chelate ring (Somasundaran and Nagaraj, 1984). This section describes the structure, coordination sites, complex formation, and selectivity (formation constants) for the complexing agents as well as the metal ion (copper) used during the study. In Chapter 5.1.2, it will be attempted to translate these fundamental concepts about chelate chemistry to flotation systems.

The structure of the complexing agents shows that DETA, EDA and TETA are all linear polyamines and EDTA is an amino acid (Chapter 2.4.2, Figures 2.5a, 2.6a, 2.7a and 2.8a). The major difference between these complexing agents is that they coordinate with copper ions differently and some are more selective than others. For example, iron(III) complexes have a very low affinity for amine ligands, except for, EDTA (Cotton and Wilkinson, 1980) and TETA (Beck and Gorog, 1958). This is evident in Table 5.1 where Fe^{3+} ions have a high log K of 25.1 and 21.7, indicating their affinity to easily coordinate with EDTA and TETA, respectively.

Table 5.1 shows the equilibrium constants used to define the reactions between metals and ligands, these constants are termed the stability constants or formation constants. They are a measure of the tendency toward formation of metal chelates in aqueous solutions, the magnitude of which gives a quantitative measure of the relative stabilities of the various chelates. A comparison of the formation constants (log K values) for different ligands shows the selectivity of one ligand over another. Selectivity can be described as the ligand's ability to preferentially bind to one metal ion, or group of metal ions, in the presence of others. It is the thermodynamic stability of the complex, which is expressed by the relative stability constants for complex formation (Cotton and Wilkinson, 1980 and Chaberek and Martell, 1959).

Complex formation can be expressed quantitatively by either stepwise stability constants: $K_2 = [ML_2]/[ML][L]$ or by cumulative stability constants: $\beta_2 = [ML_2]/[M][L]^2$. It is often convenient to consider the overall process of adding *n* ligands to a metal ion, rather than the individual stepwise equilibria. The stability constants for the sum of several reactions (or for the product of their equilibrium expressions) are called a cumulative constant. The cumulative constant is given the symbol β_n for the addition of *n* ligands to a metal ion. β is used uniquely to designate the cumulative addition of any combination of free components, M, L, and H. The stepwise and cumulative constants are related by: $\beta_n = K_1.K_2...K_n$. (Covington, 1997 and Pankow, 1991).

Metal Complex	Log K					
	Cu^{2+}	Ni^{2+}	Fe^{2+}	Fe^{3+}	Ca^{2+}	Mg^{2+}
M(DETA)	16.0	10.7	6.23			
$M(DETA)_2$	5.3	8.2				
M(EDA)	10.8	7.9	4.4			
$M(EDA)_2$	9.4	6.6	3.3			
$M(EDA)_3$	0.1	4.7	2.0			
M(TETA)	20.5	14.1	7.8	21.7*		
M(EDTA)	18.3	18.4	14.3	25.1	10.7	8.7

Table 5.1: Formation constants of metal complexes at 20°C, I = 0.1 (Chaberek and Martell, 1959, * Beck and Gorog, 1958).

As depicted in Table 5.1, DETA and EDA will only form complexes with Cu^{2+}, Ni^{2+} and Fe^{2+} ions in that order of preference, while TETA will form complexes with Fe^{3+} ions first followed by Cu^{2+}, Ni^{2+} and Fe^{2+} ions in that order of preference, depending on the concentration of the ligand. EDTA will form complexes with most of the transition and many non-transition metals and selectivity is achieved by regulation and maintenance of the pH or by the addition of masking agents. Selectivity between the complexing agents is achieved by making use of the stability constants and chelate formation under various solution conditions.

The major factors that determine the stability constants are, in order of decreasing importance,

- The p*K*a of the ligand molecule, which represents the tendency of the donor atoms to donate electrons to metal atoms to form a chelate.
- Substituents, i.e. substitution on the chelating molecule have important effects as it alters the p*K*a and/or it introduces steric factors for the formation of a chelate (electron donating or withdrawal tendencies of organic groups).
- Nature of donor atoms (weak/strong acid or base, hard or soft ligand).

- Central metal atom (hard or soft metal).
- Ring size (preferred cation size).
- Number of rings (ligand denticity, steric effects).

The first four factors are very important as they determine the nature and strength of the bonds (Somasundaran and Nagaraj, 1984).

Chaberek and Martell (1959) have observed that stable compounds are formed between ligands and copper ions until a total of four groups have become attached to the metal. Any further addition of ligands results in very little or no increase in stability, therefore copper has been assigned a coordination number of 4. A chemical reaction occurs when a chelating agent bonds to a copper ion, either in solution or at the mineral surface. The formation of the copper chelate involves bonding of the copper ion through covalent and coordination bonds with the electron-donor atoms of the functional group of the chelating reagent (Fuerstenau et al. 1999). This occurs by the exchange of water molecules, which are bound to the copper atom, for ligand molecules.

EDA is a bidentate ligand, which when unprotonated, can form two coordinate covalent bonds with a metal atom through the lone pair electrons on both nitrogens. The structure of EDA and 1:1 Cu(II)-EDA chelate was shown in Figure 2.6 (Ch. 2.4.2). In its neutral form, it forms soluble complexes with both copper(I) and copper(II) ions: i.e. $Cu(EDA)^{2+}$, $Cu(EDA)_2^{2+}$ and $Cu(OH)(EDA)^{+}$. Copper-EDA species form at pH values much lower than those at which EDA is hydrolysed in water-EDA systems, reflecting their stability (Aksu and Doyle, 2000).

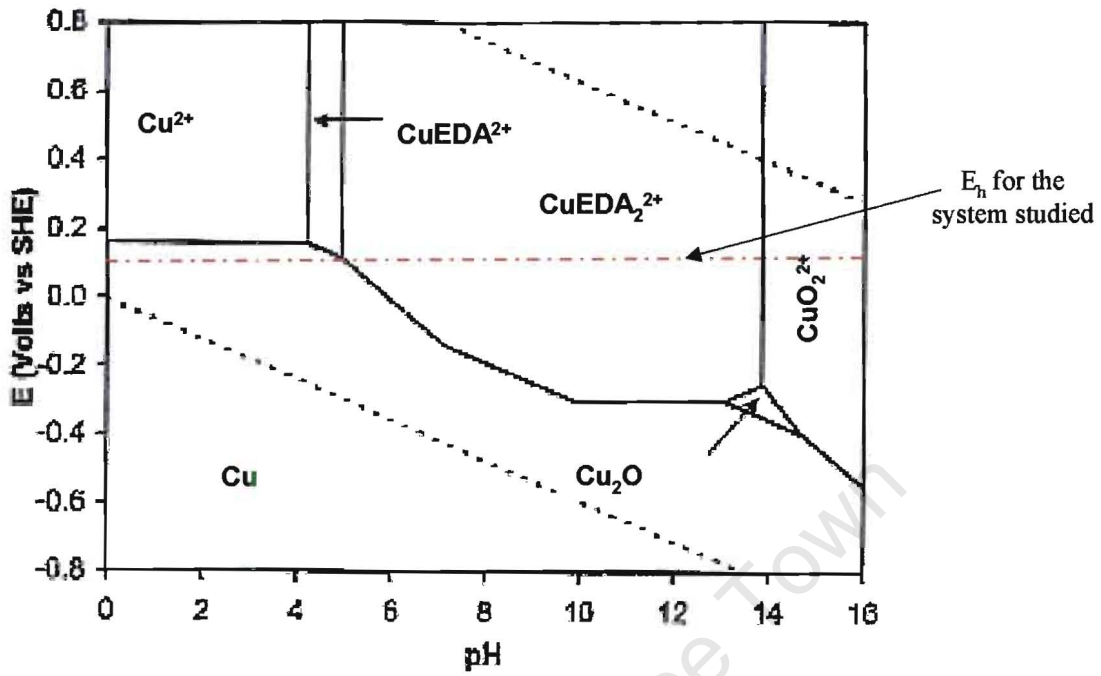

Figure 5.1: Potential-pH diagram for the copper-water-ethylenediamine (EDA) system at 25°C and 1 atm. Total EDA activity, $\{EDA_T\} = 10^{-2}M$; Total dissolved copper activity, $\{Cu_T\} = 10^{-6}M$, (Aksu and Doyle, 2000).

Figure 5.1 shows the potential-pH diagram for the copper-water-EDA system and it can be seen that at pH 9, copper is complexed by two EDA ligands to give $Cu(EDA)_2^{2+}$ species at E_h >0.2 V, the E_h for the system studied was around 0.1 V. This chelate most probably forms via a stepwise ligand substitution reaction, which will be discussed later in Chapter 5.1.2.

DETA is a terdentate ligand (Figure 2.5a, Ch. 2.4.2), which when unprotonated, can form three coordinate covalent bonds with a metal atom through the lone pair electrons on the three nitrogens. For copper metal ions, DETA coordinates through its three amine nitrogens to fill 3 of coppers 4 coordination sites to produce a stable 1:1 Cu(II)-DETA complex. The structure of DETA and 1:1 Cu(II)-DETA chelate is displayed in Figure 2.5 (Ch. 2.4.2). A 1:2 Cu-DETA chelate may be formed if the concentration of the complexing agent is sufficiently high.

TETA is a tetradentate ligand (Figure 2.7a, Ch. 2.4.2), which when unprotonated, can form four coordinate covalent bonds with a metal atom through the lone pair electrons on the four nitrogens. TETA is well adapted to the square-planar requirements of the Cu(II) ion and will produce a 1:1 Cu(II)-TETA chelate. The structure of TETA and 1:1 Cu(II)-TETA chelate is shown in Figure 2.7 (Ch. 2.4.2).

EDTA is a hexadentate ligand and can interact with up to six coordination locations of metal ions through its two amine nitrogens and four carboxylate groups and as such is an extremely effective chelating agent. The associated entropy increase gives very stable complexes. Saturation of coordination positions generally produces single stable 1:1 metal chelates. For copper metal ions, EDTA coordinates through its two amine nitrogens and two of its carboxylate groups to fill copper's coordination number of 4 to produce a stable 1:1 Cu(II)-EDTA complex. The structure of EDTA and 1:1 Cu(II)-EDTA chelate is displayed in Figure 2.8, Ch. 2.4.2.

In summary, it can be seen that there are a number of factors that play a role in complex formation and selectivity, i.e.:

- Ligand molecules should have suitable functional groups which must be situated to permit the formation of a ring with a metal as a closing member.
- Formation/stability constants define reactions between metal and ligands, the magnitude of which gives a qualitative measure of relative stability as well as selectivity of one ligand over another.
- Complex formation is facilitated by the rapid exchange of water molecules and involves the stepwise substitution of coordinated water molecules by other ligands.
- Successive substitutions require higher concentrations of the ligand. This is because successive ligands are bound less strongly to the metal ion.
- A ligand can be polydentate (have several donor atoms capable of electron pair donation to a metal ion). Ligands with 1, 2, 3 and 4 donor atoms are referred to as mono-, bi-, tri- and tetra-dentate. Adjacent donor atoms in polydentate ligands bind to adjacent coordination sites on a metal ion.

- Viewing the periodic table as a whole, major differences in metal-ligand complex stability can be seen, e.g. nature of donor atoms (weak/strong acid or base, hard or soft ligand), central metal atom (hard or soft metal). These differences are strongly related to the choice of donor atoms. In general the donor atom most strongly favoured by a metal ion in solution is the same donor that binds to the metal in its ores.
- Selectivity can be achieved by use of other ligand properties:
    - Size of a chelate ring.
    - Maximum denticity of a ligand (coordination sites).
    - Ligand field strength developed by a ligand.
    - Ability of a ligand to promote spin pairing on a metal ion
    - Steric constraints imposed on or by a ligand.

5.1.2 Solid / Solution Phase Chelate Chemistry

This section attempts to use the fundamental solution chemistry knowledge about the complexing agents to describe the possible mechanisms occurring when complexing copper is also in the solid phase during flotation for the system studied. Since EDA has been shown to be the most effective complexing agent for the system studied, it has been used as an example in copper ion removal from pyroxene mineral surfaces.

The following diagrams show the possible mechanisms of inadvertent copper activation of silicate mineral surfaces as well as the mechanisms for copper removal using EDA, which forms a 1:2 copper(II)-EDA chelate by stepwise ligand substitution. These diagrams are a schematic representation only.

Fuerstenau (1976) reported that adsorption of copper ions onto quartz surfaces may occur by three possible mechanisms. Firstly, it could be a result of hydrogen bonding between the adsorbed hydrogen ion and the hydroxy complex (Figure 5.2).

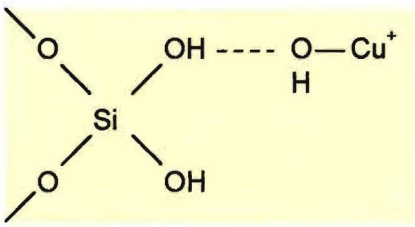

Figure 5.2: Copper adsorption by hydrogen bonding at pH 9.

Secondly, he proposed that an alternative mechanism could be the adsorption of the hydroxy complex by the formation and splitting out of water (Figure 5.3).

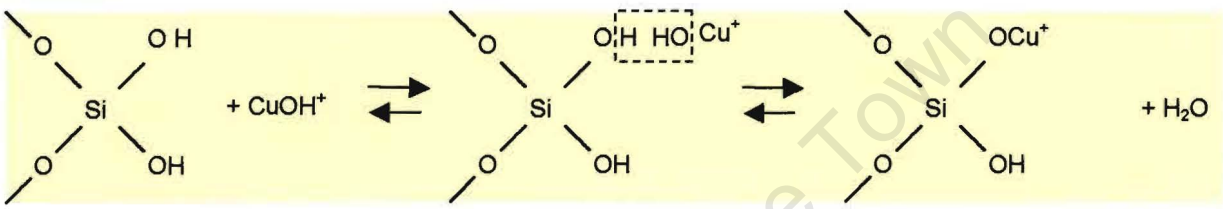

Figure 5.3: Copper adsorption by means of the formation and splitting out of water of the hydroxy complex at pH 9.

A third mechanism would involve the nucleation and growth of a copper hydroxide precipitate at the mineral surface. Any of these adsorption mechanisms would result in a more positive mineral surface charge. It is assumed that these mechanisms play a role in copper ion adsorption onto the pyroxene surfaces. The removal of the copper ion by the addition of EDA would firstly result in the formation of 1:1 Cu(II)-EDA chelate as depicted in Figure 5.4 and secondly in the formation of a 1:2 Cu(II)-EDA chelate at pH 9 (Figure 5.5).

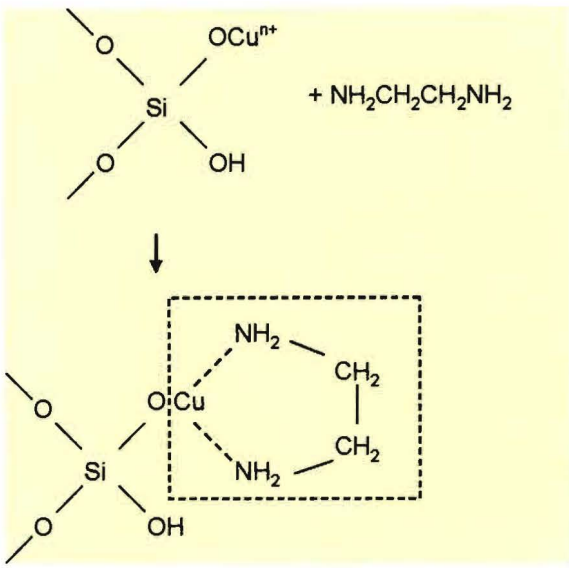

Figure 5.4: Formation of a 1:1 Cu(II)-EDA complex by exchange of water molecules for ligand molecules at pH 9.

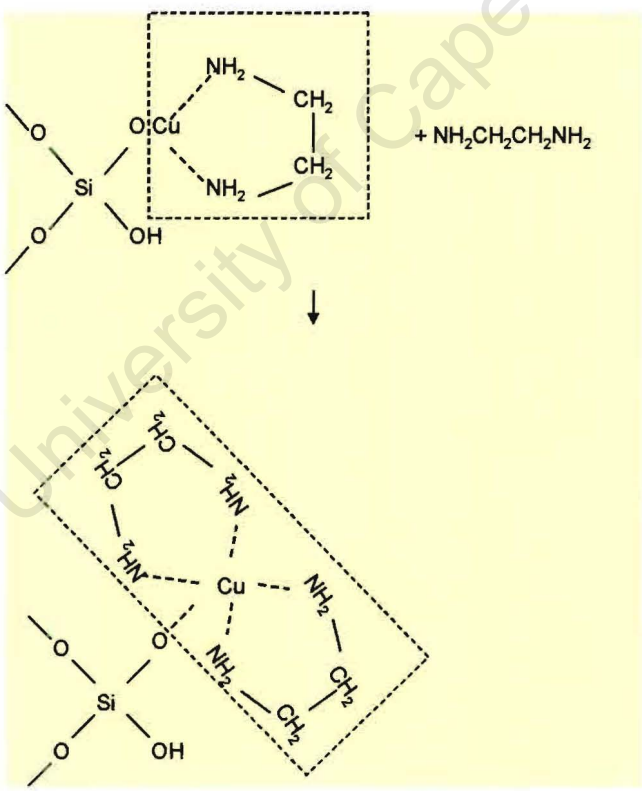

Figure 5.5: Formation of a 1:2 Cu(II)-EDA complex by stepwise ligand substitution and the exchange of water molecules for ligand molecules, sequestering the metal-ligand complex from the mineral surface into solution at pH 9.

The formation of these soluble stable metal chelates remove the inadvertently activated copper(II) and nickel(II) ions from the pyroxene mineral surfaces into solution. This is accomplished by stepwise reactions, which would occur rapidly, and the equlibria most probably overlaps since the relative magnitudes of the successive formation constants are very similar (Table 5.1). These stepwise reactions occur as a result of ligand substitution of water molecules by another ligand (EDA). The breaking of M-OH_2 bonds is an endothermic reaction and the making of the M-L bond is an exothermic process. Successive ligands are bound less strongly because each new ligand transfers electron charge to the metal and thus decreases its Lewis acid strength. A consequence of successive formation complexes, ML, ML_2, ML_3.... requires larger concentrations of the ligand to drive the equilibrium, $ML_n + L = ML_{n+1}$, to the right. Thus with increasing ligand concentration each of the following reactions will dominate in turn:

$$M + L = ML$$
$$ML + L = ML_2$$
$$ML_2 + L = ML_3$$

until the number of L donor atoms coordinated is equal to the maximum coordination of the metal ion. The coordination number is a property of the metal ion, not the ligand. For Cu^{2+}, in which the complex ion is tetragonal with 4 short and two long bonds, the coordinating number, N, is taken as 4, i.e. $L_{max} = 4$ (Cotton and Wilkinson, 1988).

For the complete formation of the metal-ligand complex to take place, it is readily seen by calculating the concentration of the ligand, [L], required to drive the conversion of ML_{n-1} into M_n to essential completion. Consider the Cu^{2+} - EDA reaction where M = Cu^{2+} and L = EDA.

For the reaction	$M + L = ML$,	$K_1 = [ML]/[M][L] = 10^{10.8} = 6.3E+10$
	$ML + L = ML_2$	$K_2 = [ML_2]/[ML] = 10^{9.4} = 2.5E+10$
	$ML_2 + L = ML_3$	$K_3 = [ML_3]/[ML_2] = 10^{0.1} = 1.26$

Starting from the aqua metal (M) ion, i.e. copper(II) ion with six water molecules attached, when 99% of the total metal is converted into ML.

$$[ML]/[M] = 99/1 = K1[L].\ \text{Thus, } [L] = 99/K_1 = 1.6E\text{-}09\ M$$

Starting from ML, when 99% of the total metal is converted into ML_2.

$$[ML_2]/[ML] = 99/1 = K2[L].\ \text{Thus, } [L] = 99/K_2 = 3.9E\text{-}08\ M$$

Starting from ML_2, when 99% of the total metal is converted into ML_3.

$$[ML_3]/[ML_2] = 99/1 = K3[L].\ \text{Thus, } [L] = 99/K_3 = 79\ M$$

The above calculations indicate that the dosage used during the study for EDA (4.0E-05M) is sufficient to form the 1:2 Cu(II)-EDA complex. Calculations were also performed for the other complexing agents that were evaluated and are shown in Table 5.2. The results indicate that there is sufficient reagent to form the 1:1 Cu(II)-DETA, TETA or EDTA complexes. DETA can form 1:2 Cu(II)-DETA complexes but the dosage (6.98E-05M) used for the study was too low for this complex to form. These ligand concentrations also show that there is only enough EDA to complex the copper(II) ions added to the system and possibly the small amount of nickel(II) ions present from pentlandite dissolution as the 1:2 metal-EDA complexes.

Metal Complex	Concentration of Ligand Required for Complete Formation of Metal-Ligand Complexes					
	Cu^{2+}	Ni^{2+}	Fe^{2+}	Fe^{3+}	Ca^{2+}	Mg^{2+}
	Mol/dm^3					
M(DETA)	9.9E-15	1.9E-09	5.8E-05			
M(DETA)$_2$	5.5E-04	6.3E-07				
M(EDA)	1.6E-09	1.3E-06	3.9E-03			
M(EDA)$_2$	3.9E-08	2.5E-05	5.0E-02			
M(EDA)$_3$	79	1.9E-03	9.9E-01			
M(TETA)	3.1E-19	7.9E-13	9.9E-15	1.9E-20		
M(EDTA)	5.0E-17	3.9E-17	9.9E-15	7.9E-24	1.9E-09	1.9E-07

Table 5.2: Ligand concentrations for complete formation of the Metal-Ligand complexes at 20°C, I = 0.1.

The chelate chemistry fundamentals have shown that the general stability trend of the complexing agents tested is EDTA>TETA>DETA>EDA with respect to the coordination sites of 1:1 copper(II) chelates (Table 5.1). However, EDA would become more stable by attaching two chelate rings to one copper ion forming a 1:2 Cu(II)-EDA chelate. The cumulative formation constant (log β) for this 1:2 Cu(II)-EDA chelate is 20.3 (Table 5.1), the increase in stability for every ring added is greatly increased in more dilute solutions for a metal and ligand at similar concentrations, this is based on the relative degrees of dissociation of metal chelates and metal complexes which can be calculated from stability constants. The interaction of metal ions with sequestering agents such as EDA is governed to a large extent by steric effects derived from both the ligand and the metal and when a number of electron donor groups are bound together into a single chelate, the importance of steric effects is greatly increased, and stability depends on a number of other ligand characteristics, such as size and number of chelate rings formed. For complete understanding of the process of the metal chelate formation in aqueous solution, it is desirable to determine the standard changes in free energy ($\Delta F°$), enthalpy ($\Delta H°$) and entropy ($\Delta S°$) (Chaberek and Martell, 1959). All the above factors become

significant to varying degrees resulting in the system that has the most disorder being favoured as this results in the greatest stability.

It has been shown that many factors affect the stability of the metal-ligand complexes and it is not fully understood why EDA is better than the other complexing agents tested except for the fact that only EDA forms a 1:2 Cu(II)-Ligand chelate for the system studied. The remaining discussions on surface alteration and floatability may highlight why EDA is such an effective complexing agent at pH 9 compared to DETA, TETA and EDTA.

5.2 Surface Analysis

5.2.1 Zeta Potential Determinations

Zeta potential determinations are used to study the electrokinetic phenomena at mineral-collector interfaces. This information can thus be used to assist in predicting flotation behaviour of a mineral in an aqueous system. Reproducibility tests were carried out to establish the reliability of the zeta potential determination procedure used during the study. As demonstrated by the zeta potential / pH curves (Figure 4.13) and the low standard deviation for each pH measured (Table 4.3), the technique and the procedure used gave reproducible results.

Zeta potential determinations for pentlandite and pyroxene using individual reagents on their own are shown in Figures 4.14 and 4.15, respectively. For pentlandite in the absence of reagents two pH_{iep} (isoelectric point pH) were observed. Unoxidised sulphides in general have a pH_{iep} of about 2 (Acar and Somasundaran, 1992) and as the mineral surfaces oxidise and become coated with impurities, a higher pH_{iep} is displayed. The lower iep value, viz 5.2, can be attributed to the formation of iron oxides [FeO (iep 6.7-8.2), Fe_3O_4 (iep 6.5), Fe_2O_3 (iep 6.7-8.2)] and iron hydroxide (FeOOH, iep 7) on the pentlandite surfaces while the higher iep value, namely 10, may be due to the formation of nickel oxide (NiO, iep 10.3) and nickel hydroxide ($Ni(OH)_2$, iep 11.1) surface precipitate (Acar and Somasundaran, 1992). Iron and nickel speciation

diagrams are given in Figures 5.6, 5.7 and 5.8. The diagrams show that Fe^{2+}, Fe^{3+} and Ni^{2+} ions are predominant at acidic pH and oxides and hydroxides are formed at alkaline pH.

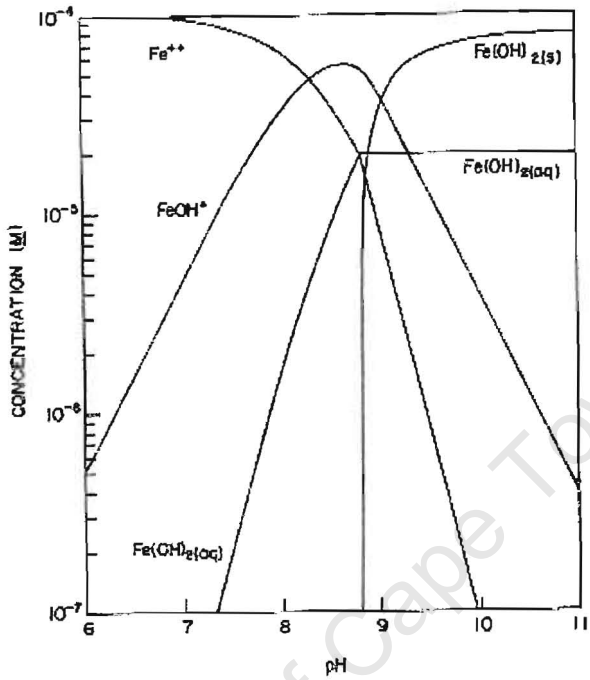

Figure 5.6: Logarithmic concentration diagram for 1X10^{-4}M Fe^{2+} (Fuerstenau, 1976).

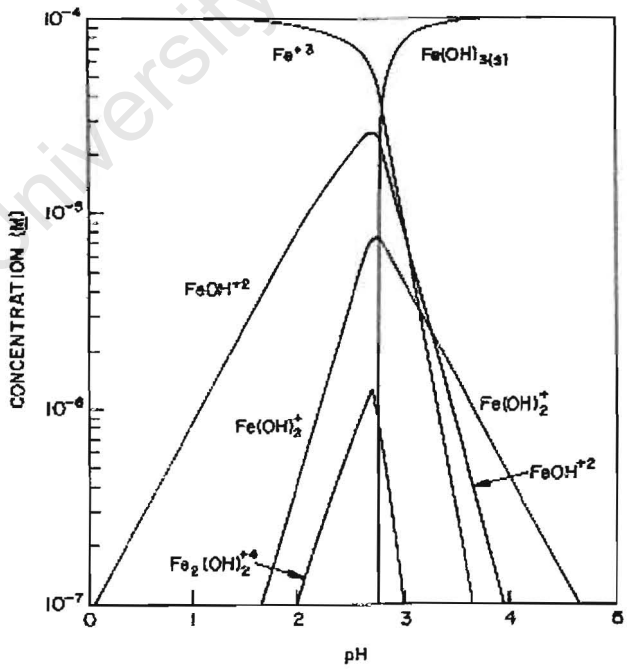

Figure 5.7: Logarithmic concentration diagram for 1X10^{-4}M $FeCl_3$ (Fuerstenau, 1976).

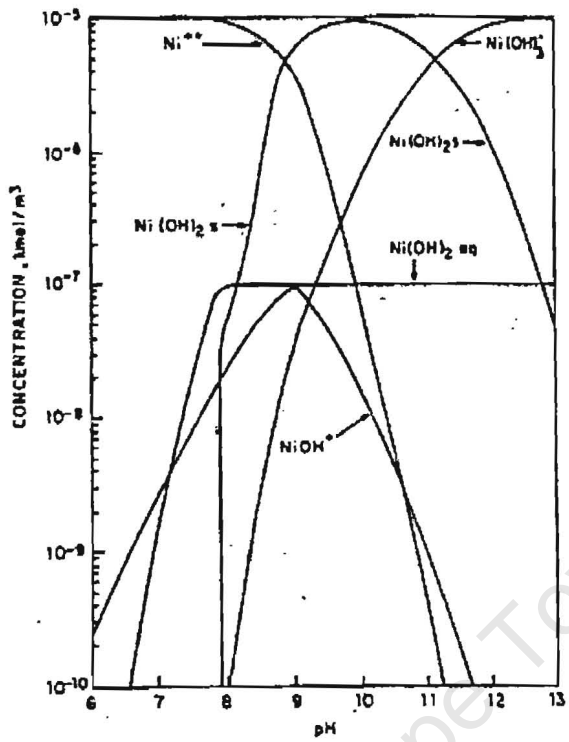

Figure 5.8: Logarithmic concentration versus pH diagram for nickel species. The $Ni(NO_3)_2$ concentration is 6.62X10^{-3}M Ni^{2+} (Mackensie and O'Brien, 1969).

The addition of copper sulphate resulted in a shift of the zeta potential / pH curves to more positive values for pentlandite and pyroxene from pH 6. This indicates that Cu^{2+} ions as well as various positively charged copper hydroxide species ($CuOH^+$, $Cu_2(OH)_2^{2+}$), which are predominant below pH 9.5 (Acar and Somasundaran, 1992), adsorb onto pentlandite and pyroxene surfaces (Figures 4.14 and 4.15). The concentrations of these species are pH dependent and they are known to specifically adsorb onto mineral surfaces (Wang et al. 1989 and Fuerstenau, 1976). The iep value of copper oxide/hydroxide occurs at pH ~ 9.5 (Fullston et al. 1998). Figure 5.9 shows the copper speciation diagram which shows that the predominant species at pH 9 at a copper concentration of 1E-05M is $Cu(OH)_2$ precipitate.

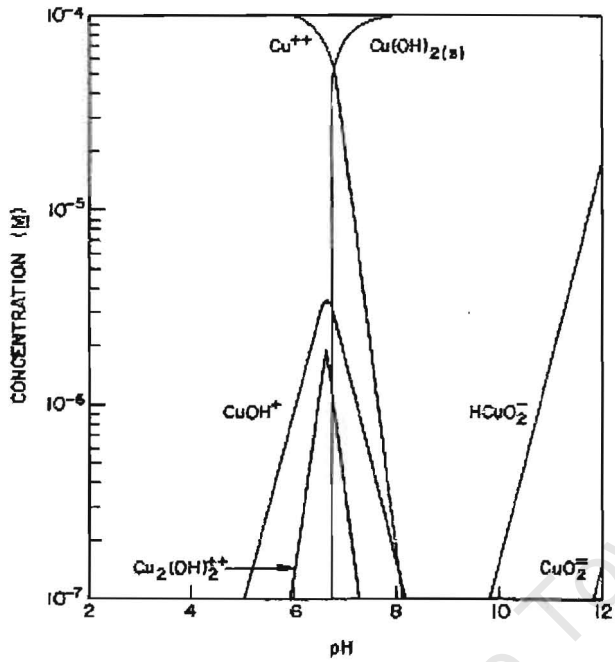

Figure 5.9: Logarithmic concentration diagram for $1X10^{-4}$M Cu^{2+} (Fuerstenau, 1976).

In the presence of xanthate the data obtained clearly showed that SIBX on its own readily adsorbs onto the pentlandite surfaces between pH 5 and 9 when compared to the zeta potential / pH curve in the absence of any reagents. This involves a reaction between xanthate and nickel sites (chemisorption) which arises from an anodic process involving oxidation of the collector, which is coupled to a cathodic process, this involves the reduction of dissolved oxygen at other surface sites to remove the electrons donated by the oxidation process (Hodgson and Agar, 1989). The data obtained also showed that SIBX on its own does not readily adsorb onto the pyroxene surfaces (Figures 4.14 and 4.15) since there is no change in the zeta potential / pH curves in the absence or presence of SIBX.

The addition of the complexing agents, DETA, EDA and TETA resulted in a positive shift of the zeta potential / pH curve at pH 4. This may be attributed to the adsorption of these reagents on minerals surfaces and/or the formation of nickel chelates on the pentlandite surfaces since they are all positively charge species when protonated or

chelated with nickel ions. EDTA on the other hand is negatively charged when protonated and would complex the positively charged iron species on the pentlandite surfaces. This would result in a negative shift in the zeta potential / pH curve, particularly for pentlandite (Chaberek and Martell, 1959).

The zeta potential results for copper activated pentlandite and pyroxene mineral surfaces in the presence of the complexing agents (Figures 4.16 and 4.17) show that at pH 4 the complexing agents adsorb onto the mineral surfaces forming positive copper(II) chelates. At pH 6 the change in zeta potential for pentlandite surfaces is minor due to the nature of the copper(II) ions bond onto the mineral surfaces. Most of the copper(II) ions would bond to sulphur forming a strong CuS bond, which the complexing agent would not be able to break. At a higher pH (>7) copper oxide and hydroxide species are prevalent (Figure 5.9) which the complexing agents will sequester (form soluble stable metal chelates) to varying degrees, depending on their coordination with copper(II) ions, from both pentlandite and pyroxene surfaces.

A comparison of the DETA, EDA, TETA and EDTA zeta potential / pH curves indicates that EDTA is less selective for copper species particularly in the case of pyroxene surfaces. This may be attributed to the fact that EDTA coordinates through its two amine and four carboxylate groups. Oxygen containing chelate compounds readily form complexes in alkaline solutions and since oxygen is the most electronegative of the O, N, S and P donor atoms, consequently, oxygen invariably forms ionic bonds with a majority of elements in the periodic table. Thus, chelating agents with O-O donors form chelates with a large number of metals and are therefore less selective (Somasundaran and Nagaraj, 1984). The results obtained show that this is the case in the system studied for pentlandite and pyroxene mixtures. The formation constants for iron(III) compared to copper(II) EDTA complexes is much higher and this would result in the reagent being consumed with complexing iron(III) ions (Table 5.1). This would explain why EDTA does not show any selectivity for copper ions although the XPS data showed that some copper was being removed. To achieve selectivity between pentlandite and pyroxene using EDTA, an increase in reagent dosage is necessary, however, the

addition of an excess of EDTA is known to depress sulphide minerals in flotation (Wang and Forssberg, 1990).

Further testwork investigated the effect xanthate has on copper activated mineral surfaces in the presence and absence of the complexing agents. For both pentlandite and pyroxene, the results (Figures 4.18 and 4.19) show that where copper was adsorbed on mineral surfaces, xanthate would also adsorb which is indicated by the shift in zeta potential/pH curve to more negative values. The copper-xanthate complex on pyroxene may introduce hydrophobicity and thus true flotation. However, for pyroxene, where the complexing agents have been added the addition of xanthate resulted in a lower degree of xanthate adsorption. This is shown by a smaller shift in the zeta potential / pH curve to less negative values compared to the copper sulphate and xanthate trial. This is attributed to a lower copper surface coverage (Figure 4.19) thus reducing pyroxene recovery.

In summary, the zeta potential determinations have shown:

- Pentlandite and pyroxene become copper activated in the presence of copper sulphate and therefore copper adsorption is non-selective.
- Xanthate adsorption was observed on copper activated mineral surfaces.
- The addition of the complexing agents reduced the concentration of copper oxide and hydroxide species from pentlandite and pyroxene minerals surfaces but predominantly from pyroxene surfaces.

5.2.2 ToF-SIMS and XPS Analyses

ToF-SIMS and XPS analyses were carried out with the aim of gaining an understanding of mineral surface alterations and linking those to flotation recovery.

ToF-SIMS and XPS data have shown, like the zeta potential determinations, that pyroxene becomes copper(II) activated in the presence of copper sulphate (Figures 4.22 and 4.33). The ToF-SIMS data has also revealed that pyroxene is inadvertently

activated by Ni(II) ions as a result of pentlandite dissolution due to superficial oxidation (Figure 4.27). This would result in a higher pyroxene recovery in a pentlandite-pyroxene mixture and thus lower selectivity. ToF-SIMS images of pyroxene mineral surfaces that have been treated with copper sulphate and xanthate are shown in Figure 5.10. These images clearly demonstrate that pyroxene is inadvertently activated by copper and nickel ions due to the addition of copper sulphate and dissolution of pentlandite, respectively.

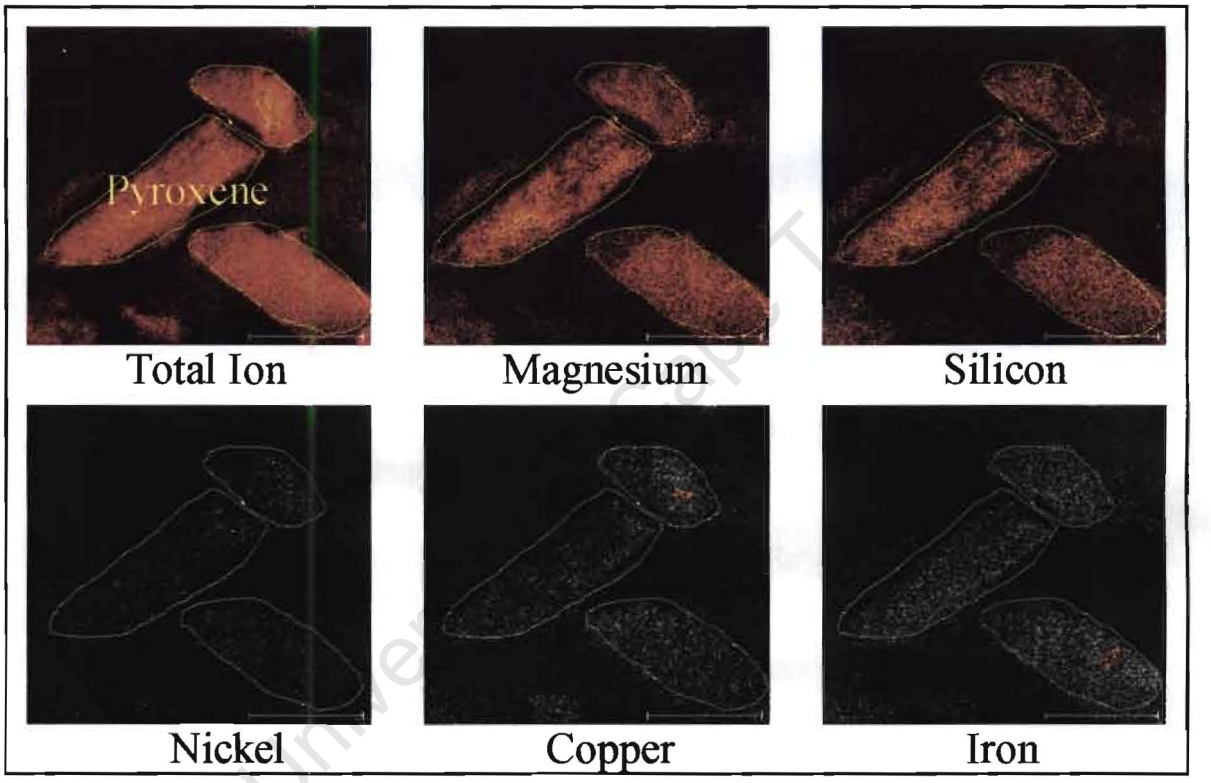

Figure 5.10: Images of pyroxene grains which were treated with copper sulphate (5.00E-05M) and xanthate (5.00E-05M) in mixture with pentlandite using synthetic water, *I* = 2.0E-02 at pH 9.

The ToF-SIMS data indicated that in the presence of DETA, EDA and TETA, the concentration of copper(II) and nickel(II) ions found on pyroxene and pentlandite surfaces were reduced to varying degrees, but predominantly on pyroxene (Figures 4.22, 4.23, 4.26 and 4.27). The ToF-SIMS images of pentlandite and pyroxene grains that have been treated with copper sulphate, EDA and xanthate in that sequence are

shown in Figure 5.11. The images show that the copper and nickel concentrations on the pyroxene mineral surfaces are significantly lower relative to Figure 5.10, thereby reducing the ultimate hydrophobicity of the pyroxene mineral surface.

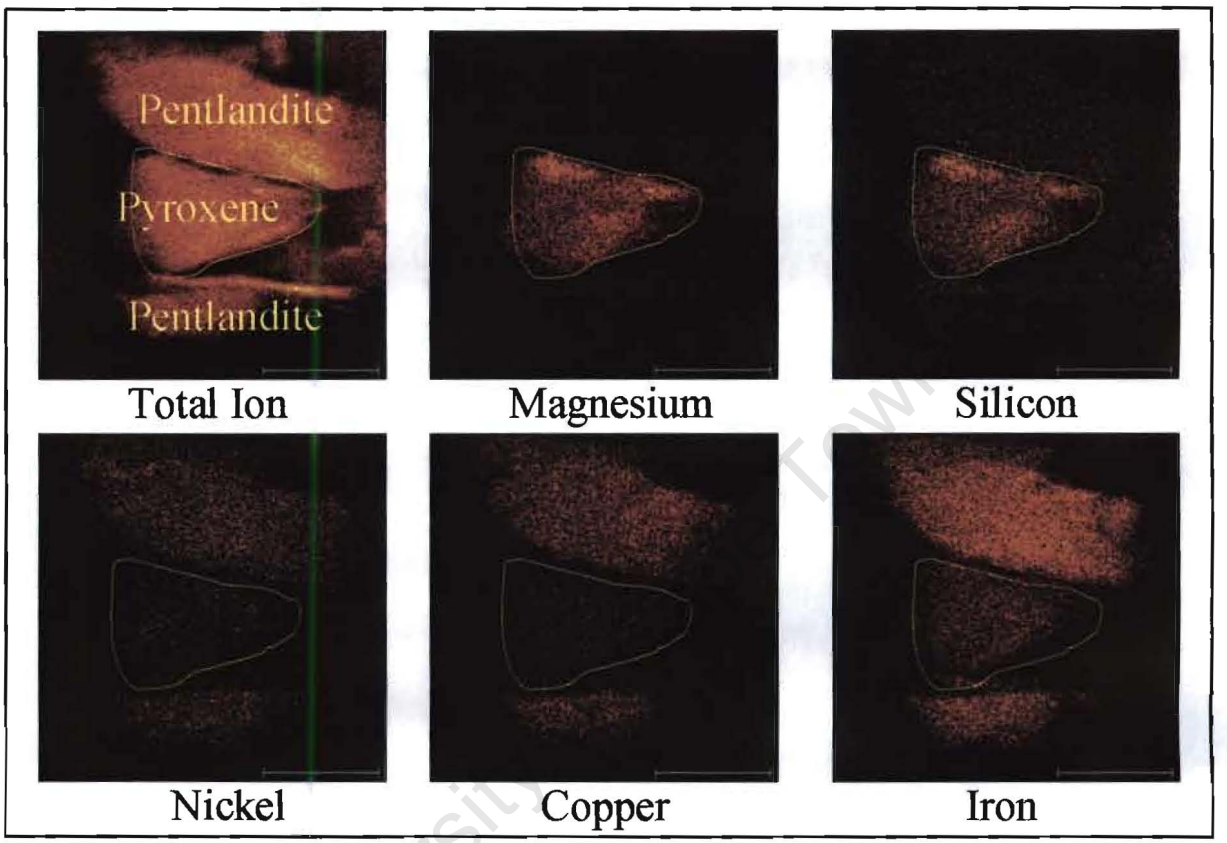

Figure 5.11: Images of pentlandite and pyroxene grains treated with copper sulphate (5.00E-05M), followed by EDA (4.00E-5M) and xanthate (5.00E-05M) in synthetic water, *I* = 2.0E-02 at pH 9.

The XPS data for pentlandite and pyroxene in the presence and absence of EDA and EDTA with respect to copper concentrations on the mineral surfaces followed similar trends to those observed for the zeta potential determinations; EDA reduced the copper concentration significantly from pyroxene surfaces compared to EDTA. The results for the ToF-SIMS showed opposite trends compared with the XPS data for pentlandite, i.e. a higher copper concentration was observed for the EDA case compared to the EDTA case (Figures 4.22 and 4.33a, b and c). This may be attributed to a number of impurities observed in the spectra during the analysis of the samples where EDTA was

added; this would result in lower copper intensities. Another possible explanation could also be that the ToF-SIMS technique analyses the very top monolayer of the mineral surface and depending on the uniformity of the copper coverage, variation in intensities would be observed while the XPS technique analyses around a depth of 4 nm and would therefore account for all the copper on the mineral surfaces.

The ToF-SIMS data showed that the xanthate coverage on the pentlandite mineral surfaces was approximately 10 times higher compared to that of pyroxene indicating the affinity of xanthate for pentlandite surfaces irrespective of copper activation or not.

Varying the addition point of EDA negatively affected the flotation response by altering surface characteristics. A brief discussion of the results is presented here since the possible mechanisms involved in surface alteration and recoveries are discussed in detail in Chapter 5.3. Figure 4.30 shows the Cu/Ni ratio surface coverage for pentlandite. It is evident that a higher copper concentration is observed when EDA is added after copper sulphate and prior to xanthate compared to the cases where EDA is added prior to the copper sulphate and xanthate and after copper sulphate and xanthate. This observation is due to a higher degree of copper adsorption onto sulphur sites, which would not be sequestered by the addition of EDA. In the case where EDA is added first it will complex with nickel and any excess EDA will sequester the copper ions from solution before they have time to adsorb onto the mineral surfaces. When EDA is added after copper sulphate and xanthate, it would sequester any copper and nickel oxide and hydroxide as well as any weakly attached copper-hydroxy-xanthate species. Zhenghe et al., 1997 has shown that amine complexing agents will sequester precipitated copper/nickel-xanthate complexes in solution at pH 9. The opposite is seen for pyroxene mineral surfaces (Figures 4.31 and 4.32) where lower nickel and copper concentrations are obtained when EDA is added after copper sulphate and prior to xanthate addition. The lowest nickel surface coverage for pyroxene is observed when EDA is added before copper sulphate, this is attributed to nickel being chelated first since no copper is present in solution.

5.3 Microflotation

Mineral recovery by flotation can be used as an indicator of hydrophobicity in a given chemical and electrochemical system. Small-scale flotation experiments have been found to be a useful tool to investigate flotation behaviour of the various constituents of the ore. A study of the effect of reagent adsorption on a specific mineral can be carried out, since the influence of froth phase and cell dynamics in the pulp phase are not present. Reproducibility tests were performed to evaluate the reliability of the procedure and apparatus used for the microflotation testwork. As demonstrated by the recovery-time curves (Figures 4.1 and 4.2) and the low standard deviation (Tables 4.1 and 4.2) for each concentrate collected, the procedure and apparatus used gave consistent results.

Optimal dosages were determined for each complexing agent at pH 9 and the dosages chosen were based on the best selectivity obtained between pentlandite and pyroxene without significantly reducing the pentlandite recovery. A cut-off of 80% for pentlandite recovery was used. These dosages were used throughout the study (Table 4.3).

Recovery-time curves comparing different chemical treatment regimes are shown in Figures 4.7 and 4.8. The addition of copper sulphate, prior to xanthate addition, improved the flotation kinetics, particularly for pentlandite relative to the xanthate trial (Figure 4.7). A schematic representation of the possible mechanisms for the interaction of copper sulphate followed by xanthate addition in a 1:1 pentlandite-pyroxene mixture at pH 9 for pentlandite and pyroxene are shown in Figures 5.12 and 5.13.

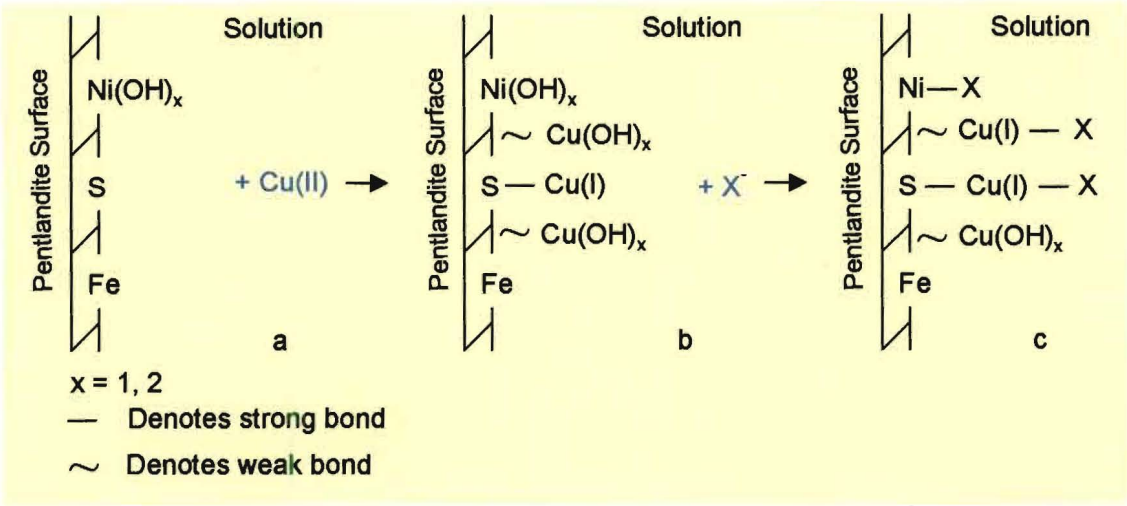

Figure 5.12: Schematic representation of copper sulphate and xanthate interactions for pentlandite mineral surfaces at pH 9.

For pentlandite, (Figure 5.12);

Diagram a) Shows the mineral surface at pH 9. According to the speciation diagram for nickel (Figure 5.8), the predominant species would be $NiOH^+$ and $Ni(OH)_2$.

Diagram b) After copper(II) ion addition; this shows copper adsorption onto the mineral surface by, 1) an oxidation-reduction reaction during which the copper(II) ion oxidises the sulphur of the mineral ($S^2 - S_{oxid}$) and in the process Cu(II) ions are reduced to Cu(I) and, 2) $Cu(OH)_2$ precipitation. Although the speciation diagram (Figure 5.9) shows $Cu(OH)_2$ precipitation at pH 9, Cu-S species would also be present. This is attributed to the reaction between Cu(II) ions and sulphur in the mineral lattice, which is kinetically faster compared to $Cu(OH)_2$ precipitation (Gerson, personal communication). The Cu-S bond formation reduces the Cu(II) ion concentration in solution and therefore a lower degree of $Cu(OH)_2$ precipitation would be observed.

Diagram c) After addition of xanthate; this diagram shows that xanthate ions will adsorb onto the copper and nickel sites thus increasing the hydrophobicity and flotation response due to the formation of copper and nickel xanthate complexes. Residual xanthate ions will react with the precipitated $Cu(OH)_2$ colloids, which are likely to be converted to hydrophobic colloids [$2Cu(OH)_2$

$\rightarrow 2Cu(II)X_2 \rightarrow 2Cu(I)X + X_2]$, assuming that the system is not kinetically controlled (Gerson, personal communication).

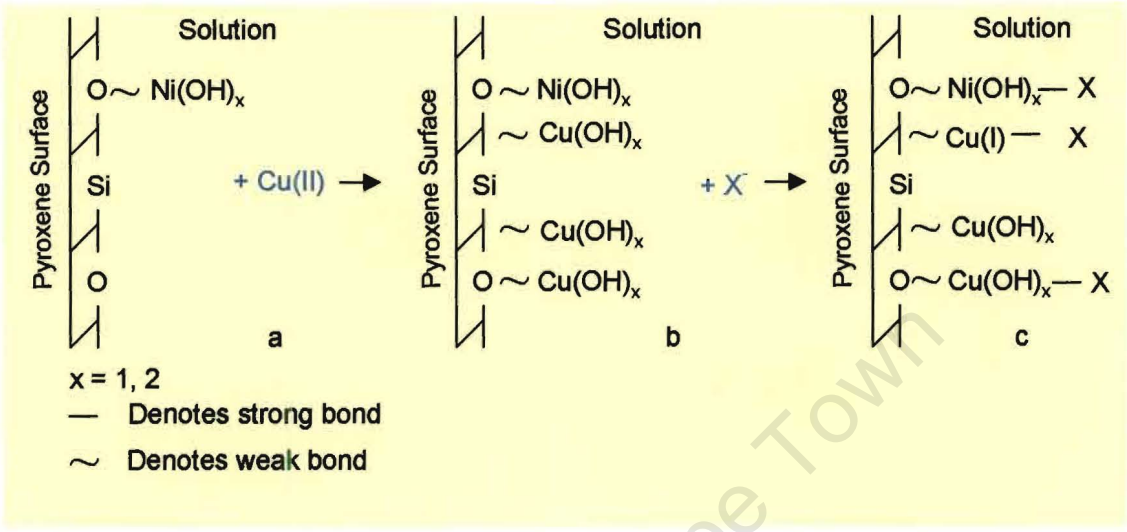

Figure 5.13: Schematic representation of copper sulphate and xanthate interactions for pyroxene mineral surfaces at pH 9.

For pyroxene, (Figure 5.13);

Diagram a) Shows the mineral surface at pH 9. $NiOH^+$ and $Ni(OH)_2$ species (Figure 5.8) will also be present on the pyroxene surface as a result of pentlandite dissolution.

Diagram b) After copper(II) ion addition; this floatability observed at pH 9 is attributed to two competing processes taking place, viz. adsorption of copper(II) ions from solution onto the minerals surfaces by, 1) electrostatic attraction of copper(II) ions species, ($CuOH^+$, $Cu_2(OH)_2^{2+}$) and, 2) $Cu(OH)_2$ precipitation (Acar and Somasundaran, 1992).

Diagram c) After addition of xanthate, residual xanthate ions will react with the precipitated $Cu(OH)_2$ (as discussed for pentlandite in Figure 5.12, Diagram c) thus rendering these previously hydrophilic colloids hydrophobic and increasing the flotation response of pyroxene. Xanthate anions will also adsorb onto the positively charged nickel hydroxide ($NiOH^+$) species, which

are predominant at pH 9 (Figure 5.8), due to electrostatic attraction, and thus enhance pyroxene floatability. The possible mechanisms involved in Ni(II) ion adsorption onto the pyroxene surfaces were previously described in Chapter 2.2 (Mackenzie and O'Brien, 1969).

The degree of collector adsorption onto the copper activated mineral surfaces is evident in the recovery data obtained for pentlandite and pyroxene, 97% and 77%, respectively, relative to the recovery obtained for the xanthate trial only, which yielded recoveries of 30% for pentlandite and 8% for pyroxene (Figures 4.7 and 4.8).

A comparison of the microflotation results for the complexing agents (Figures 4.7 and 4.8) has shown that EDA gives the best selectivity between pentlandite and pyroxene at pH 9 without reducing the pentlandite recovery to any significant degree. The results also show the need for a complexing agent when compared to the standard copper sulphate and xanthate case. The reason for this effect, using EDA, is that it probably deactivates the pyroxene surfaces by sequestering (forming soluble stable metal chelates) the copper(II) and nickel(II) oxide and hydroxide species which are the predominant species observed at pH 9 (Figures 5.8 and 5.19. Thus in the presence of sufficient EDA hydrophilic oxide layers involving Cu(II) ions on pentlandite surfaces will be removed into solution via the complexation with EDA, yielding a mineral surface with a more hydrophobic surface.

The use of DETA, TETA and EDTA showed no significant benefit in terms of pentlandite recovery as well as selectivity, and gave very similar results to those obtained in the presence of copper sulphate and xanthate (Figures 4.7 and 4.8).

Since EDA has been shown to be the most effective complexing agent of those tested for the system studied, further microflotation trials were performed to evaluate the effect of varying the sequence of EDA addition on selectivity and floatability. The results (Figures 4.9 and 4.10) indicated that varying the EDA addition point negatively affected the pentlandite recovery as well as selectivity over pyroxene thus validating the

reasoning for adding the reagents in the following sequence: copper sulphate followed by EDA and then followed by xanthate. The reason for this order of addition was, in the case of copper sulphate; to activate the mineral surfaces, followed by the complexing agent, which reduces the inadvertent copper activation of the pyroxene surfaces. Finally xanthate was added as the collector. Figures 5.14 and 5.15 show the schematic representation of the possible mechanisms involved for pentlandite and pyroxene, respectively, when copper sulphate, EDA and xanthate are added sequentially to the 1:1 pentlandite-pyroxene mixture at pH 9.

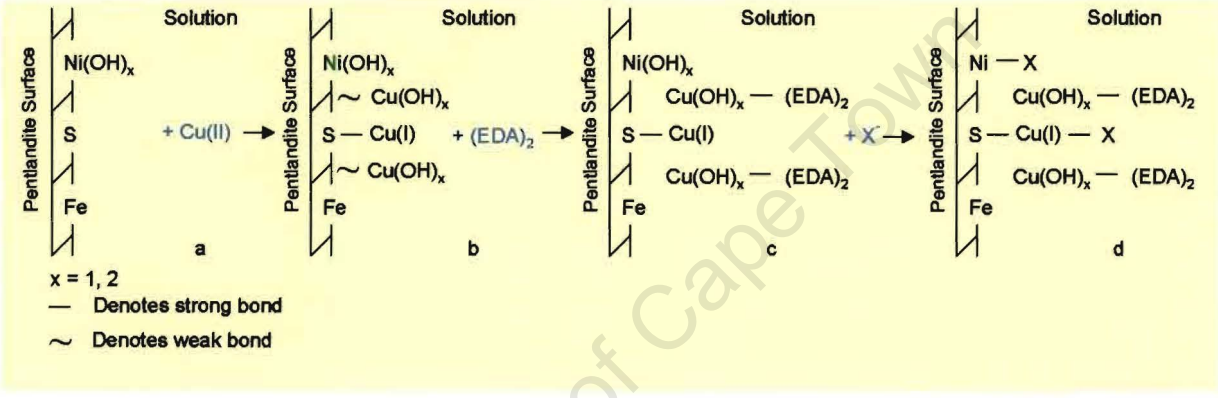

Figure 5.14: Schematic representation of copper sulphate, EDA and xanthate interactions for pentlandite mineral surfaces at pH 9.

For pentlandite, (Figure 5.14);

Diagram a) Shows the pentlandite surface prior to copper(II) ion addition as discussed previously for Figure 5.12, diagram a.

Diagram b) Shows copper adsorption onto the mineral surface, which has previously been described in Figure 5.12, Diagram b.

Diagram c) EDA addition to solution; EDA will sequester copper oxide and hydroxide species into solution, leaving an enriched copper(I) mineral surface, EDA would not remove any copper or nickel attached to the sulphur atom in the mineral surface lattice due to the relative bond strengths of the Cu-S and Ni-S (Kelebek et al. 1996).

Diagram d) Xanthate addition to solution; shows the formation of copper and nickel xanthate complexes as described for Figure 5.12, Diagram c, but only on the sites that are bound to sulphur in the mineral lattice which induces hydrophobicity on the pentlandite surfaces. It is assumed that no interaction between X^- and the copper-hydroxy-EDA complexes will occur.

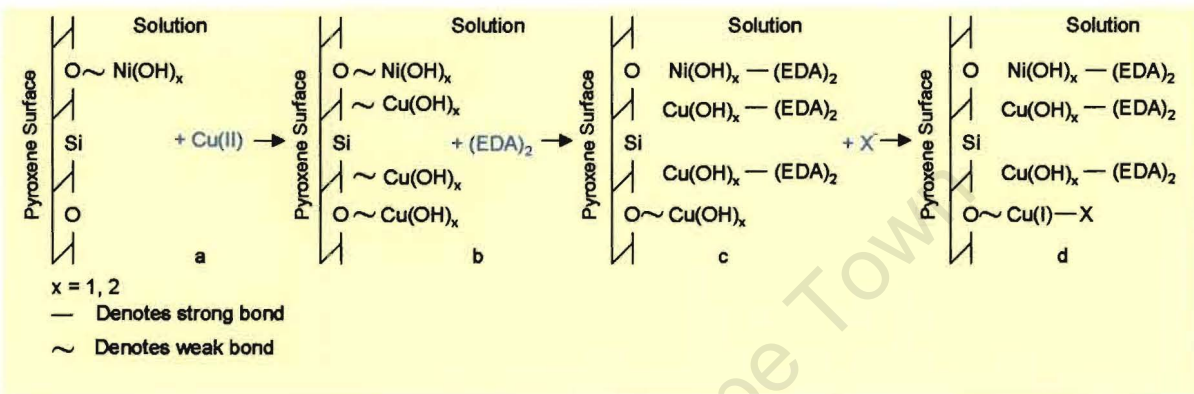

Figure 5.15: Schematic representation of copper sulphate, EDA and xanthate interactions for pyroxene mineral surfaces at pH 9.

For pyroxene, (Figure 5.15);

Diagram a) Shows the pyroxene surface prior to copper(II) ion addition (previously discussed for Figure 5.13, Diagram a).

Diagram b) Shows copper adsorption onto the mineral surface, which has previously been described in Figure 5.13, Diagram b.

Diagram c) EDA addition to solution; EDA will sequester the copper oxide and hydroxide species into solution, leaving a mineral surface with significantly reduced concentrations of copper(II) and nickel(II) species.

Diagram d) Xanthate addition to solution; shows the formation of copper and nickel xanthate complexes as described in Figure 5.13, Diagram c, which would induce some hydrophobicity on the pyroxene surfaces since a significant amount of the inadvertently activating ions species would have been removed into solution via the complexation with EDA.

The drop in pentlandite recovery to 92% compared to that obtained for the copper sulphate and xanthate trial (Figures 4.7 and 4.8) is probably due to a lower degree of xanthate adsorption. It has been proposed in Figure 5.14, Diagram c, that EDA would complex with most of the copper hydroxide colloids on the pentlandite surfaces and remove them into solution and they would therefore not be available for conversion to Cu(I) complexes and xanthate adsorption, which would affect the recovery. The large reduction in pyroxene recovery to 45% (Figures 4.9 and 4.10), relative to the copper sulphate and xanthate trial (Figures 4.7 and 4.8) is attributed to EDA deactivating the pyroxene surfaces by sequestering the copper(II) and nickel(II) oxide and hydroxide species into solution and therefore having less sites available for xanthate adsorption, thereby reducing the pyroxene floatability.

Schematic representation of the possible mechanisms involved for pentlandite and pyroxene, respectively, when EDA, copper sulphate and xanthate are added sequentially to the 1:1 pentlandite-pyroxene mixture at pH 9 is shown in Figures 5.16 and 5.17.

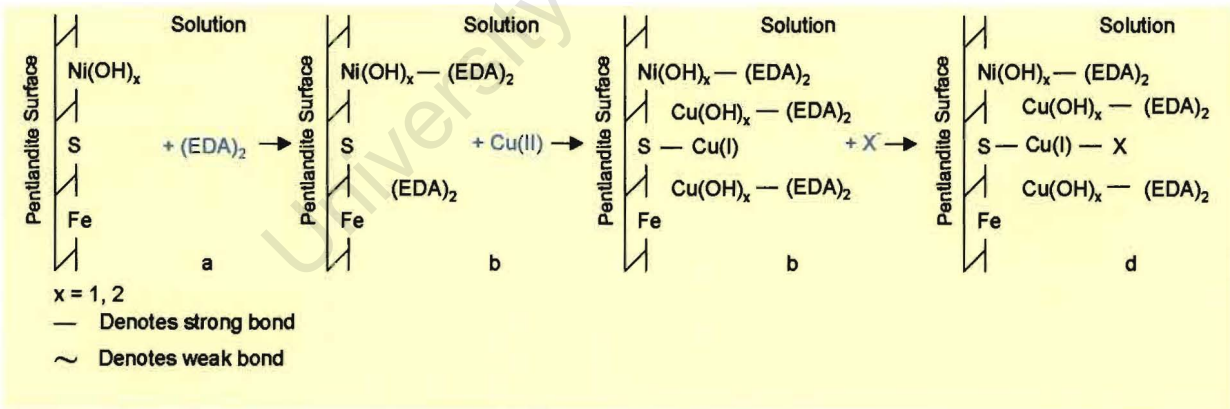

Figure 5.16: Schematic representation of EDA, copper sulphate and xanthate interactions for pentlandite mineral surfaces at pH 9.

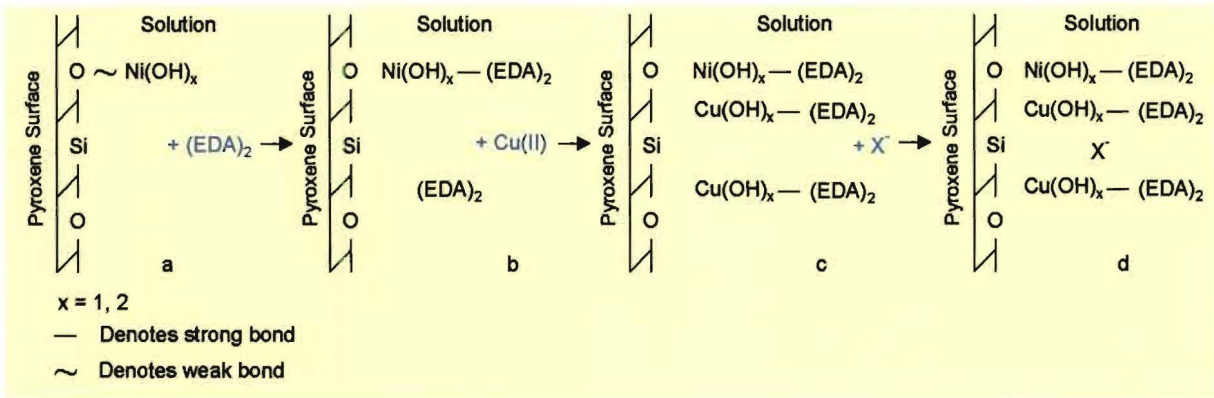

Figure 5.17: Schematic representation of EDA, copper sulphate and xanthate interactions for pyroxene mineral surfaces at pH 9.

For pentlandite and pyroxene, (Figures 5.16 and 5.17);

Diagram a) Shows the pentlandite and pyroxene mineral surface prior to EDA addition.

Diagram b) EDA addition to solution; when EDA is added it would form metal complexes in the following order of affinity since the magnitude of log K represents the relative affinities of the metal ion for the ligands (Table 5.1):

Cu>Ni>Zn>Co>Cd>Cr>Fe

Since no copper is present EDA would complex with any Ni(II) oxide or hydroxide species on the mineral surface and for pentlandite surfaces, block these sites for collector adsorption and for pyroxene surfaces, sequester these ions into solution.

Diagram c) When copper(II) ions are added, EDA ligand sites would most likely still be available for complexation and these would be filled by the added copper(II) ions which would be complexed before they have chance to activate the mineral surfaces. This is evident in the reduction of both pentlandite and pyroxene recoveries to 65% and 22% respectively compared to the copper sulphate, EDA and xanthate case (Figures 4.9 and 4.10).

Diagram d) Addition of xanthate; shows the formation of a few copper and nickel xanthate complexes on any free copper(II) and nickel(II) species as previously described for pentlandite and pyroxene, Figures 5.12 and 5.13,

Diagrams c, respectively. It should be pointed out that the degree of xanthate adsorption would be low particularly for pyroxene, which would reduce hydrophobicity on both mineral surfaces compared to the copper sulphate, EDA and xanthate trial (Figures 4.9 and 4.10).

Schematic representation of the possible mechanisms involved for pentlandite and pyroxene when copper sulphate, xanthate and EDA are added sequentially to the 1:1 pentlandite-pyroxene mixture at pH 9 is shown in Figures 5.18 and 5.19, respectively.

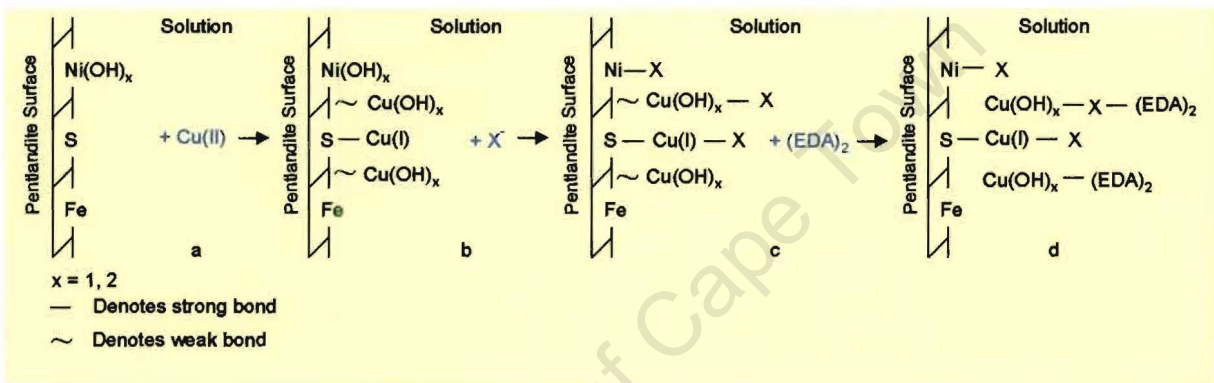

Figure 5.18: Schematic representation of copper sulphate, xanthate and EDA interactions for pentlandite mineral surfaces at pH 9.

For pentlandite, (Figure 5.18);

Diagram a) Shows the pentlandite mineral surface prior to copper(II) ion addition which has previously been described in Figure 5.12.

Diagram b) Shows copper adsorption onto the mineral surface, which has previously been described in Figure 5.12, Diagram b.

Diagram c) Shows the formation of copper and nickel xanthate complexes, which induce hydrophobicity on the pentlandite surfaces as previously discussed for Figure 5.12, Diagram c.

Diagram d) EDA addition to solution; EDA will sequester copper oxide and hydroxide as well as weakly attached copper-hydroxy-xanthate species (Zhenghe et al., 1997) into solution, leaving a mineral surface with only the xanthate bonded

to the Cu-S and Ni-S in the pentlandite lattice, due to bond strengths as previously discussed in Figure 5.14, Diagram c.

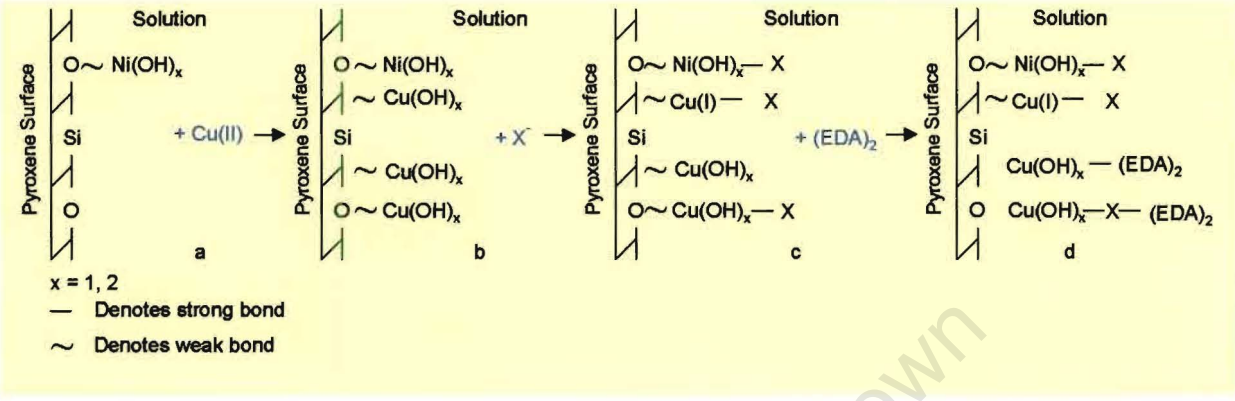

Figure 5.19: Schematic representation of copper sulphate, xanthate and EDA interactions for pyroxene mineral surfaces at pH 9.

For pyroxene, (Figure 5.19);

Diagram a) Shows the pyroxene surface prior to copper(II) ion addition. Previously explained in Figure 5.13, Diagram a.

Diagram b) Shows copper adsorption onto the mineral surface, which has previously been described in Figure 5.13, Diagram b.

Diagram c) After xanthate addition; shows the formation of copper and nickel xanthate complexes, which induce hydrophobicity on the pyroxene mineral surfaces as previously discussed in Figure 5.13, Diagram c.

Diagram d) EDA addition to solution; EDA will sequester copper oxide and hydroxide as well as weakly attached copper-hydroxy-xanthate species into solution (Zhenghe et al. 1997). This would result in lower pyroxene recovery compared to the copper sulphate, EDA and xanthate case leaving a mineral surface with only a few copper and nickel xanthate species introducing some hydrophobicity to pyroxene surfaces.

The recovery obtained for pentlandite and pyroxene was 65% for both minerals (Figures 4.9 and 4.10). The drop in recovery for both minerals compared to the copper sulphate and xanthate case (Figures 4.7 and 4.8) has been attributed to the complexation of copper oxide and hydroxide as well as weakly attached copper-hydroxy-xanthate species into solution thereby reducing the degree of copper and nickel xanthate species being formed.

Variations in the concentration of copper sulphate and xanthate were investigated with and without the addition of EDA to determine the effect lowering the concentration of these reagents would have on the flotation response and selectivity of pentlandite and pyroxene (Figures 4.11 and 4.12).

1) Lowering of the copper sulphate and xanthate concentrations, independently, in the presence and absence of EDA resulted in a reduction of the pentlandite recovery. This is attributed to a lower concentration of copper and xanthate on the mineral surface. The psuedo-monolayers calculated for copper and xanthate at the 5.0E-05M concentration (Table 4.3) show that there were 3.5 and 6.3 monolayers compared to only 0.35 and 0.63 monolayers, for the lowered copper and xanthate concentrations. It therefore proposed that there was insufficient copper available to fully activate the mineral surfaces and in the case of xanthate (with and without the lower copper concentration) there was insufficient collector coverage to induce hydrophobicity.

2) When EDA was added to the lowered copper sulphate and xanthate concentration test, the results (Figures 4.11 and 4.12) showed an increase in ultimate recovery by around 20% compared to the case without EDA addition (Figure 4.11). The reason for this is that there is 10 times less copper present; EDA would sequester not only copper and nickel but other oxide or hydroxide species, such as iron, etc. from the mineral surfaces, leaving a 'clean' mineral surface for the xanthate ions to attach and thereby increase the pentlandite recovery. For pyroxene, EDA would sequester most of the copper and nickel oxide and hydroxide species into solution, leaving a low concentration of copper and nickel sites available for xanthate adsorption. There may also be agglomeration of the pentlandite and pyroxene

particles, due to electrostatic forces of attraction between the minerals as shown for the zeta potential determinations (Figures 4.14 and 4.15), which would significantly increase the pyroxene recovery.

In summary, the microflotation results have shown:

- A high flotation response for pentlandite and pyroxene in the presence of copper sulphate and xanthate.
- The need for the use of a complexing agent to reduce the pyroxene recovery by removing the activating metal ions from the mineral surface.
- EDA has proved to be the best complexing agent for the system studied at pH 9 with respect to pentlandite recovery and selectivity over pyroxene.
- Varying the addition point of EDA negatively affected the flotation response by altering surface characteristics.

Lowering the copper and xanthate concentrations independently, also negatively affected the flotation response due to an insufficient amount of copper and collector to enhance mineral surface hydrophobicity.

CHAPTER 6

CONCLUSIONS

This study has examined the role of complexing agents in pentlandite-pyroxene flotation and focused on the surface chemistry and interaction between valuable and gangue minerals as well as the interaction of complexing agents and reagents (xanthate, copper sulphate) in the system at pH 9.

This study has shown that pentlandite recovery can be increased in a 1:1 pentlandite-pyroxene mixture with the addition of an activator such as copper sulphate. Collector adsorption is maximised by the formation of copper and nickel xanthate complexes, which induce hydrophobicity on the mineral surfaces. This results in a high pentlandite recovery of 97% compared to 30% for the case without copper sulphate addition.

In this event pyroxene also becomes inadvertently copper activated, which is evident from the zeta potential, ToF-SIMS and XPS data. When xanthate ions are added to the copper activated minerals true flotation of pyroxene occurs. The floatability observed at pH 9 would suggest that the precipitated $Cu(OH)_2$ colloids on the mineral surfaces form Cu(I)-X complexes, thus rendering these previously hydrophilic colloids hydrophobic. In addition, the flotation and surface analysis data revealed that pyroxene could also be inadvertently activated by Ni(II) ions, which would result in a higher pyroxene recovery.

To minimise the pyroxene recovery without negatively affecting the pentlandite recovery, complexing agents were considered since they have been recognised as potential reagents in flotation for many decades. Amine complexing agents are known to specifically complex with copper and nickel ions in solution. Many studies of pyrrhotite surfaces have shown that complexing agents remove oxide and hydroxide layers from the mineral surfaces and reduce the concentration of ions that cause inadvertent activation of pyrrhotite. It was hypothesised that this will also hold true for siliceous gangue minerals since the complexing agents do not distinguish between gangue or sulphide mineral surfaces and only complexes with the hydrophilic oxide and

hydroxide layers involving Cu(II), Ni(II) and other ions. DETA, EDA, TETA and EDTA were evaluated for the use in the flotation of a 1:1 pentlandite-pyroxene mixture at pH 9. The results have shown the need for a complexing agent when compared to the standard copper sulphate and xanthate case.

A comparison of the microflotation results for the complexing agents has shown that EDA gave the best selectivity between pentlandite and pyroxene at pH 9 without reducing the pentlandite recovery to any significant degree. This is due to the formation and stability of the 1:2 Cu(II)-EDA chelate. EDA deactivates the pyroxene surfaces by sequestering the copper(II) and nickel(II) oxide and hydroxide species which are the predominant species observed at pH 9. It should be pointed out that the complexing agents tested do not compete with the surface lattice Cu-S and Ni-S bond due to the relative strength of the bonds formed. It is worth noting that the optimum dosage for EDA was lower compared to the other complexing agents tested, which would have favourable cost implications. The results also showed that the other two amines, DETA and TETA, behaviour was intermediate between EDA and EDTA.

Variation in the sequence of addition of EDA negatively affected the flotation response by altering surface characteristics. The drop in pentlandite and pyroxene recovery is mainly due to a lower degree of xanthate adsorption which is attributed to, 1) EDA deactivating the pentlandite and pyroxene surfaces by sequestering the copper(II) and nickel(II) oxide and hydroxide as well as weakly attached copper hydroxy xanthate species into solution and 2) blocking of nickel sites by the complexation of EDA onto the pentlandite mineral surface, thereby having less sites available for xanthate adsorption and a reduction in floatability.

Lowering the copper and xanthate concentrations independently in the presence and absence of EDA, also negatively affected the flotation response due to an insufficient amount of copper and collector to enhance mineral surface hydrophobicity.

The optimum conditions, in terms of pentlandite recovery and selectivity over pyroxene, appeared to be the combination of copper sulphate (5.0E-05M), EDA (4.0E-05M), SIBX (5.0E-05M), at pH 9.

Further testwork in this area could focus on a similar study at pH 6 since preliminary testwork has revealed a potentially improved performance of pH 6 over pH 9. It has also been suggested that the complexing agents tested form copper and nickel complexes at much lower pHs of between 3 and 6.5 (Hubbard et al. 1996) compared to the working pH of 9 for this study. Additional work could also include the evaluation of the synergistic effects between ethylenediamine (EDA) and polyphosphate as well as the effect of polyphosphate chain lengths. Internal testwork has shown that the addition of a dispersant was beneficial in terms of the valuable minerals grade-recovery relationship.

LIST OF REFERENCES

Acar, S. and Somasundaran, P., 1992. Effect of dissolved mineral species on the electrokinetic behaviour of sulphides. Minerals Engineering, Vol. 5, No.1, pp. 27-40.

Agar, G.E., Kipkie, W.B. and Wells, P.F., 1982. The separation of chalcopyrite and pentlandite from INCO Metals' Sudbury area ores. XIV International Mineral Processing Congress, Toronto, Canada, pp. IV-1.1- 1.12.

Aksu, Sedar and Doyle, Fiona M., 2000. Potential-pH diagrams for copper in aqueous solutions of various organic complexing agents. Electrochem. Soc. Proc., vol 200-14, pp. 258-269.

Barskii, L.A., Rybas, V.V., Fat'yanova, M.A. and Ponomarev, G.P., 1986. Influence of sulphur-containing ions on selective flotation of copper-nickel ores. Fiziko-Tekhnicheskie Problemy Razrabotki Poleznykh Iskopaemykh, No.4, pp. 99-106.

Beck, M.T. and Gorog, S., 1958. Acta Phys et Chem, 4, 59.

Boyd, D.A., 1979. An investigation into electron spectroscopy as a means of studying the chemistry of froth flotation. Johnson Matthey Report No. 78J1.

Bozkurt, V., Xu, Z. and Finch, J.A., 1997. Pentlandite/pyrrhotite interaction: xanthate adsorption in presence of Ni ions. In Processing of complex ores. Ed. J.A. Finch, S.R. Rao and I. Holubec, CIM, Montreal, pp. 101-114.

Bozkurt, V., Xu, Z. and Finch, J.A., 1998. Xanthate adsorption on pentlandite and pyrrhotite: Effect of mineral interactions. In Innovations in mineral and coal processing, Ed. Atak, Onal and Celik, Rotterdam, pp. 93-98.

Bozkurt, V., Xu, Z. and Finch, J.A., 1999. Effect of depressants on xanthate adsorption on pentlandite and pyrrhotite: single vs. mixed minerals. Canadian Metallurgical Quarterly, Vol. 38, No. 2, pp. 105-112.

Bradshaw, D.J., 1997. Synergistic effects between thiol collectors used in the flotation of pyrite. PhD Thesis, University of Cape Town.

Bradshaw, D.J. and O'Connor, C.T., 1996. Measurement of the sub-process of bubble loading in flotation. Minerals Engineering, Vol. 9, No. 4, pp. 443-448.

Broomhead, J.A. and Layers, G., 1976. Leaching studies with pentlandite and pyrrhotite. Proc. Australas. Inst. Min. Metall., No. 259, pp. 19-22.

Buckley, A.N. and Woods, R., 1991. Surface composition of pentlandite under flotation-related conditions. Surface and Interface Analysis, Vol. 17, pp. 675-680.

Chaberek, S. and Martell, A.E., 1959. Organic sequestering agents. John Wiley & Sons, Inc., New York.

Clarke, P., Fomasiero, D., Ralston, J. and Smart, R.St.C., 1995. A study of the removal of oxidation products from sulphide mineral surfaces. Minerals Engineering, Vol. 8, No.11, pp. 1347-1357.

Cotton, F. A. and Wilkinson, G., 1980. Advanced inorganic chemistry, a comprehensive text, fourth edition. A Wiley-Interscience Publication, John Wiley & Sons.

Cotton, F. A. and Wilkinson, G., 1988. Advanced inorganic chemistry, fifth edition, sections 2.5 and 29.3. A Wiley-Interscience Publication, John Wiley & Sons.

Covington A., 1997 Compendium of analytical nomenclature, IUPAC.

Deju, R.A. and Bhappu, R.B., 1965. Surface properties of silicate minerals. State Bureau of Mines and Mineral Resources, New Mexico Institute of Mining and Technology, Circular 82, pp. 1-6.

Deju, R.A. and Bhappu, R.B., 1966. A chemical interpretation of surface phenomena in silicate minerals. Society of Mining Engineers, December, pp. 329-332.

de Vaux. D., 1997. An introduction to Time of Flight Secondary Ion Mass Spectrometry. Anglo bi-annual operations director's technical seminar.

Finkelstein, N.P. and Allison, S.A., 1976. The chemistry of activation, deactivation and depression in the flotation of zinc sulphide: a review. In Fuerstenau, M.C. (Ed.), A.M.

Gaudin Memorial Volume, Flotation. 1: American Institute of Mining, Metallurgical and Petroleum Engineers, New York, pp. 414-451.

Finkelstein, N.P., 1997. The activation of sulphide minerals for flotation: a review. International Journal of Mineral Processing, 52, pp. 81-120.

Forssberg, K.S.E. and Jonsson, H., 1981. Absorption of heavy metal ions on pyrrhotite. Scandinavian Journal of Metallurgy, Vol. 10, pp. 225-230.

Forward, F.A., Veltman, H. and Vizsolyi, A., 1960. Production of high purity lead by amine leaching. Proc. International Mineral processing Congress, London: IMM, pp. 823-837.

Fuerstenau, D.W., 1982. Activation and flotation of sulphide minerals. In King R.P. (Ed.), Principles of Flotation, S.A. Inst. Min. Metall. , Johannesburg, pp. 188-198.

Fuerstenau, M.C., 1975. Role of metal ion hydrolysis in oxide and silicate flotation systems. Advances in Interfacial Phenomena, AICHE Symposium Series, No. 150, Vol.71, pp.16-23.

Fuerstenau, M.C., 1976. Flotation. A.M. Gaudin Memorial Volume, Volume 1, Published by American Institute of Mining, Metallurgical, and Petroleum Engineers, Inc., New York, pp. 148-196.

Fuerstenau, M.C., Palmer, B.R. and Gutierrez, B., 1977. Mechanisms of flotation of selected iron-bearing silicates. Society of Mining Engineers, Vol. 262, pp. 234-236.

Fullston, D., Fornasiero, D. and Ralston, J., 1998. Zeta potential study of the oxidation of copper sulphide minerals. Colloids and Surfaces, A: Physicochemical and Engineering Aspects, pp. 1-9.

Fuerstenau, D.W., Herrera-Urbina, R. and McGlashan, D.W., 1999. Studies on the applicability of chelating agents as universal collectors for copper minerals. Int. J. Miner. Process. 58, pp 15-33.

Gaudin, A.M., Fuerstenau, D.W. and Mao, G.W., 1959. Activation and deactivation studies with copper on sphalerite. Mining Engineering, SME, 11, pp. 430-436.

Hayes, R.A., 1987. The effect of E_h on the collectorless flotation of sulphide minerals. M. Appl. Sci. Thesis, South Australian Institute of Technology, Adelaide, Australia.

Healy and Trahar, 1989. Challenges in Mineral Processing, ed. by K.V.S. Sastry and M.C. Fuerstenau, pp. 3-14, AIME, Littleton, CO.

Heiskanen, K., Kirjavainen, V. and Laapas, H., 1991. Possibilities of collectorless flotation in the treatment of pentlandite ores. International Journal of Mineral Processing, 33, pp. 263-274.

Heyes, G.W. and Trahar, W.J., 1984. The flotation of pyrite and pyrrhotite in the absence of conventional collectors. Electrochemistry in Mineral and Metal Processing, P.E. Richardson, et al., Ed., Vol. 84-10, The Electrochem. Soc., Inc. Pennington, NJ, pp. 219-232.

Hodgson, M. and Agar, G.E., 1989. Electrochemical investigations into the flotation chemistry of pentlandite and pyrrhotite: Process water and xanthate interactions. Canadian Metallurgical Quarterly, Vol. 28, No.3, pp. 189-198.

Hubbard, K.L., Darling, G.D. and Finch, J.A., 1999. Screening ligands for metallurgical applications by the determination of pH of complexation with metals. Minerals Engineering, Vol. 10, No. 1, pp. 41-54.

Hunter, R.J., 1993. Introduction to modern colloid science. Oxford University Press.

Ishihara, T. and Kagami, Y., 1964. Nippon Kogyo Kaishi, 80:881.

Jonassen, H.B. and Dexter, T.H., 1949. Inorganic complex compounds containing polydentate groups. I. The complex ions formed between copper (II) ions and ethylenediamine. Journal of the American Chemical Society, Issue 71, pp. 1553-1556.

Kakovskii, I.A., 1957. Physical properties of some flotation reagents and their salts with ions of heavy non-ferrous metals. Proc. 2nd Int. Conf. Surface Activity, London, pp. 225-237.

Kakovskii, I.A. and Arashkevich, V.M., 1968. The study of properties of organic disulphides. Preprint, VIIIth I.M.P.C., Leningrad.

Kant, C., Rao, S.R. and Finch, J.A., 1994. Distribution of surface metal ions among the products of chalcopyrite flotation. Minerals Engineering, Vol. 7 No. 7, pp. 805-916.

Kartio, I.J., Basilio, C.I. and Yoon, R.H., 1996. An XPS study of sphalerite activation by copper. In Woods, R., Doyle, F., Richardson, P.E. (Eds.), Electrochemistry in Mineral and Metal Processing IV, The Electrochemical Society, pp. 25-34.

Kelebek, S., 1993. The effect of oxidation on the flotation behaviour of nickel-copper ores. XVIII International Mineral Processing Congress, Sydney, 23-28 May, pp. 999-1005.

Kelebek, S., 1996. Effect of polyamines on mineral separation of nickel-coppper ores: chelation equilibria in collectorless flotation with DETA. Trans. Instn. Min. Metall. (Sect. C: Mineral Process. Extr. Metall.), 105, pp. C75-C81.

Kelebek, S., Wells, P.F. and Fekete, S.O., 1996. Differential flotation of chalcopyrite, pentlandite and pyrrhotite in Ni-Cu sulphide ores. Canadian Metallurgical Quarterly, Vol. 35, No.4, pp. 329-336.

Kelebek, S. and Tukel, C., 1999. The effect of sodium metabisulphite and triethylenetetramine system on pentlandite-pyrhotite separation. Int. J. Miner. Process. 57, pp. 135-152.

Kirjavainen, V., Schreithofer, N. and Heiskanen, K., 2002. Effect of calcium and thiosulfate ions on flotation selectivity of nickel-copper ores. Minerals Engineering, 15, pp. 1-5.

Klein, C. and Hurlbut, Jr. C.S., 1985. Manual of mineralogy (after J. D. Dana), 20th Edition, John Wiley & Sons, Inc.

Legrand, D.L., Bancroft, G.M. and Nesbitt, H.W., 1997. Surface characterization of pentlandite, $(Fe,Ni)_9S_8$, by X-ray photoelectron spectroscopy. International Journal of Mineral Processing, 51, pp. 217-228.

Liu, L., Rao, S.R. and Finch, J.A., 1993. Laboratory study of effect of recycle water on flotation of a Cu/Zn sulphide ore. Minerals Engineering, Vol. 6, No.11, pp. 1183-1190.

Mackenzie, J.M.W. and O'Brien, R.T., 1969. Zeta potential of quartz in the presence of nickel (II) and cobalt (II). Society of Mining Engineers, Vol. 244, pp. 168-173.

Malvern Instruments, 1996. PCS Training Manual, Issue 1.3.

Marticorena, M.A., Liechti, D. and Kerr, A.N., 1995. The role of diethylenetiamine as a gangue sulphide depressant. Proc. Copper 95-Cobre 95 International Conference, Volume II – Mineral Processing and Environment, (Eds.) A. Casali, G.S. Dobby, M. Molina and W.J. Thoburn, The Metallurgical Society of CIM.

McNeil, M. Rao, S.R. and Finch, J.A., 1994. Technical Note, Oxidation of amyl xanthate by pentlandite. Canadian Metallurgical Quarterly, Vol. 33, No.2, pp. 165-167.

Moulder, John F., Stickely, William F., Sobal, Peter E. and Bomben, Kenneth D., 1995. Handbook of X-ray Photoelectron Spectroscopy, reference book of standard spectra for identification and interpretation of XPS data. Pyhsical Electronincs, Inc. USA.

Nagaraj, D.R. and Brinen, J., 1995. SIMS study of metal ion activation in gangue flotation. Proceedings XIX International Mineral Processing Congress, SME, Chapter 43, pp. 253-257.

Nagaraj, D.R. and Brinen, J., 1996. SIMS and XPS study of the adsorption of sulphide collectors on pyroxene: a case for inadvert metal in activation. Colloids and Surfaces, A: Physicochemical and Engineering Aspects 116, pp. 241-249.

Pankow J.F., 1991. Aquatic chemistry concepts, Lewis Publishers, Chelsea, Michigan, USA.

Perry, D.L., Tsao, L. and Taylor, J.A., 1984. Surface studies of the interaction of copper ions with sulphide minerals. In Electrochemistry in Minerals and Metal Processing, Electrochemical Society, Pennington, pp. 169-184.

Prestidge, C.A., Thiel, A.G., Ralston, J. and Smart, R.St.C., 1994. The interaction of ethyl xanthate with copper(II)-activated zinc sulphide: Kinetic effects. Colloids Surface, A. Physicochem. Eng. Aspects, 85, pp. 51-68.

Prestidge, C.A., Skinner, W.M., Ralston, J. and Smart, R.St.C., 1997. Copper(II) activation and cyanide de-activation of zinc sulphide under mildly alkaline conditions. Appl. Surf. Sci., 108, pp. 333-344.

Ralston, J. 1991. E_h and its consequences in sulphide mineral flotation. Minerals Engineering, Vol. 4, Nos. 7-11, pp. 859-878.

Ralston, J., Alabaster, P. and Healy, T.W., 1981. Activation of zinc sulphide with Cu II), Cd(II), and Pb(II): III. The mass spectrometric determination of elemental sulphur. International Journal of Mineral Processing, 7, pp. 279-310.

Rao, S.R. and Finch, J.A., 1991. Adsorption of amyl xanthate at pyrrhotite in the presence of nitrogen and implications in flotation. Canadian Metallurgical Quarterly, Vol. 30, No. 1, pp. 1-6.

Reich, F., 1997. The operators Guide for the 2100 TRIFT II ToF SIMS", Physical Electronics.

Richardson, S. and Vaughan, D.J., 1989. Surface alteration of pentlandite and spectroscopic evidence for secondary violarite formation. Mineralogical Magazine, Vol. 53, pp. 213-22.

Somasundaran, P. and Nagaraj, D.R., 1984. Chemistry and applications of chelating agents in flotation and flocculation. Reagents in the Minerals Industry.

Schueler, B.W., 1992. Microscope imaging by time of flight secondary ion mass spectrometry. Microsc. Microanal. Microstruct. 3, pp. 119-139.

Skoog, Douglas A. and West, Donald M., 1982. Fundamentals of analytical chemistry, fourth edition. Saunders college printing, Holt-Saunders Japan.
Smart, R.St.C., 1994. Chemical and structural alteration in the surface layers of oxides. In Science of ceramic interfaces II, Ed. J. Nowotny, Elsevier Science, pp. 311-339.

Thomber, M.R., 1983. Mineralogical and electrochemical stability of the nickel-iron sulphides-pentlandite and violarite. Journal of Applied Electrochemistry, 13, pp. 253-267.

Trahar, W.J., 1983. In Principles of Flotation, The Wark Symposium.

Trahar, W.J., 1984. The influence of pulp potential in sulphide flotation. In M.H. Jones and J.T. Woodcock (Editors), Principles of Mineral Flotation, The Wark Symposium, Australasian Institute of Mining and Metallurgy, Symposia Series No. 40, Melbourne, pp. 117-135.

Vreughenhil, A., Markwell, R., Finch, J.A. and Butler, I., 1997. Formation and characterization of nickel-DETA complexes related to flotation systems. Met. Soc., CIM, Sudbury, pp. 283-289.

Wang, X., Forssberg, K.S.E. and Bolin, N.J., 1989. Thermodynamic calculations on iron-containing sulphide mineral flotation systems, I. The stability of iron-xanthate. International Journal of Mineral Processing, 27, pp. 1-19.

Wang, X., Forssberg, E. and Bolin N.J., 1989 a, b, c. Scand. J. Met. 18, pp. 243-272.

Wang, X., Forssberg, E. and Bolin N.J., 1989 d and e. The aqueous surface chemistry of activation in the flotation of sulphide minerals – A review. Part II: A surface precipitation model. Miner. Process. Ext. Met. Rev. Vol. 4, pp. 167-199.

Wang, Xianghuai and Forssberg, Eric, 1990. EDTA-induced flotation of sulphide minerals. Journal of Colloid and Interface Science, Vol. 140, No. 1.

Wesseldijk, Q.I., Reuter, M.A., Bradshaw, D.J. and Harris, P.J., 1999. The flotation behaviour of chromite with respect to the beneficiation of UG2 ore. Minerals Engineering, Vol. 12, No. 10, pp. 1177-1184.

Xu, Z., Rao, S.R., Finch, J.A., Kelebek, S. and Wells, P., 1997. Role of diethylene triamine (DETA) in pentlandite-pyrrhotite separation-Part 1: Complexation of metals with DETA. Trans. Instn Min. Metall. (Sect.C: Mineral Process. Extr. Metall.), 106, pp. C15-C20.

Yoon, R.H., Basilio, C.I., Marticorena, M.A., Kerr, A.N. and Stratton-Crawley, R., 1995. A study of the pyrrhotite depression mechanism by diethylenetriamine. Minerals Engineering, Vol. 8, No. 7, pp. 807-816.

Zhenghe, Xu, Rao, S.R., Finch, J.A., Kelebek, S. and Wells, P., 1997. Role of diethylenetriamine (DETA) in pentlandite-pyrrhotite separation-Part 1: complexation of metals with DETA. Trans. Instn Min. Metall. (Sect.C: Mineral Process. Extr. Metall.), 106, pp. C15-C20.

APPENDIX A: Xanthate and Copper Surface Coverage Calculations

It is instructive to carry out semi-quantitative exploratory calculations of estimates of the particle surface coverage by various reagents. The case of copper sulphate and xanthate used during the study is shown below as an example.

Mineral Surface Area Determined Using BET Method:

Pyroxene:	$0.59\ m^2/g = 0.59 \times 10^{20}\ Å^2/g$
Pentlandite:	$0.30\ m^2/g = 0.30 \times 10^{20}\ Å^2/g$
1:1 Pentlandite-Pyroxene Mixture:	$0.89\ m^2/2g = 0.89 \times 10^{20}\ Å^2/2g$
	$= 0.45 \times 10^{20}\ Å^2/g$

Copper Surface Coverage:

Cu Concentration:	$5 \times 10^{-5}\ mol.dm^{-3}$
Grams of Cu in 250 cm^3 (cell volume):	8×10^{-4}
Number of Cu Moles:	$8 \times 10^{-4}/63.5 = 1.2598 \times 10^{-5}$
Number of Cu Atoms:	$1.2598 \times 10^{-5} \times 6.023 \times 10^{23} = 7.5878 \times 10^{18}$

Gaudin et al. (1959) assumed that the possible copper uptake for sphalerite was one ion for each 20.8 $Å^2$. Assuming that the same copper surface area is relevant for the pentlandite-pyroxene and pentlandite-feldspar mixture uptake, the required surface area for pseudo-monolayer coverage would be:

$$7.5878 \times 10^{18} \times 20.8\ Å^2 = 1.5783 \times 10^{20}\ Å^2/g$$

This implies that 3.5 pseudo-monolayers of copper could be formed on pentlandite-pyroxene mixtures.

Xanthate Surface Coverage:

Xanthate Concentration:	5×10^{-5} mol.dm^{-3}
Grams of Xanthate in 250 cm^3:	1.9×10^{-3}
Number of Xanthate Moles:	$1.9 \times 10^{-3}/149 = 1.2752 \times 10^{-5}$
Number of Xanthate Atoms:	$1.2752 \times 10^{-5} \times 6.023 \times 10^{23} = 7.6805 \times 10^{18}$

Bradshaw (1997) assumed that the possible thiol collector uptake for pyrite is one ion for each 37 Å^2. Assuming that the same xanthate surface area is relevant for the pentlandite-pyroxene and pentlandite-feldspar mixture uptake, the required surface area for pseudo-monolayer coverage would be:

$$7.6805 \times 10^{18} \times 37 \text{ Å}^2 = 2.8418 \times 10^{20} \text{ Å}^2/\text{g}$$

This implies that 6.3 pseudo-monolayers of xanthate could be formed on pentlandite-pyroxene mixtures.

APPENDIX B: Zeta Potential Determination Procedure

A detailed zeta potential determination procedure used throughout the study is shown below. This procedure was used to ensure accuracy and repeatability of zeta potential data.

- Crush 0.3 g of a mineral sample to 100% -25µm in an agate mortar and pestle.
- Add 240 cm^3 of $Na_2B_4O_7$ solution (0.001M) and/or synthetic water.
- Stir well and split into 4 beakers (60 cm^3).
- Adjust pH to 4, 6, 8 and 10 with Na_2CO_3 or HCl.
- Condition for 20 minutes.
- Measure electrophoretic mobility, (volume used +/- 10 cm^3).
- Add reagent, e.g. copper sulphate (5×10^{-5}M), and condition for 5 minutes.
- Measure electrophoretic mobility.

APPENDIX C: Microflotation Test Procedure

The microflotation test procedure, given below, was followed during the study in order to obtain reproducible data.

- For a single mineral study, weigh 2 grams of a mineral sample after crushing and screening (38-106µm size fraction). For mineral mixtures study, weigh 1 gram of each mineral after crushing and screening (38-106µm size fraction).
- Add the mineral sample to 50 cm^3 of $Na_2B_4O_7$ solution and/or synthetic water adjusted to the desired pH.
- Transfer the solution to the microflotation cell and fill the cell to just below the overflow lip.
- Circulate pulp with peristaltic pump, set at 60 rpm / 1 min.
- Condition for 1 minute, add reagents as required and condition for the time required.
- Top up the cell volume to 250 cm^3, put cone in place and introduce the air (5 cm^3/min) through a syringe at the base of the cell.
- Remove the syringe and collect flotation products after:
  - 3 min - 1st Conc.
  - 20 min - 2nd Conc.
- Collect tailings sample.
- Filter each product on weighed filter paper and rinse with deionised water adjusted to the desired pH.
- Dry under argon if ToF-SIMS analysis is required.
- Conditioning times used during the study:
  - SIBX: 2 min
  - $CuSO_4$: 5 min
  - DETA: 5 min
  - Polyphosphate: 5 min

An example of microflotation test spreadsheet is shown below:

Pentlandite + Pyroxene, SIBX, Synthetic water, pH 9

Product	Mass (FP)	Mass (FP+S)	Mass (S)	Mass Pull	S		Pentlandite	Pentl. Rec.	Pyroxene	Pyrox.Rec.
	g	g	g	%	%		g	%	g	%
Concentrate 1	0.0000	0.0000	0.0000	0.00	0	0.0000	0.0000	0.00	0.0000	0.00
Concentrate 2	2.7470	3.1212	0.3742	18.80	26.21	82.8775	0.3101	30.95	0.0641	6.48
Tailings	1.3952	3.0112	1.6160	81.20	13.54	42.8142	0.6919	69.05	0.9241	93.52
			1.9902	100.00			1.0020	100.00	0.9882	100.00
Total Concentrate			0.3742	18.80				30.95		6.48

APPENDIX D: Example of ToF-SIMS Analysis Spreadsheet

A typical ToF-SIMS automated spectra evaluation report is shown below. The intensities obtained would be normalised for the elements of interest and presented as the relative percent surface coverage.

AUTOMATED SPECTRA EVALUATION REPORT

Grain Number	#Si	#Ni	#Ni+o	#Ni+o+h	#Na	#Ca	#Mg	#al	#fe	#fe+o	#fe+o+h	#cu	#cu+o+h	#cr	#c5+h9+o+	#s
02425p.tdc	3225	143	3	20	213	1178	4621	740	1837	38	15	20	3	65	0	573
02426p.tdc	3822	94	8	24	951	720	4903	759	1734	33	24	22	5	58	1	520
02427p.tdc	2668	315	4	7	110	411	3671	508	1049	18	5	15	4	35	0	55
02428p.tdc	14703	325	44	41	1127	2650	17779	3485	6084	118	78	76	12	218	0	80
02429p.tdc	2722	46	0	1	69	399	3006	443	997	9	0	6	1	40	0	2
02430p.tdc	4037	569	5	25	611	484	6022	731	1066	28	4	18	5	31	0	190
02431p.tdc	527	11	0	1	31	72	798	92	174	1	5	3	1	5	0	15
02432p.tdc	1597	211	0	0	37	70	2025	147	244	6	0	5	0	11	0	0
02433p.tdc	1482	55	1	0	52	59	1474	133	186	2	0	1	0	13	0	0
02434p.tdc	2698	74	4	10	145	1625	3728	367	1521	18	25	10	3	42	1	172
02435p.tdc	1598	35	0	0	69	184	1575	232	320	3	0	4	0	16	0	0
02436p.tdc	155	3	1	1	10	28	225	24	57	1	0	0	0	0	0	1
02437p.tdc	5111	187	14	43	408	1136	7429	1114	2439	49	49	29	10	86	0	225
02438p.tdc	36694	2774	65	113	1165	1406	49502	5516	11975	277	204	69	12	346	0	322
02439p.tdc	16867	236	18	21	1002	1327	22756	1822	3992	114	36	37	6	112	0	67
02440p.tdc	4058	263	4	4	206	145	5577	307	754	26	7	2	2	19	0	0
02441p.tdc	6387	52	4	3	477	790	8137	1627	1740	48	10	6	2	80	0	0
02442p.tdc	3518	231	1	4	330	188	4854	1004	2016	30	20	11	2	43	0	0
02443p.tdc	7865	219	5	8	234	116	9910	403	1121	32	12	2	0	19	1	1063
02444p.tdc	418	11	0	3	119	334	741	130	67	2	0	3	0	12	0	0
02445p.tdc	3548	19	0	1	90	118	4785	254	478	8	0	2	0	13	0	877
02446p.tdc	5300	37	0	2	453	478	7544	921	838	22	7	8	1	48	0	693
02447p.tdc	1589	24	2	0	186	240	2545	389	174	3	0	1	0	21	0	56
02448p.tdc	1811	168	2	2	192	360	2445	298	635	4	1	13	0	25	1	60
02449p.tdc	10023	1143	22	40	460	644	15042	2319	3929	71	65	33	3	110	1	384
02450p.tdc	15668	161	9	22	1091	1127	22583	1923	3458	97	33	27	5	80	0	144
02451p.tdc	21737	1146	33	62	1093	1073	31219	3082	7134	144	92	47	17	247	0	145
02452p.tdc	1988	85	5	6	192	363	3154	467	617	15	10	10	1	32	0	114
02453p.tdc	4062	1048	21	36	1825	778	6209	1113	3503	52	48	29	13	81	0	1
02454p.tdc	5458	183	9	12	296	574	7776	756	1480	32	8	13	4	47	0	8
02455p.tdc	814	12	5	4	45	117	1096	100	219	6	15	7	1	12	0	80
02456p.tdc	299	4	0	1	22	22	361	42	68	3	1	2	1	3	0	67
02457p.tdc	464	13	3	1	32	51	606	83	152	8	4	1	1	7	0	1
02458p.tdc	4552	138	9	8	281	205	6686	486	1454	27	18	11	6	26	0	129
02459p.tdc	2183	34	2	11	970	1099	2451	1670	365	7	4	7	1	14	0	417
02460p.tdc	6723	260	13	37	402	1135	11225	1348	2474	45	52	35	11	114	2	127
02461p.tdc	8563	266	11	20	1668	1254	13537	2027	2920	84	39	22	10	109	1	222
02462p.tdc	7386	764	3	14	223	311	10311	1190	2219	42	8	13	3	78	0	166
02463p.tdc	18177	1018	26	30	802	918	25317	2197	5071	131	71	34	6	201	0	214
02464p.tdc	11873	3079	50	105	8796	2616	18575	2967	8597	131	105	75	14	223	0	222
02465p.tdc	15580	441	25	39	1474	2293	22994	2896	4320	106	46	45	7	154	2	86
02466p.tdc	5728	103	7	11	268	890	8060	700	1282	53	16	10	4	65	0	89
02467p.tdc	142	1780	13	21	124	188	188	60	3875	26	35	61	3	12	3	1080
02468p.tdc	560	5905	30	132	356	2194	606	166	9085	101	82	115	8	27	87	9491
02469p.tdc	156	837	4	5	38	828	251	53	2350	10	4	20	3	6	57	3226
02470p.tdc	234	541	38	15	138	66	32	510	845	3	4	16	1	5	2	73
02471p.tdc	4	94	1	0	2	181	0	9	107	2	0	0	0	7	0	0
02472p.tdc	276	2595	18	45	225	442	94	40	3927	43	21	43	3	10	22	1376
02473p.tdc	1390	3671	29	32	60	1042	1122	267	9828	89	39	90	4	26	79	6864
02474p.tdc	810	6865	45	41	494	1636	533	149	9732	82	44	119	6	17	145	9091
02475p.tdc	822	4571	17	43	216	257	996	151	3061	38	7	26	0	10	71	2895
02476p.tdc	0	0	0	0	0	0	0	0	0	0	0	0	0	0	2	262
02477p.tdc	568	3441	18	24	55	3086	986	95	5983	58	5	59	3	22	49	3362
02478p.tdc	588	4899	13	35	71	1042	655	118	5620	50	13	145	0	18	44	4105
02479p.tdc	652	4781	21	18	81	309	579	165	7062	60	5	111	2	10	58	4101
02480p.tdc	1560	14463	116	163	294	1118	1332	533	27776	258	403	317	16	112	4	3195
02481p.tdc	1108	5210	37	71	329	2974	957	214	10031	90	96	156	10	35	1	1005
02482p.tdc	212	2632	25	44	87	681	208	60	4413	48	91	60	2	28	1	656
02483p.tdc	261	3702	24	35	135	878	304	90	5311	72	79	85	6	21	6	1062
02484p.tdc	72	1417	6	5	96	50	60	16	1258	12	0	24	2	5	15	3290
02485p.tdc	458	2641	26	32	78	675	310	77	5310	56	143	57	5	20	11	1102
02486p.tdc	198	2310	26	18	44	566	177	55	4272	34	29	60	1	8	8	1097
02487p.tdc	67	48	2	2	105	103	11	228	121	17	32	3	3	26	0	18
02488p.tdc	1268	7174	41	71	267	552	1052	272	13237	117	160	141	5	27	24	2423
02489p.tdc	1470	10737	73	104	544	4837	1435	549	16764	160	77	171	8	43	27	2312
02490p.tdc	101	309	1	0	10	59	62	11	478	4	3	6	0	2	9	307
02491p.tdc	310	2027	9	10	115	648	354	63	2359	17	6	35	0	12	42	1755
02492p.tdc	409	2779	32	50	50	146	110	108	3880	83	85	59	5	28	120	6425
02493p.tdc	272	943	1	0	9	55	70	28	1389	6	0	32	0	5	130	6061
02494p.tdc	0	0	0	0	0	0	0	0	0	0	0	0	0	0	74	3169
02495p.tdc	0	0	0	0	0	0	0	0	0	0	0	0	0	0	54	1205